ANALYSIS OF MICRORNA FUNCTION IN THE GASTROINTESTINAL TRACT

Bailey Cristina Eileen Peck

A dissertation submitted to the faculty at the University of North Carolina at Chapel Hill in partial fulfillment of the requirements for the degree of Doctor of Philosophy in the Curriculum in Genetics & Molecular Biology in the School of Medicine.

Chapel Hill
2016

Approved by

Brian J Bennett

Pauline K Lund

Scott T Magness

John F Rawls

Praveen Sethupathy

ABSTRACT

Bailey Cristina Eileen Peck: Analysis of microRNA function in the gastrointestinal tract
(Under the direction of Praveen Sethupathy)

microRNAs (miRNAs) are a group of small non-coding RNAs that regulate gene expression through post-transcriptional targeting of messenger RNAs (mRNAs). Discovered in mammals in 2001, miRNAs have since become appreciated as both biomarkers and drivers of disease, including metabolic diseases such as type 2 diabetes. Metabolic diseases are characterized by systemic energy imbalance, which involve diverse tissues such as liver, pancreas, adipose, brain, muscle, and intestine. Understanding the role of miRNAs in the regulation of these organ systems during normal physiology and disease pathogenesis is a necessary step to help develop effective miRNA-based therapeutics. Toward this goal, in my dissertation research I identify miRNAs that act as biomarkers of metabolic and gastrointestinal (GI) diseases and evaluate their role in gene regulatory networks in the liver and small intestine. miRNAs are severely understudied in the intestine compared to most other metabolic tissues, and specifically in the intestinal epithelium, so I extended my research objective to help bridge this gap by identifying diet- and microbiota-sensitive miRNAs in distinct cell populations of the intestinal epithelium. I found that intestinal epithelial stem cells (IESCs) respond most robustly to these environmental stimuli. Furthermore, I demonstrated that specific microbiota-sensitive miRNAs regulate IESC proliferation, which is a key process underlying intestinal homeostasis. The findings of my research represent key advances in the GI field, and serve as a strong foundation for future research into the role of miRNAs in metabolic and GI disease.

To the duck whose one leg was both the same.

ACKNOWLEDGMENTS

A doctoral dissertation is never completed in solitude, and there are many, many people whom I have to thank for providing me support, encouragement, mentorship, friendship and the resources necessary to complete this stage of my education.

I will start by thanking my generous funding sources that have taken a chance on me and made my graduate studies possible through various fellowship awards. Specifically, the Initiative for Maximizing Student Diversity (IMSD), the Curriculum in Genetics & Molecular Biology, the Sarah Graham Kenan-Edwards Hobgood fellowship, the National Institute of Diabetes and Digestive and Kidney Disorders (NIDDK), the University of North Carolina at Chapel Hill (UNC), and the UNC Biological and Biomedical Sciences Program.

My dissertation would not have been completed without the endless support and mentorship from my advisor, Praveen Sethupathy. Praveen is a one-of-a-kind mentor whom I am so thankful to have met even before starting my graduate career. Several years ago, he selflessly guided me not only to UNC, but also to his lab, where I have had one of the most positive and inspiring graduate careers. As a PI, Praveen has kept me confident in the midst of the discouraging, helped identify hidden gems among dead ends, and taught me the art of telling stories of great scientific discoveries. As a mentor and advisor, Praveen has been my champion, encouraging my professional and personal development and cheering my successes, and my challenger, pressing me to do more than I thought possible.

Kay Lund, my mentor and chair, who has been one of my favorite sources of advice throughout my graduate career, also deserves special thanks. Her guidance and support over the past four years have helped shape my career aspirations. She is a constant source of inspiration, and I am so thankful that she listened to my risky project idea and helped me turn it into an exciting reality. As her career has progressed, I am also thankful for the generous amount of time she has lent to read my manuscripts and grant applications, and talk me through various career choices and pitfalls. I am so grateful for her ongoing grounded, constructive, thorough, and much needed guidance.

I would also like to thank the other members of my thesis committee, Brian Bennett, Scott Magness, and John Rawls, who despite being in different institutions, departments, and campuses were always available to meet, provide advice, critique my research, and offer diverse and interesting perspectives and suggestions. I would like to thank Brian for providing his expertise on diet and nutrition, giving me genuine career advice, and for advocating for me throughout my graduate career. I would like to thank Scott for challenging me, questioning me, and, above all, supporting me. His advice and innovative perspectives have constantly inspired me to do better science and take my questions one step further. Finally, I would like to thank John for the many, many hours of discussion and debate regarding microbiota, the host-epithelium, conventionalization, and overall strategy during the initial stages of my thesis project. He opened up the world of the microbiome to me and has since been an avid supporter and priceless mentor. A committee is a family, and I am glad I picked these five!

Several past and present mentors who guided me and encouraged me to continue this journey deserve recognition. I'd like to start by acknowledging Peggy Daugherty of Colorado College, who allowed me the first glimpse of myself as a scientist; Leona Gagnon of The

Jackson Laboratory, for introducing me to experimental biology and mouse genetics; Francis Collins of the National Institutes of Health, for the ongoing, thoughtful guidance and inspiration; and Samir Kelada of UNC, for preparing me for the challenges of research.

I have recognized my mentors, but I also need to thank all of my lab mates over the past decade that have listened to my problems and provided advice on troubleshooting, next steps, and interpretation. Lab mates have laughed with me, sympathized with me, and have generally been my favorite people I have had the pleasure to see every day. I want to give a special shout out to Jeanette Baran-Gale and Sara Selitsky, who as senior graduate students in Praveen's lab have been there for me every step of the way. I would like to thank them for the advice, assistance, mentorship, critical ear, and helping hands. They are not only my lab mates, but also two of my closest friends. Jeanette has provided countless hours of technical support and many refreshing lunch dates and coffee breaks discussing science, the future, career paths, and life in general. I would like to thank her for being by my side both in and out of the lab and classroom. Despite the oceans that may separate us, I know that she will be a constant friend, colleague, collaborator, and mentor. Since joining Praveen's lab, I would also like to thank Lisa Kurtz, who has always been 'home base' in the lab, keeping us grounded, but not too serious. Thanks Tim Dinh, Alisha Coffey, Nev Kazgan, Eva Vitucci, Rowan Beck, Wendy Pitman, Ben Keith, Mi Zhou, Emily Fannin, John Sincavage, Sydney Feinstein, and the rest of the miRcats for keeping lab real. I would also like to thank the members of Kay's lab, including Amanda Mah, Emily Moorefield, Shengli Ding, Eric Blue, Jim Simmons, and Sara Andres, for teaching me about the gut, supporting my projects, and lending hours of troubleshooting advice and assistance.

The experiments and published manuscript described in Chapter 2 would not have been possible without my co-authors, Lisa Kurtz, Emily Fannin, Carine Beysen, Ji Miao, Stuart R.

Landstreet, Shengli Ding, Vandana Turaga, Kay Lund, Scott Turner, Sudha B. Biddinger, and Kasey C. Vickers. Additional acknowledgment must also be given to Michael Erdos, Samir Kelada, Jeanette Baran-Gale, and Jonathan Haldeman for their helpful suggestions regarding the study and manuscript, Stanley Lemon for generously sharing Huh7 cells, and Brad Hoffman of the University of British Columbia for sharing the chromatin occupancy sites for FOXA2 in mouse liver and islet based on a previously published study.

I would like to thank Shehzad Sheikh for sharing his exciting Crohn's disease data, his knowledge and excitement for IBD research, and his mentorship over the last couple years; and Terry Furey for his ability to simplify complex ideas and his close eye for details. Chapter 3 would not have been possible without their assistance and support. I also want to thank my co-authors for the research presented in Chapter 3, including Matt Weiser, Eric Lee, Greg Gipson, Vishal Iyer, Balfour Sartor, Hans Herfarth, Millie Long, Jonathan Hansen, Kim Isaacs, Dimitri Trembath, Reza Rahbar, and Timothy Sadiq.

Many helping hands assisted the experiments and published manuscript described in Chapter 4 over the past couple of years. This 'side-project' became quite a beast with plot twists, dead-ends, and a few surprises, which I have my many co-authors to thank for helping untie. They include John Sincavage, Sydney Feinstein, Amanda Mah, Jim Simmons, and Kay Lund. I also must acknowledge the Beaulieu laboratory for provision of the HIECs, the UNC Flow Cytometry Core Facility, the UNC High Throughput Sequencing Facility, the UNC Bioinformatics Core Facility, and specifically Barry Udis, Joel Parker, Eric Blue, and Scott Magness for technical assistance and useful discussions.

The data included in Chapter 5 could not have been generated without Amanda Mah, who helped generate the germ-free mice, train me on the many techniques needed to analyze the

intestine, troubleshoot FACS, and manage the challenges of graduate school. She has been a patient and supportive mentor, despite my flaws, and I appreciate all of her help on the various projects I have undertaken. Additionally, many thanks are due to Eric Blue for his help in developing the GF Sox9-EGFP resource; Elaine Glenny for critical assistance with the anaerobic chamber and the protocol for conventionalization; Lisa Kurtz, Emily Moorefield, Shengli Ding, and Jeanette Baran-Gale for technical assistance and training; John Rawls and Scott Magness for helpful discussions; as well as Felicia Heyward and UNC Flow Cytometry Core Facility, the UNC Gnotobiotic Core Facility, Dr. Zhao Lai and the UTHSCSA Genome Sequencing Facility, and Dr. Bob Bagnell and the UNC Microscopy Services Laboratory for critical services rendered for the experiments presented in Chapter 5.

Toward the completion of this dissertation as a whole, I also must thank the many friends and colleagues who volunteered their time to read through and copyedit the very rough versions of this document. Specifically, thank you to Deirdre Sackett and Jonathan Susser, both of whom served with me on the executive board of the UNC Science Writing and Communication club; Sydney Feinstein, a fellow miRcat who worked with me on the results presented in Chapter 4; Kelsey Gray and Michelle Engle, who are both GMB peers and friends; and Kate Kutchko, a close friend and colleague.

Outside of lab, I have my peers in GMB, FYG, and IMSD to thank for their friendship, support, and shoulders to lean on (during both the tough times and the best of times). In particular, I would like to mention Kate Kutchko, a fellow CC Tiger, who became one of my closest friends during my time at UNC. I want to thank her for the many passionate and thought-provoking debates on science, policy, and life, which I am ever thankful we can continue our friendship through. I so appreciate her advice, shared ideas, moral support, game nights, movie

dates, and happy hours, all of which have helped me get through graduate school in one piece.

Finally, I must acknowledge my family, who has truly made the greatest sacrifices to get me to and through grad school. They are my constant support network. My father, who passed away in 2015, was a lifelong inspiration. His intelligence, love of science, hard work ethic, and many still top-secret projects are the traits and memories that continue to push me to do better. My mom, who has been my greatest supporter for as long as I can remember, deserves special recognition. Her love of life, thoughtfulness, patience, drive, and confidence are traits that I will forever attempt to emulate. My Gramma Ruby, who immigrated to the US to pursue higher education, has always been a present advocate and supporter. Her sacrifices paved the way for my successes, and I am truly thankful for everything she has done for me. My stepfather, Tom, I would like to thank for his quick wit, unique perspectives, friendship, and support. My siblings Kilian, Teghan, Ivan, and Sara, who have all pursued and achieved successful careers in their own right, deserve thanks for celebrating the good times and supporting me during the difficult times. I would also like to thank my best friend, Ashley, for the last 18 years of friendship. Despite the distance, my love of vegetables, and her two days of age maturity over me, she has been one of my greatest cheerleaders, confidantes, and companions. I have Ashley to thank for the many rides home from the airport, hours-long phone conversations, personal advice, and loving support over the years. May we forever be related through our dogs.

Finally, I would like to thank my partner, David, for his love and support over the last decade. His quick humor, love, thoughtfulness, patience, presence, and companionship persevered despite the long work hours, missed dates, and staggered schedules. These past four years had their challenges and blessings, and I am so thankful for his generosity, kindness, forgiveness, commitment, and understanding. I can't think of a better person with whom to raise

our dog-children, Getty and Maccabee. In 2010, David chose to move across the country with me, and I am forever appreciative that he chooses to stand by my side, to share and celebrate our successes, and to plan for the future with me.

PREFACE

In each chapter, there are portions of work that were completed by other talented scientists, and most chapters contain published work that I have been granted access to use as part of this dissertation.

The full citation for the published work found in Chapter 2 is as follows:

> Kurtz, C. L.*, Peck, B. C. E.*, Fannin, E. E., Beysen, C., Miao, J., Landstreet, S. R., Ding, S., Turaga, V., Lund, P. K., Turner, S., Biddinger, S. B., Vickers, K. C., and Sethupathy, P. (2014) MicroRNA-29 fine-tunes the expression of key FOXA2-activated lipid metabolism genes and is dysregulated in animal models of insulin resistance and diabetes. *Diabetes*. **63**, 3141–3148.

This project evolved from results generated during my first graduate research rotation in the Sethupathy lab. Lisa Kurtz, who serves as a co-first author with me on the manuscript (as designated by the asterisk), continued and confirmed many of the initial transfection studies using LNAs, FOXA2 ORF, and luciferase vectors after the completion of my research rotation. After I joined the Sethupathy lab for my thesis work, she and I were responsible for completing the remaining experiments, editing the manuscript, and generating figures. Permission to include the published article in its entirety is given by the journal *Diabetes* for educational purposes as explained on their website (http://www.diabetesjournals.org/content/reprints-permissions).

The full citation for the published work found in Chapter 3 is as follows:

> Peck, B. C. E., Weiser, M., Lee, S. E., Gipson, G. R., Iyer, V. B., Sartor, R. B., Herfarth, H. H., Long, M. D., Hansen, J. J., Isaacs, K. L., Trembath, D. G., Rahbar, R., Sadiq, T. S., Furey, T. S., Sethupathy, P., and Sheikh, S. Z. (2015) MicroRNAs Classify Different Disease Behavior Phenotypes of Crohn's Disease and May Have Prognostic Utility. *Inflammatory Bowel Diseases*. **21**, 2178–2187.

Permission to use the work in whole was provided free of charge from *Inflammatory*

Bowel Diseases, Wolters Kluwer Health, and Lippincott Williams & Wilkins through RightsLink, which can be found in the online version of the article (http://journals.lww.com/ibdjournal/Fulltext/2015/09000/MicroRNAs_Classify_Different_Disease_Behavior.20.aspx).

The full citation for the published work found in Chapter 4 is as follows:

> Peck, B. C. E., Sincavage, J., Feinstein, S., Mah, A. T., Simmons, J. G., Lund, P. K., and Sethupathy, P. (2016) miR-30 family controls proliferation and differentiation of intestinal epithelial cell models by directing a broad gene expression program that includes SOX9 and the ubiquitin ligase pathway. *J. Biol. Chem*, **291**(31), 15975-15984.

The *Journal of Biological Chemistry* automatically grants authors the right to reuse their published material in a thesis and/or dissertation. Details of this permission can be found on their website (http://www.jbc.org/site/misc/Copyright_Permission.xhtml).

The material included in Chapter 5 has been submitted for publication. Rights and usage will be discussed with the publisher upon acceptance. A full citation for the current version of this work, which can be found on the preprint server *bioRxiv*, is as follows:

> Peck, B. C. E., Mah, A. T., Pitman, W. A., Ding, S., Lund, P. K., and Sethupathy, P. (2016) Functional transcriptomics in diverse intestinal epithelial cell types reveals robust gut microbial sensitivity of microRNAs in intestinal stem cells. *bioRxiv*. 10.1101/087882 http://dx.doi.org/10.1101/087882.

TABLE OF CONTENTS

LIST OF TABLES

LIST OF FIGURES

LIST OF ABBREVIATIONS

3'UTR	3-prime untranslated region
B1	Crohn's disease subtype based on Montreal scoring system that describes B1 patients as having a non-stricturing and non-penetrating disease phenotype
B2	Crohn's disease subtype based on Montreal scoring system that describes B2 patients as having a stricturing phenotype
B3	Crohn's disease subtype based on Montreal scoring system that describes B3 patients as having a penetrating phenotype
CD	Crohn's disease, see UC and IBD
cDNA	complementary DNA, produced upon reverse transcription of RNA
CPM	Counts per million, a normalization method for messenger RNA-sequencing
DE	Differential expression, or differentially expressed
ECM	Extracellular matrix genes, which include *COL6A1*, *COL6A3*, *COL21A1*, and *ELN*
EEC	Enteroendocrine cells, a population of intestinal cells with endocrine function, including the release of hormone and signaling molecules in response to environmental stimuli
FC	Fold change, see RQV
FDR	False discovery date, a multiple testing correction
FFPE	Formalin-fixed and paraffin-embedded
GEO	Gene Expression Omnibus repository
GI	Gastrointestinal
GLM	Generalized linear model
GO	Gene ontology
GRN	Gene regulatory network
GWAS	Genome-wide associate study
HFD	High-fat diet

HIECs	Human intestinal epithelial cells, acquired from the Beaulieu laboratory
IBD	Inflammatory bowel diseases, which include Crohn's disease and ulcerative colitis
IE	Intestinal epithelium
IEC	Intestinal epithelial cell
IESC	Intestinal epithelial stem cells, includes reserve IESCs (abbreviated rIESCs) and actively-cycling IESCs (abbreviated aIESCs)
IF	Inflamed tissue, as defined by the presence of inflammatory immune cells
IQR	Interquartile range
LFD	Low-fat diet
LNA	Locked nucleic acid. If followed by a number, refers to complementary LNA to the miRNA. If followed by 'Scr,' refers to a control scramble LNA
miRNA	microRNA. Individual miRNAs are abbreviated as miR followed by a numeric identifier. For example, miR-29.
MG132	Z-Leu-Leu-Leu-al, a potent proteasome inhibitor
mRNA	Messenger RNA
NI	Non-inflamed tissue, see IF
NIBD	Non-inflammatory bowel disease control sample or patient
NGS	Next-generation sequencing. Typically refers to high-throughput sequencing technologies
PIO	Pioglitazone, an antidiabetic prescription medication
qRT-PCR	Quantitative reverse-transcription polymerase chain reaction
RIN	RNA integrity index, ranges from 0 to 10
RPMM	Reads per million mapped, a normalization means for small RNA-sequencing
RPMMM	Reads per million mapped to microRNAs, a normalization means for microRNAs
RQV	Relative quantitative value. Similar to fold change, in this case first normalizing to a control gene

SI	Small intestine, which consists of duodenum, jejunum, and ileum. If italicized, refers to gene *SI*, which codes for sucrase isomaltase
SNP	Single nucleotide polymorphism
TER	Transepithelial electrical resistance, a tool commonly used to evaluate the differentiation of Caco-2 and other intestinal cells, which by forming a single-layer with tight junctions, show increased TER
TF	Transcription factor
TLR5	Toll-like receptor 5
TMAO	Trimethylamine N-oxide
TSS	Transcription start site
UC	Ulcerative colitis, see CD and IBD
ZDF	Zucker Diabetic Fatty rat strain

CHAPTER 1 – INTRODUCTION

Metabolic diseases, including obesity and type 2 diabetes, represent a global health crisis. Particularly prevalent in the Western world, these diseases affect approximately one in three adults in the United States(Aguilar et al. 2015). During disease progression, systemic dysregulation occurs in tissues including the liver(Rottiers and Naar 2012), adipose(Grundy 2015), skeletal muscle(Marette et al. 2014), brain(Codocedo et al. 2016), and intestine(Changting Xiao et al. 2015). There are clear environmental risk factors for disease onset, including diet and gut microbiota(Tremaroli and Bäckhed 2012), as well as diverse and numerous genetic components that modify and personalize metabolic disease progression.

In my thesis research, I sought to understand the role of a subclass of regulatory RNAs, microRNAs, in regulating and driving metabolic disease pathogenesis. I began my studies in the liver, one of the most well studied organ systems with regard to type 2 diabetes and microRNAs (Figure 1.1). My research eventually led me to the intestine, where nearly 25% of the body's glucose is produced(Mithieux et al. 2009), a feat which is vital to maintaining fasting glycaemia levels(Penhoat et al. 2014). Importantly, the intestine houses the gut microbiota, a metabolic organ in its own right. microRNAs are known to respond to a wide variety of environmental stimuli and are released into the blood stream where they may communicate with distant tissues. Yet little is known about the role of microRNAs in regulating normal physiological, let alone disease, processes in the intestine. In this dissertation, I evaluate microRNAs as tissue

biomarkers of type 2 diabetes (liver) and Crohn's disease (CD; colon), identify two microRNAs of critical importance in maintaining physiological homeostasis in the liver and intestine, and establish microRNAs as key microbiota-sensitive regulators of physiological processes in the intestine (Figure 1.1C).

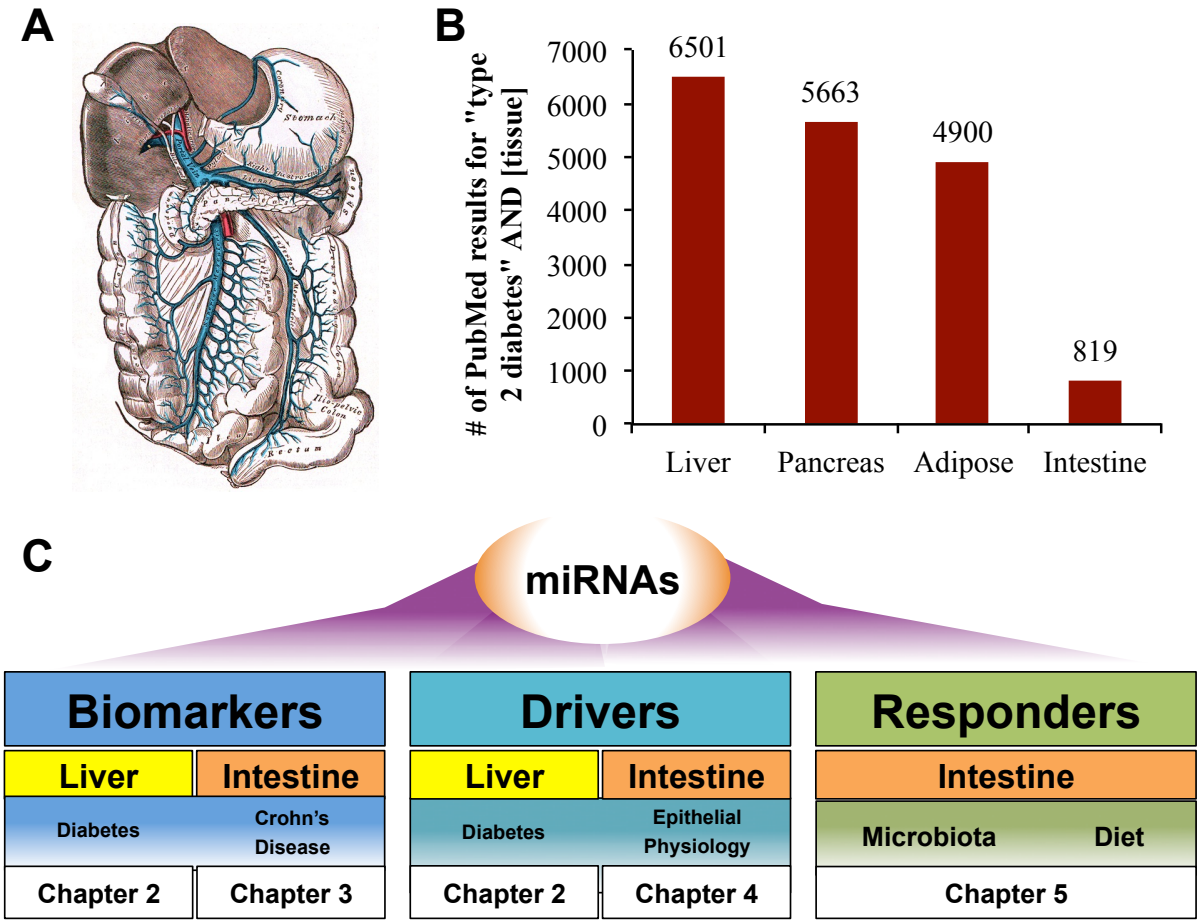

Figure 1.1. The gastrointestinal tract and type 2 diabetes. (**A**) Medical illustration showing the interconnected organ systems that compose the GI tract. The liver receives blood, metabolites, and other molecules from the pancreas, visceral adipose (not shown), stomach, and intestine through a vascular network that feeds into the portal vein (blue). Image labeled free for reuse and acquired via Wikimedia. (**B**) The number of results are shown following a PubMed search for "type 2 diabetes" AND [tissue], which was conducted on 7/11/16. (**C**) Outline depicting the flow of my dissertation investigating miRNAs as biomarkers and drivers of disease, as well as responders to environmental risk factors for the development of metabolic diseases.

microRNA biogenesis and function

microRNAs (miRNAs) are a population of small (18-24 nucleotide), noncoding RNAs that regulate gene expression through post-transcriptional targeting of messenger RNAs(Bartel 2009). This relatively recently discovered class of RNA can be used as biomarkers of physiological states, but have also emerged as drivers of disease and responders to environmental stimuli. miRNAs have their own promoters and are endogenously transcribed (Figure 1.2), typically in a RNA polymerase II-dependent manner, before being capped, polyadenylated, cleaved by the RNase III Drosha, and actively transported to the cytoplasm(X. Liu et al. 2008). Once in the cytoplasm, miRNAs are processed into their mature form by Dicer, which loads them onto the multiprotein RNA-induced silencing complex (RISC)(X. Liu et al. 2008). An active metazoan miRNA on RISC will scan the transcriptome searching for accessible target sites typically located within 3'UTRs that are complementary to the miRNA's seed region, bases 2-8 at the 5'-end of a miRNA. A bound miRNA typically acts to repress a target gene by sequestering and preventing translation or by destabilizing the target RNA(X. Liu et al. 2008).

Due to the short sequence-specific targeting requirement, a single miRNA has the potential to target hundreds of genes, and a single gene may be targeted by several different miRNAs(Mukherji et al. 2011; Bhajun et al. 2016). Complex miRNA and gene regulatory networks (GRNs) exist and may help a cell or organism respond to a diverse array of stimuli. miRNA degeneracy, which describes how multiple different miRNAs can perform the same or highly overlapping functions, contributes to the ability of a cell or system to adapt to diverse environmental perturbations(Bhajun et al. 2016). Most miRNAs singularly have a relatively modest repressive effect. They generally work to fine-tune and buffer gene expression(Tsang et al. 2007; Herranz and Cohen 2010; Su et al. 2011) and can also serve as switches to modulate the

output of large GRNs(X. Liu et al. 2008; H. Guo et al. 2010; Mukherji et al. 2011; Bhajun et al. 2016). Researchers believe that single nucleotide polymorphisms (SNPs) located within miRNA target sites and miRNA promoter/enhancer regions may underlie some of the identified genome-wide association study (GWAS) hits across various complex diseases(Bulik-Sullivan et al. 2013; Delay et al. 2016; Mullany et al. 2016), which strengthens evidence for a strong functional role of miRNAs in disease pathogenesis. Indeed, one prominent example is a SNP in the target site of miR-196 within the gene *IRGM* that significantly increases risk for CD(Brest et al. 2011).

miRNAs may also act as intercellular communicators. Cells package miRNAs into exosomes and other microparticles, which may be released and taken up by distant cells to regulate gene expression(Mittelbrunn et al. 2011; Boon and Vickers 2013; L. Xu et al. 2013). miRNAs in exosomes appear to be targeted for loading, as specific miRNAs may be enriched and/or depleted relative to intracellular levels(Squadrito et al. 2014). miRNAs have been found circulating in various bodily fluids, including blood, breast milk, and feces, potentiating wide regulation of distant cells within and without the body. Moreover, patients with certain metabolic diseases have altered expression of miRNAs in these fluids, which provides a possible mechanism by which miRNAs may be involved in the systemic dysregulation(Karolina et al. 2012). Environmental stimuli, such as hormones, cytokines, and nutrients/metabolites, are also established modulators of miRNA expression(Dalmasso et al. 2011; Dumortier et al. 2013; García-Segura et al. 2013; Nguyen et al. 2014). Because metabolic diseases include both genetic and environmental components, evaluating the contribution of miRNAs is of particular interest.

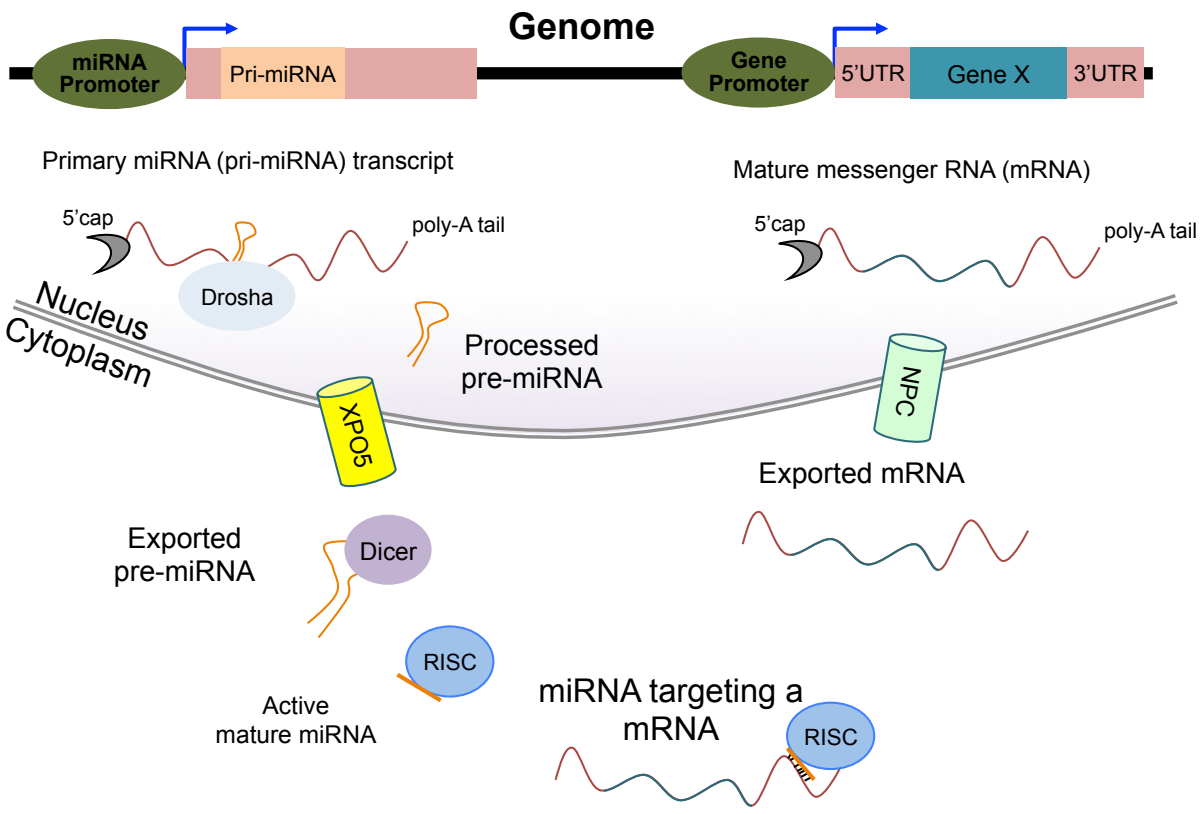

Figure 1.2. Cartoon depicting microRNA and mRNA biogenesis. This simplified cartoon contrasts canonical miRNA (left) and mRNA biogenesis (right).

microRNAs in metabolic disease

A number of miRNAs have already been identified as biomarkers and regulators of metabolic disease, and multiple reviews have been published on the topic(Rottiers and Naar 2012; Dumortier et al. 2013; Rotllan et al. 2016). However, in this section I will briefly detail a few of the most recognized miRNAs associated with metabolic disease, as well as others more recently identified. I hope to emphasize the diversity of roles for miRNAs across tissues, cell types, and developmental time points, all of which can lead to disease when dysregulated.

microRNA-33

miR-33a and miR-33b are isomiRs, miRNAs with identical targeting seed regions, and best known for their sophisticated regulation of lipid metabolism in the liver. These miRNAs are located within and processed from their respective host genes, *SREBF1* and *SREBF2*, which encode transcription factors (TFs) that serve as master regulators of lipid homeostasis(Horie et al. 2010; Najafi-Shoushtari et al. 2010) in part by driving the expression of genes that encode enzymes in the fatty acid and cholesterol synthesis pathways in the liver, including *FASN*, *SCD*, *SQLE*, and *HMGCR*(Rottiers and Naar 2012; Dumortier et al. 2013; Rotllan et al. 2016). miR-33 directly targets a number of hepatic mRNAs coding for fatty acid oxidation proteins, as well as negative regulators of fat production, cholesterol efflux, and glucose metabolism(Ramírez et al. 2013). miR-33 acts to maintain lipid homeostasis, but when dysregulated can also lead to diseases such as hypercholesterolemia and atherosclerosis(Rayner, Sheedy, et al. 2011). Moreover, research shows that miR-33 mediated regulation of lipid metabolism pathways is conserved in both rodents(Rayner, Sheedy, et al. 2011) and non-human primates(Rayner, Esau, et al. 2011), strengthening the importance of research into its role and use as a potential therapeutic in the treatment of human diseases. Interestingly, miR-33-mediated regulation of

cholesterol pathways has also been linked to the control of the cell cycle and proliferation(Cirera-Salinas et al. 2012; Inukai and Slack 2012).

microRNA-375

The first miRNA to be attributed to taking part in insulin secretion, miR-375 was originally described as pancreatic islet cell specific. It has critical roles in regulating both the development and function of the pancreatic β-cells(Poy et al. 2004; Poy et al. 2009) and therefore is an important modulator of glucose homeostasis. More recently, miR-375 has been identified outside of the islet. Similar to its role in development, miR-375 has been shown to be downregulated in various cancer subtypes, which enhances proliferation(Yan et al. 2013). In healthy intestinal tissue, it drives enteroendocrine cell (EEC)(Knudsen et al. 2015) and possibly Goblet cell differentiation(Biton et al. 2011). Both the pancreas and intestine function as important metabolic and endocrine organ systems, making miR-375 a particularly relevant miRNA in the study of type 2 diabetes and other metabolic diseases.

microRNA-378

miR-378 is a notable miRNA in that both the -5p and -3p ends of the precursor miRNA are loaded onto RISC and have regulatory function. Interestingly, *PPARGC1B*, which codes for the energy metabolism transcription factor PGC-1β, is the host gene for miR-378. In adipocytes, miR-378-5p and miR-378-3p regulate differentiation and function of white adipose tissue(Romao et al. 2011). Knockout mice for miR-378a are resistant to HFD-induced weight gain and have increased oxidative capacity, and mitochondrial function across multiple metabolic tissues(Carrer et al. 2012). miR-378 is also established as a regulator of angiogenesis, muscle development, differentiation, and regeneration(Krist et al. 2015).

microRNA-24

miR-24 was more recently identified as a metabolic disease-relevant miRNA, and has been shown to be dysregulated in the blood plasma and tissues of type 2 diabetics(Xiang et al. 2015) and in animal models of metabolic disease(Zhu et al. 2013). miR-24 is a direct regulator of diabetes-linked TF *Neurod1*, which is involved in islet and endocrine development(Zhu et al. 2013). miR-24 targets von Willdebrand factor, of which elevated levels are associated with thrombotic cardiovascular diseases, the leading cause of death for patients with type 2 diabetes (Xiang et al. 2015). Expression levels of miR-24 are responsive to glucose(Zhu et al. 2013; Xiang et al. 2015) and fatty acids(Ng et al. 2014), which is interesting given that miR-24 also acts to regulate lipid metabolism, in part through the targeting of *Insig1* in the liver(Ng et al. 2014). Knockdown of miR-24 in mice on a HFD, improves circulating plasma and hepatic triglyceride and cholesterol levels(Ng et al. 2014). miR-24, much like miR-33, miR-378, and miR-375, has also been attributed a role in regulating proliferation and differentiation, including in adipocytes and T-cells(Kang et al. 2013; Cho et al. 2016; Jin et al. 2016).

microRNA-30

miR-30 has recently been identified as a regulator of cholesterol synthesis and secretion in the liver. In 2013, Soh *et al*. showed that miR-30 directly targets MTP to reduce lipid synthesis in the liver(Soh et al. 2013). They showed in mice fed a HFD that hepatic overexpression of miR-30 reduced lipid synthesis. Moreover, in mice at risk for atherosclerosis ($ApoE^{-/-}$), transduction of mice with a miR-30 overexpression vector reduced plasma cholesterol and resulted in fewer atherosclerotic plaques(Soh et al. 2013). Recently, researchers evaluated treatment with miR-30 mimic in models of metabolic disease. This approach has the benefit of not requiring viral vectors for overexpression, which are currently not feasible as therapeutic

vehicles. In this paper, on which I serve as co-author, we showed similar beneficial effects of reducing hypercholesterolemia, hepatic lipid synthesis, and atherosclerosis progression(Irani et al. 2016), suggesting miR-30 may be a highly promising therapeutic for patients with cardiovascular diseases. Outside of the regulation of lipid synthesis and secretion, miR-30 has also been linked to the regulation of proliferation and differentiation in a number of tissues and in the progression of cancer(F. Yu et al. 2010; T. Wu et al. 2012; Guess et al. 2015; B.-W. Zhang et al. 2016).

microRNAs as therapeutics and therapeutic targets in the treatment of metabolic disease

miRNAs are particularly attractive therapeutic targets. They can be inhibited using antisense oligonucleotides, or antimiRs, which sequester or inhibit miRNA action, and target miRNAs for degradation. Chemical modifications to these oligonucleotides, such as locked nucleic acids, increase the stability of the antimiRs *in vitro* and *in vivo*(van Rooij et al. 2012). Pharmaceutical companies have already designed antimiRs that have entered clinical trials for the treatment of various diseases. For example, miR-122, one of the first miRNAs to be developed as a therapeutic, is in phase II trials for the treatment of hepatitis C(Lindow and Kauppinen 2012; Sethupathy 2016). miR-122 is hijacked by the hepatitis C viral genome to assist in replication and miR-122 inhibitors have been shown to be effective at reducing viral activity(Lindow and Kauppinen 2012). Since this landmark development in miRNA therapeutics, several additional antimiR drugs have entered the preclinical arena, including several for the treatment of metabolic diseases including obesity and type 2 diabetes, such as miR-103/107 for treatment of type 2 diabetes associated hepatic steatosis(Sethupathy 2016). Interestingly, miRNA

mimics may also have some therapeutic potential. Anti-cancer miR-34 mimics, such as the drug MRX34, are in Phase 1 clinical trials and are showing promising results(Beg et al. 2015).

A major identifiable theme across these metabolically relevant miRNAs is their context-specific actions. A miRNA can have very different (though not necessarily incoherent) functions across diverse tissues. This is due to the very different gene expression profiles, 3'UTRs, and the environmental stimuli encountered by each cell population. Due to these considerations, several challenges still exist toward effective delivery and disease amelioration using miRNA therapeutics. As miRNAs have diverse, context-dependent functions, off-target effects may prove problematic. Additionally, certain organs like liver and kidney take up oligos more effectively than other tissues like brain and pancreas(Sethupathy 2016), identifying delivery vehicles or oligo modifications that improve this uptake with be key to solidifying the therapeutic potential of miRNAs in the future.

Importantly, many of these metabolically-relevant miRNAs appear to have roles in both energy homeostasis and in regulating cell proliferation and fate decisions. While these diverse functional roles may complicate treatment strategies due to off-target effects, they also have important implications in terms of disease etiology. There is no tissue more pertinent to metabolism and proliferative capacity than the intestinal epithelium (IE), which is an essential regulator of energy homeostasis and the most rapidly renewing tissue in adult mammals.

The intestinal epithelium as a metabolic tissue

The IE is vital for a wide range of physiological functions, including pathogen defense, nutrient absorption, and metabolic homeostasis. It is also the most rapidly renewing tissue in the body, with cellular turnover occurring every 3-5 days in humans. This rate depends on the

stability of intestinal epithelial stem cells (IESCs), which give rise to transit amplifying progenitor cells that go on to differentiate into various types of mature intestinal epithelial cells (IECs), such as enterocytes, EECs, Paneth cells, and goblet cells. Precisely regulating gene expression in these cell types is critical for properly balancing proliferation and differentiation in the IE.

While fasting, select tissues must carry out gluconeogenesis to maintain normoglycaemia levels. In addition to absorbing nutrients from diet during the fed state, the IE is responsible for 20-25% of the body's glucose production during fasting, which once released into the portal vein by the IE is able to signal to the brain through the periportal neural system to induce hunger-stimulating hormone secretion(Mithieux and Gautier-Stein 2014). Interestingly, Roux-en-Y gastric bypass surgery ameliorates type 2 diabetes by improving glycemic control, and the effect can be seen in the hours following surgery before any weight loss is observed(le Roux et al. 2007; Schauer et al. 2012; Schauer et al. 2014). Recent reports have linked IE gluconeogenesis and hormone production to this effect(le Roux et al. 2007; Reinehr et al. 2007; Troy et al. 2008; Schauer et al. 2014).

The functions of miRNAs in the IE are understudied, particularly in relation to other metabolic tissues such as the liver and muscle. The limited number of published studies suggest that miRNAs are likely important in shaping IE architecture, barrier function, and proliferation(McKenna et al. 2010; Dalmasso et al. 2011; Ye et al. 2011). More recently, it has been proposed that miRNAs likely produced from IECs may regulate resident microbial communities(S. Liu et al. 2016). Because miRNAs are attractive therapeutic targets in an increasing array of disorders(van Rooij et al. 2012), it is important to identify specific miRNAs and their regulatory pathways that govern key physiological processes in the intestine. Such an

undertaking would provide a strong foundation for the development of novel, effective miRNA-based therapeutic targets for gastrointestinal (GI) and metabolic disease.

Gut microbiota and diet in metabolism and metabolic disease

The intestine houses the gut microbiota, a collection of greater than 10^{12} commensal and symbiotic of bacteria, fungi, viruses, and more(Tremaroli and Bäckhed 2012; Devaraj et al. 2013; Aron-Wisnewsky and Clément 2016), the largest density of which reside in the large intestine. The gut microbiome influences the host by modulating nutrient absorption(Semova et al. 2012), hormone secretion(Tolhurst et al. 2012; Chimerel et al. 2014), inflammation(Bonamichi-Santos et al. 2015; Zaiss et al. 2015), angiogenesis(Schirbel et al. 2013), and intestinal physiology(Larsson et al. 2012; Aidy et al. 2013; Becker et al. 2013). High-throughput sequencing technology has expanded our ability to analyze the complexity of the microbiome in real time without independent culturing, which has allowed researchers to evaluate how microbial diversity changes over time and in response to various stimuli. As such, a number of factors are known to influence the microbiome, including diet(David et al. 2014), ethnicity(Prideaux et al. 2013), drug and antibiotic use(Carvalho et al. 2012; Forslund et al. 2015; Mikkelsen et al. 2015), age(Odamaki et al. 2016), and disease status(Tlaskalová-Hogenová et al. 2011; Qin et al. 2012; Forslund et al. 2015). To characterize the diversity of microbiomes, researchers in 2011 took a modeling approach to identify enterotypes, which are classified by the presence and abundance of three genera of bacteria(Arumugam et al. 2011). However, intra-individual microbial composition varies widely based on localization within the intestinal tract and a number of environmental factors(Aidy et al. 2012). More research is needed to understand

not only the relationships within the microbial community, but also how various compositions might affect human health and disease.

Metabolites generated by certain microbial species have also been associated with higher risk for metabolic diseases. One metabolite associated with disease risk is trimethylamine N-oxide (TMAO). Hepatic flavin monooxygenase converts a metabolite of microbial digestion of phosphotidylcholine/choline/betaine into TMAO, which is a strong risk factor for adverse cardiovascular events(Z. Wang et al. 2011; Loscalzo 2013). Other byproducts are thought to be protective. For example, short chain fatty acids like butyrate act against colorectal cancer(Hu et al. 2011) and conjugated linoleic acid modulates hepatic and adipose fatty acid composition(O'Shea et al. 2012). Given the diversity of microbial metabolites, understanding the mechanism of their effect on other microbes and on host-physiology is a daunting but extremely important area of scientific research.

Certain gut microbial profiles and byproducts are well appreciated as key environmental risk factors in metabolic disease pathogenesis(Larsen et al. 2010; Qin et al. 2012; Karlsson et al. 2013; X. Zhang et al. 2013) and may also be important in developing personalized therapeutics. As mentioned in the previous section, Roux-en-Y surgery results in the rapid amelioration of type 2 diabetes. Robust changes in microbial composition have also been observed following surgery(Furet et al. 2010; J.V. Li et al. 2011), suggesting an additional role for the microbiota in mediating the beneficial effect of the surgery. Mice deficient for Toll-like receptor 5 (TLR5), which is expressed on IECs and recognizes bacterial flagellar ligands, will develop severe colitis, obesity, hypercholesterolemia, insulin resistance, and elevated blood pressure(Vijay-Kumar et al. 2010). These metabolic phenotypes are corrected by treatment with antibiotics, implicating gut microbiota and their interactions with the host epithelium(Vijay-Kumar et al. 2010).

Interestingly, a dominant nonsense mutation in human *TLR5* is also associated with type 2 diabetes, but was found to be protective against obesity. The slight phenotypic dissimilarities between mice and humans lacking *TLR5* may stem from differences in microbial composition or from slight functional variances(Al-Daghri et al. 2013).

Notably, even microbially-derived drug byproducts are relevant in the study of metabolic disease pathogenesis. Recently, a meta-analysis of published metagenomic data found that Metformin treatment was a significant confounding variable(Forslund et al. 2015) in the comparison of microbiomes from type 2 diabetics and controls. Understanding the effect of Metformin on the GI tract is therefore relevant to the treatment of diabetes. Treatment with Metformin in mice reduces overall microbial diversity, but increases the amount of *Akkermansia muciniphila*, a bacterial species already linked to the improvement of metabolic disease(Everard et al. 2013; H. Lee and Ko 2014; Shin et al. 2014), which provides a possible mechanism of action and explanation for the variability of Metformin efficacy. These preliminary studies suggest a substantial role for microbiota in mediating the beneficial and off-target effects of Metformin. Understanding how the microbiome helps regulate metabolic disease, drug response, and IE physiology are important next steps toward developing novel, effective therapeutics for treating GI and metabolic disease.

To study the role of gut microbiota, researchers have developed germ-free (GF) animals, which are housed and bred under gnotobiotic conditions. GF mice are leaner than conventional mice and are resistant to HFD-induced obesity, endotoxaemia and inflammation, steatosis, and insulin resistance(Rabot et al. 2010; Everard et al. 2013; Aron-Wisnewsky and Clément 2016). Antibiotic treatment of mice on a HFD has similar beneficial effects(Carvalho et al. 2012), emphasizing the importance of microbiota in regulating metabolic disease outcomes.

Conventionalization of GF animals using one or more microbial species provides great insight into the effect of these species on host-physiology. For example, conventionalization of GF animals with a full cohort of microbiota from an obese human or mouse induces more weight gain and insulin resistance than when conventionalized with microbiota from lean individuals(Turnbaugh et al. 2008). Similarly, monocolonization studies have shed light on the role of the innate and adaptive immune system(Duan et al. 2010; D. Kim et al. 2016), both of which demonstrate the role of microbiota in host physiology.

GF rodents have substantially altered intestinal physiology. Morphologically, rodents lacking microbiota have reduced IE renewal, increased passage rate, reduced IEC migration, shorter villi, longer microvilli, and reduced surface area, though some regional differences have been reported(Khoury et al. 1969; Gordon and Pesti 1971; Clarke 1975; Abrams 1977). Because microbiota are important in the conversion of primary bile acids, it is no surprise that GF animals have reduced secondary bile acids within the ileum, despite having greater total levels of bile acids(Wostmann 1973; Wostmann 1996). In other GF mammals, increased numbers of Goblet cells have been reported relative to conventionalized or conventionally-raised counterparts. GF mice have also been shown to have increased mucin production(Wostmann 1996). Elevated levels of hormones, including peptide YY and enteroglucagon, have been observed in GF animals, as well as increased numbers of EECs(Uribe et al. 1994; Arantes and Nogueira 1997), though this may be diet dependent(Sharma and Schumacher 1996). Nutrient absorption is also altered: GF animals better absorb calcium and magnesium(Reddy 1972), exhibit reduced intestinal tyrosine(Lifshitz et al. 1978) and cholesterol absorption, and increased sterol excretion(Zhong et al. 2015). Moreover, GF mice have impaired mucosal barrier function(Hernández-Chirlaque et al. 2016 Apr 26). In sum, GF animals show altered

proliferation, differentiation, nutrient absorption, and hormone secretion, most of which is rescued upon conventionalization.

The role of miRNAs in responding to microbiota in the intestine is very poorly characterized. Interestingly, mice deficient for miRNAs show some similar phenotypes as GF animals, suggesting that perhaps miRNAs contribute to some of the microbiota-driven effects on intestinal physiology. For example, mice with inducible whole body knockout of *Dicer1*, a key enzyme in miRNA biogenesis pathway (Figure 1.2), undergo severe GI distress days after homozygous deletion, leading to death. Histological analyses of their intestines revealed distorted and disorganized IE morphology and lipid accumulation in small intestine enterocytes, which corresponds to the dysregulation of small intestinal proteins involved in fatty acid and triglyceride metabolism in these mice(T.-C. Huang et al. 2012). In IEC-specific *Dicer1* knockout mice, crypt-villus architecture is disorganized, and mice have impaired barrier function and infiltration of immune cells into the lamina propria and reduced numbers of Goblet cells and mucin production(McKenna et al. 2010; Biton et al. 2011; Yoshikawa et al. 2013). These mice show reduced growth, impaired intestinal barrier function(McKenna et al. 2010; Biton et al. 2011; S. Liu et al. 2016), and altered gut microbiota composition(S. Liu et al. 2016). Interestingly, mice heterozygous for IEC-specific *Dicer1* deletion, but not homozygous deletion, show elevated risk for tumor development in a colitis-associated tumor mouse model, though no change in inflammation is observed(Yoshikawa et al. 2013). IEC-specific *Dicer1* knockout mice have increased apoptosis in the crypt zone(McKenna et al. 2010; Nakato et al. 2016), unusual proliferation near the top of the crypt-villus junction(McKenna et al. 2010), and an overall elevated rate of cellular migration(McKenna et al. 2010), all of which suggest that miRNAs are key players in the regulation of IE proliferation, differentiation, migration, and function.

Moreover, given the similarities that can be drawn between GF and miRNA-deficient mice, it is possible that miRNAs mediate communication between gut microbes and the host epithelium.

In this dissertation, I explore miRNAs as biomarkers and drivers of hepatic and intestinal physiology and disease (Figure 1.1C). As miRNAs are important signaling and gene regulatory molecules that have therapeutic potential, understanding their expression and action in key metabolic tissues of relevance is of critical importance. Leveraging the power of cell culture lines, mouse and human patient samples, with *in silico*, *in vitro*, *ex vivo*, and *in vivo* approaches, I make important contributions to the understanding of hepatic and intestinal miRNAs in health and disease. Both the liver and intestine play key roles in maintaining systemic energy homeostasis. The liver responds to circulating hormones and molecular ligands by modulating gluconeogenic, lipogenic, and glucogenolytic pathways. In Chapter 2, I evaluate miR-29, a biomarker of type 2 diabetes, as a regulator of hepatic insulin-responsive and lipogenic pathways. Recently, the contribution of intestinal microbiota in regulating metabolic disease has gained wider appreciation. The intestine, and specifically the IE, provides a barrier between enteric bacteria, food and other ingested material, and the rest of the body. Importantly, it also is responsible for nutrient absorption, gluconeogenesis, release of hormones and other signaling molecules in response to luminal stimuli (including diet), and communicating with the gut microbiota. Yet, little is understood about the role of miRNAs in regulating these fundamental processes in the intestine. To work toward addressing this limitation, I profile miRNAs in colonic mucosa to identify potential tissue biomarkers and prognostic indicators of CD in Chapter 3, evaluate the role of miR-30 in regulating key intestinal physiological processes in Chapter 4, and in Chapter 5, profile the intestinal epithelial miRNA landscape, and determine whether and how miRNAs respond to dietary and microbial stimuli in the IE. Combined, this

interdisciplinary dissertation research lays the groundwork for understanding the role of miRNAs in the IE as both drivers of physiological processes, and also as signaling molecules mediating communication between the host and gut microbiota.

CHAPTER 2 – MICRORNA-29 FINE-TUNES THE EXPRESSION OF KEY FOXA2-ACTIVATED LIPID METABOLISM GENES AND IS DYSREGULATED IN ANIMAL MODELS OF INSULIN RESISTANCE AND DIABETES[*]

Type 2 diabetes is characterized in part by resistance to insulin action in the liver and other metabolic tissues(Kadowaki 2000). MicroRNAs (miRNAs) are widely recognized as important regulators of a diverse array of biological processes(Bartel 2009), including metabolism(W. Kim and Kyung Lee 2012). Recently, miRNAs have also emerged as stable plasma biomarkers of physiologic and metabolic status(P.S. Mitchell et al. 2008; Karolina et al. 2012), etiological factors in complex disease(Couzin 2008 Mar 28), and promising therapeutic targets(Jackson and A.A. Levin 2012; van Rooij et al. 2012). miRNA-mediated gene regulation occurs principally at the post-transcriptional level and has been the subject of intense research over the past decade. Several miRNAs have been implicated in the pathobiology of a variety of metabolic disorders, including type 2 diabetes(Fernandez-Valverde et al. 2011), cardiovascular disease(Quiat and Olson 2013), and obesity(Williams and G.M. Mitchell 2012). We reported that miR-27b is a post-transcriptional regulatory hub in liver lipid metabolism and is altered in dyslipidemia(Vickers et al. 2013). Another group of studies demonstrated that miR-33 modulates lipoprotein metabolism in mice(Horie et al. 2010; Marquart et al. 2010; Najafi-Shoushtari et al.

[*] Portions of this chapter previously appeared as a journal article in *Diabetes*. The original citation is as follows: *Kurtz, C. L., *Peck, B. C. E., Fannin, E. E., Beysen, C., Miao, J., Landstreet, S. R., Ding, S., Turaga, V., Lund, P. K., Turner, S., Biddinger, S. B., Vickers, K. C., and Sethupathy, P. (2014) MicroRNA-29 fine-tunes the expression of key FOXA2-activated lipid metabolism genes and is dysregulated in animal models of insulin resistance and diabetes. *Diabetes*. **63**, 3141–3148. http://doi.org/10.2337/db13-1015
**Denotes co-first authorship.*

2010; Rayner et al. 2010; Rayner, Sheedy, et al. 2011) and non-human primates(Rayner, Esau, et al. 2011), as well as insulin signaling in cultured human hepatocytes(Dávalos et al. 2011). Most recently, both miR-103/107 and miR-802(Kornfeld et al. 2013) were shown to regulate insulin sensitivity and glucose tolerance in mice(Trajkovski et al. 2011; Kornfeld et al. 2013). These findings strongly support the notion that miRNAs are critical players in pathways that underlie metabolic disease etiology, thus raising the possibility that miRNA-based therapy could be relevant for type 2 diabetes and related metabolic syndromes.

miR-29 has been demonstrated to be an important regulator of numerous biological processes, including neuronal maturation(Kole et al. 2011), fibrosis(van Rooij et al. 2008)3, hematopoiesis(Han et al. 2010), replicative senescence(Martinez et al. 2011), and immune response(Ma et al. 2011). Our recent *in silico* work identified miR-29 as the strongest candidate miRNA regulatory hub in the type 2 diabetes gene network(Baran-Gale et al. 2013). Other groups have shown that miR-29 is highly responsive to glucose and may regulate β-cell proliferation and insulin secretion(Pullen et al. 2011; Bagge et al. 2012). We sought to investigate miR-29 in the liver, which is a metabolic tissue of critical relevance to type 2 diabetes etiology.

In this study, we demonstrate that: 1) hepatic miR-29 and *Foxa2* mRNA are significantly up-regulated in two different animal models of insulin resistance; 2) the insulin-sensitizing drug Pioglitazone corrects hepatic miR-29 and *Foxa2* levels in the Zucker Diabetic Fatty (ZDF) rat model of diabetes; 3) miR-29 levels in hepatocytes are controlled in part by the insulin-regulated transcription factor FOXA2; and 4) miR-29 fine-tunes FOXA2-mediated regulation of key lipid metabolism genes. Taken together, our findings implicate miR-29 as an important regulatory factor for lipid homeostasis and motivate future studies to investigate the utility of miR-29 as a

tissue biomarker of type 2 diabetes drug efficacy, as well as a potential therapeutic target in metabolic syndromes.

Research Design and Methods

Animal studies

Female C57BL/6J mice were from a UNC Chapel Hill colony and started at 4 weeks of age on high-fat diet (D01060502, 45% kcal from fat) or matched low-fat diet (D01060501, 10% kcal from fat) (Research Diets, New Brunswick, NJ). Livers were isolated after 16 weeks of diet and RNA was isolated using the Norgen Total RNA Purification kit (Thorold, ON, Canada). Male Zucker Diabetic Fatty (ZDF) rats (Charles River, Wilmington MA) were acclimated for two weeks and had access to a standard chow diet (Lab Diet). Four weeks of Pioglitazone treatment (30 mg/kg/day) started at 8 weeks of age. Blood was collected once per week during treatment in order to measure glucose levels. Livers were isolated at 12 weeks of age and RNA was isolated using TRiZol.

Cell culture

Huh7 cells (human hepatoma) were obtained from Dr. Stanley Lemon's laboratory at UNC Chapel Hill. Huh7 cells were maintained in 5 mM glucose DMEM (Sigma-Aldrich, St. Louis, MO) supplemented with 10% FBS, 2 mM L-glutamine, 1 mM Na-pyruvate and 1X NEAA (Invitrogen, Grand Island, NY), in 100 mm collagen 1 coated cell culture dishes (Becton-Dickinson, Bedford, MA). For transfections, cells were split into 6-well collagen-1 coated plates (Becton-Dickinson) to approximately 70-80% confluency and allowed 24 hours to adhere. All cells were cultured in a humidified incubator at 37^{o}C and 5% CO_2.

Transfection studies

Huh7 cells were plated on collagen-1-coated 6-well plates (Becton-Dickinson, Bedford, MA) 1 day before transfection. At ~70-80% confluency, the cells were transfected with either 10 ηM miRIDIAN hsa-miR-29a mimic (ThermoScientific; Waltham, MA), 10 ηM mmu-miR-29a-3p LNA inhibitor (Exiqon; Woburn, MA), or 100 ηM ON-TARGET plus human siRNA against FOXA2 (ThermoScientific; Waltham, MA) using either Dharmafect 4 (ThermoScientific; Waltham, MA) or Lipofectamine 2000 (Life Technologies, Grand Island, NY) transfection reagent. A human FOXA2 expression vector containing FOXA2 transcript variant 1 in the pCMV6-XL5 plasmid (Origene, Rockville, MD) was transfected (1 μg) using Dharmafect Duo transfection reagent (ThermoScientific; Waltham, MA). Forty-eight hours after transfection, total RNA was isolated from the cells using the Total RNA Purification Kit from Norgen (Thorold, ON, Canada).

Small RNA-sequencing analysis

Total RNA was extracted from mouse liver tissue using the Norgen total RNA purification kit (Norgen; Thorold, ON, Canada). RNA quality was assessed by Agilent 2100 Bioanalyzer, and only very high quality samples with RNA Integrity Number (RIN) above 8.0 were considered further. Small RNA libraries (n = 2 for each of HFD-fed and LFD-fed mice) were generated using the Illumina TruSeq small RNA library preparation kit. These libraries were then sequenced on the Illumina HiSeq 2000 platform (50 bp reads). miRNA and isomiR identification and quantitation was performed as described previously(Baran-Gale et al. 2013).

Gene expression (RNA) analysis

Total RNA was isolated from cultured Huh7 cells or mouse liver tissue using the Total

RNA Purification kit (Norgen; Thorold, ON, Canada), and subject to DNase treatment using the TURBO DNA-free kit (Applied Biosystems; Grand Island, NY). Complementary DNA (cDNA) was synthesized using either the TaqMan microRNA Reverse Transcription kit (Applied Biosystems; Grand Island, NY) or the High Capacity RNA to cDNA kit (Applied Biosystems; Grand Island, NY) according to the manufacturer's instructions. Quantitative real-time PCR amplification was performed using TaqMan miRNA or gene expression assays in TaqMan Universal PCR Master Mix (miRNA qPCR) or TaqMan Gene Expression Master Mix (gene expression qRT-PCR) on a BioRad CFX96 Touch Real Time PCR Detection system (Bio-Rad Laboratories, Inc., Richmond, CA). Reactions were performed in triplicate using either *U6* (miRNA expression) or *RPS9* (gene expression) as the internal control. miRNA and mRNA levels were expressed as relative quantitative values (RQVs). All TaqMan assays used in this study where purchased from Applied Biosystems, Inc. (Grand Island, NY) and include: miR-29a (4427975, 002112), miR-29b (4427975, 000412), miR-29c (444087, 000587), miR-15a (4427975, 000389), *U6* (4427975-001973), *RPS9* (human – 4331182, Hs02339424_g1; mouse – 4331182, Mm00850060_s1), *ABHD5* (4331182, Hs01104373_m1), *HMGCS2* (4331182, Hs00985427_m1), *G6PC* (human – 4331182, Hs00609178_m1; mouse – 4331182, Mm00839363_m1), *PPARGC1A (*4331182, Hs01016719_m1), and *FOXA2* (human – 4331182, Hs00232764_m1; mouse – 4331182, Mm01976556_s1; rat – 4331182, Rn0145600_m1).

Western blotting

Protein was isolated forty-eight to seventy-two hours after transfection. RIPA buffer (Sigma Aldrich, St. Louis, MO), supplemented with complete protease inhibitor (Roche, Indianapolis, IN), phosphatase inhibitor (ThermoScientific, Waltham, MA), 100 mM PMSF in 100% isopropanol, 0.1% beta-mercaptoethanol (VWR International, Radnor, PA) and 1 mM

DTT (Fisher Scientific, Pittsburgh, PA) was used to passively lyse adhered cells. The lysate was collected and flash frozen before clarification by centrifugation. Protein concentration was calculated using the Pierce® Microplate BCA Protein Assay Kit – Reducing Agent Compatible (ThermoScientific, Waltham, MA) and run on an Any kD™ Mini-Protean TGX™ precast gel (Bio-Rad; Hercules, CA). Transfer was conducted using Bio-Rad Midi Transfer Packs on the Bio-Rad Trans-Blot® Turbo Blotting System. The membranes were blocked in 5% non-fat dry milk (Sigma-Aldrich, St. Louis, MO) in TBST and probed with 1:800 anti-ABHD5 antibody (Abnova, Cat# H00051099-M01, Taiwan) in 4% BSA (Applied Biosystems, Cat# AM2616) in TBST. Goat anti-rabbit secondary antibody (Abcam, Cat# ab131366) was diluted 1:3,000 in 1% milk/TBST. β-actin peroxidase (Sigma-Aldrich, St. Louis, MO, Cat# A3854) or GAPDH (Cell Signaling; Danvers, MA, Cat# 8884s) diluted 1:40,000 in 1% milk/TBST were used as controls. Signal was detected using the Amersham™ ECL™ Prime Western Blotting Detection Reagent (GE Healthcare Life Sciences; Piscataway, NJ) following manufacturer instructions and exposed using the LiCor C-DiGit Blot scanner (LiCor, Lincoln, NE). Signal intensity was determined by densitometry using LiCor Biosciences Image Studio Software.

Reporter gene (Luciferase) assays

Human embryonic kidney 293T (HEK293T) cells were plated at $1x10^5$ cells/mL for 24 hours prior to transient transfection using DharmaFect 4 and 500 ηg/mL MT01 Firefly/Renilla luciferase reporter with the entire 3' UTR of *HMGCS2* cloned immediately downstream of Firefly luciferase (Genecopoeia). Cells were dual transfected with 10 ηM of miR-29a mimic for 48 hours prior to cell lysis and dual luciferase assays (Genecopoeia). Site-directed mutagenesis was completed using QuickChange II XL kits (Stratagene) and the following primers – Reverse 5'-agccgttgcaccgtcaggcacaggg-3' and Forward 5'-ccctgtgcctgacggtgcaacggct-3'. A 3 base deletion

was created in the middle of the predicted "seed" target site for miR-29 (…tgcctgacggt**ggt**gcaacggctgatgga…).

Bioinformatics

ChIP-seq data for Foxa2 in mouse liver and islet were published previously(Hoffman et al. 2010). Chromatin occupancy sites based on these ChIP-seq data were obtained directly from the lead author of the study (Brad Hoffman, University of British Columbia). Candidate Foxa2 target genes in mouse liver and islet were assembled by cross-referencing the chromosomal locations of Foxa2 occupancy sites with gene promoter regions (defined as windows 5 kb upstream of transcription start sites as annotated in the RefSeq database). The miR-29ab promoter region was identified as recently described(Sethupathy 2013). Target site prediction for miR-29 was performed with TargetScan 6.2 (downloaded from http://targetscan.org). Statistical enrichment of predicted miR-29 target sites among Foxa2 target genes in the mouse liver and islet was assessed according to our recently published method, mirHub(Baran-Gale et al. 2013), using the "non-network" mode and requiring a predicted target site to be conserved among at least three mammalian species including mouse.

Results

Hepatic miR-29 is up-regulated in animal models of insulin resistance and is corrected by treatment with the insulin-sensitizing drug Pioglitazone

To determine if hepatic miR-29 levels are altered in the insulin resistant state, we investigated two different animal models of metabolic dysfunction. First, we studied female C57BL/6J mice placed on a 16-week high-fat diet (HFD; 45% kcal from fat), which resulted in

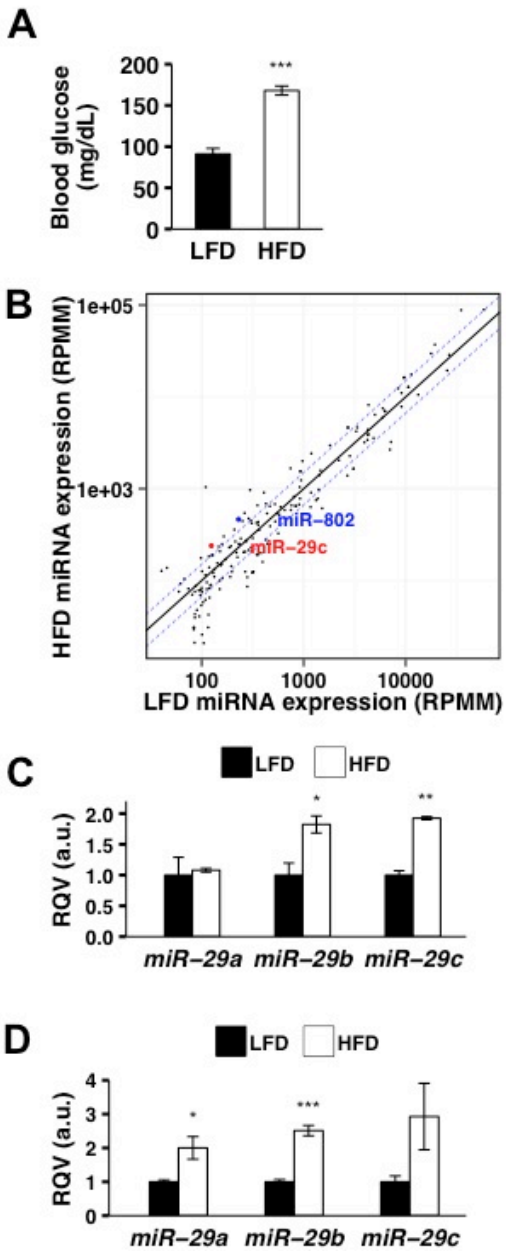

Figure 2.1. Hepatic miR-29 levels are upregulated in diet-induced insulin resistance in mice. (A) Fasting blood glucose levels of C57BL/6J female mice on HFD for 16 weeks (n = 3) and matched LFD for 16 weeks (n = 3) are shown. (**B**) miRNA expression levels (RPMM, reads per million mapped reads) based on deep sequencing analysis of small RNAs from the livers of HFD-fed (n = 2) and LFD-fed (n = 2) C57BL/6J female mice are shown. Each circle represents a miRNA that is expressed at RPMM >100 in at least one murine liver sample. Dashed blue lines represent 1.5-fold difference in expression between HFD-fed and LFD-fed mice. (**C**) Relative levels (based on sequencing) of miR-29a, miR-29b, and miR-29c in the livers of HFD-fed (n = 2) and LFD-fed (n = 2) C57BL/6J female mice are shown. (**D**) Relative levels (based on qRT-PCR) of miR-29a, miR- 29b, and miR-29c in the livers of HFD-fed (n = 3) and LFD-fed (n = 3) C57BL/6J female mice are shown. P-values were calculated according to the one-tailed unpaired Student t test. a.u., arbitrary unit. *$p < 0.05$; **$p < 0.01$; ***$p < 0.001$.

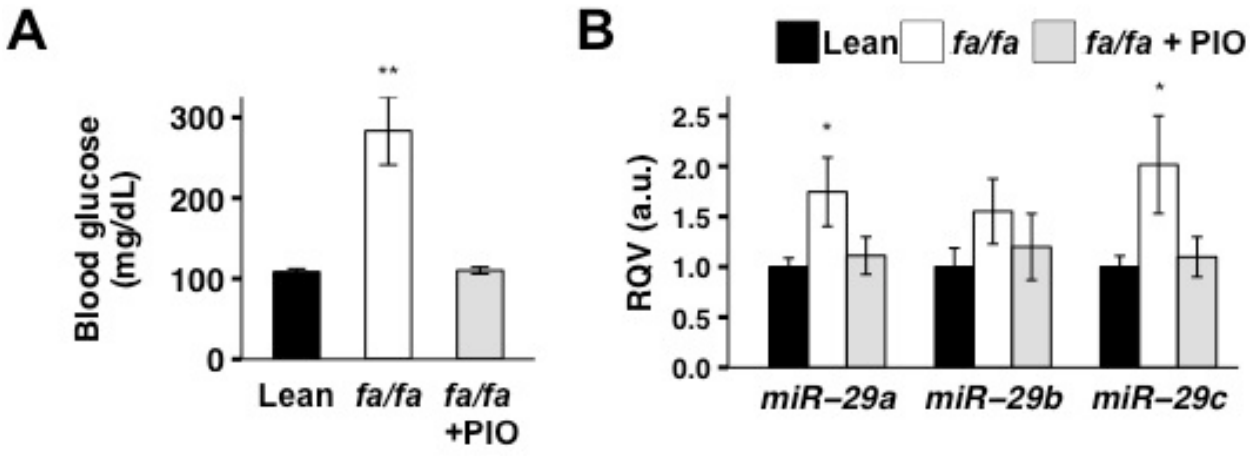

Figure 2.2. Hepatic miR-29 levels are elevated in a rat model of diabetes and corrected by treatment with the insulin-sensitizing drug pioglitazone (PIO). Fasting blood glucose levels (**A**) and relative hepatic levels (based on qRT-PCR) of miR-29a, miR-29b, and miR-29c (**B**) in 12-week-old healthy male rats (n = 8), ZDF fa/fa male littermates (n = 11), and pioglitazone-treated (4 weeks) ZDF fa/fa male rats (n = 6) are shown. P-values were calculated according to the one-tailed unpaired Student t test. a.u., arbitrary unit. *$p < 0.05$; **$p < 0.01$.

significantly elevated (~1.8-fold; $p < 0.001$) fasting blood glucose levels relative to age-, gender- and strain-matched mice on low-fat diet (LFD; 10% kcal from fat) (Figure 2.1A). We performed deep sequencing of liver small RNAs and found that miR-29b (~1.8-fold, $p < 0.05$) and miR-29c (~1.9-fold, $p < 0.001$) were significantly elevated in HFD-fed mice (Figure 2.1B & C, Supplementary Table 2.1[†]), matching the fold increase in miR-802 (Figure 2.1B, Supplementary Table 2.1[2]), which was previously identified as a critical mediator of obesity-induced glucose intolerance(Kornfeld et al. 2013). To validate this finding, we performed real time quantitative PCR (qRT-PCR) and confirmed that hepatic levels of miR-29 were significantly increased in HFD-fed mice (Figure 2.1D).

Next, we examined the Zucker Diabetic Fatty (ZDF) *fa/fa* rat model, which closely

[†] Supplementary Table 2.1 is available online at http://diabetes.diabetesjournals.org/lookup/suppl/doi:10.2337/db13-1015/-/DC1

mimics human adult onset diabetes(Yokoi et al. 2013). We showed that, as expected, fasting blood glucose levels

were significantly elevated (~2.5-fold, $p < 0.005$) in 12-week old male obese *fa/fa* rats compared to age- and gender-matched lean healthy littermates (Figure 2.2A). We then demonstrated by qRT-PCR that hepatic miR-29a and miR-29c levels were significantly ($p < 0.05$) higher for the *fa/fa* rats compared to the lean littermate controls (Figure 2.2B). Strikingly, we also observed that treatment with the insulin-sensitizing drug Pioglitazone for four weeks, which markedly improved glycaemia (Figure 2.2A), reduced hepatic miR-29 expression to levels comparable to that of the lean controls (Figure 2.2B).

Hepatic miR-29 expression is controlled in part by the insulin-regulated transcription factor FOXA2

To investigate the molecular mechanism(s) that mediate the up-regulation of miR-29 in insulin resistance, we sought to identify hepatic transcription factors (TFs) regulated by insulin signaling that could be involved in the control of miR-29 expression. First, we identified the transcription start sites (TSS) of miR-29a/b-1 (chromosome 7) and miR-29b-2/c (chromosome 1) in human hepatoma cells (HepG2) by analyzing chromatin data from ENCODE using our previously described bioinformatic pipeline(Sethupathy 2013). This strategy revealed that the most proximal active TSS for miR-29a/b-1 is ~36.5 kb upstream of the mature miR-29a sequence and for miR-29b-2/c is ~20kb upstream of the mature miR-29c sequence. We scanned these regions for areas of open chromatin and TF occupancy in HepG2 cells, as determined by ENCODE, and found >10 binding sites for FOXA2 at the miR-29a/b-1 locus and 4 binding sites at the miR-29b-2/c locus (Figure 2.3A). FOXA2 is negatively regulated by insulin(Yoon et al. 2001; Wolfrum et al. 2004), and opposes insulin action(Puigserver and Rodgers 2006) by

promoting hepatic lipid catabolism and fatty acid oxidation(Wolfrum and Stoffel 2006). To further support the finding in HepG2 cells, we mined a recently published TF ChIP-seq dataset from adult mouse liver(Hoffman et al. 2010) and detected Foxa2 chromatin occupancy at the mouse miR-29 promoter regions (data not shown).

We next performed real time quantitative PCR and observed that hepatic *Foxa2* mRNA levels were increased in both HFD-fed mice (Figure 2.3B) and diabetic *fa/fa* rats ($p < 0.05$; Figure 2.3C). Moreover, as with miR-29 (Figure 2.3D), hepatic *Foxa2* expression in the *fa/fa* rats returned to that of the lean controls upon treatment with Pioglitazone (Figure 2.3C). To more directly evaluate the potential for FOXA2 to regulate hepatic miR-29 levels, we performed siRNA-mediated knockdown of *FOXA2* in Huh7 cells. After 48 hours of siRNA treatment, *FOXA2* mRNA was significantly reduced ($p < 10^{-12}$; Figure 2. 3D). Under these conditions, we observed an almost 2-fold down-regulation of miR-29a ($p < 0.001$), miR-29b ($p < 0.05$), and miR-29c ($p < 0.01$; Figure 2. 3D). We also transiently transfected Huh7 cells with a FOXA2 expression vector (1 μg), which led to a ~172-fold up-regulation in *FOXA2* mRNA levels ($p < 0.05$), and a concomitant >2-fold increase in miR-29a ($p < 0.05$), miR-29b ($p = 0.06$), and miR-29c ($p < 0.05$). Collectively, these data suggest that the insulin-regulated FOXA2 is a transcriptional activator of miR-29.

miR-29 fine-tunes FOXA2 mediated regulation of key hepatic lipid metabolism genes

Recent studies of GRNs indicate that coordinated regulation by TFs and miRNAs confer robustness against environmental fluctuation(Osella et al. 2011). We assembled a list of high-

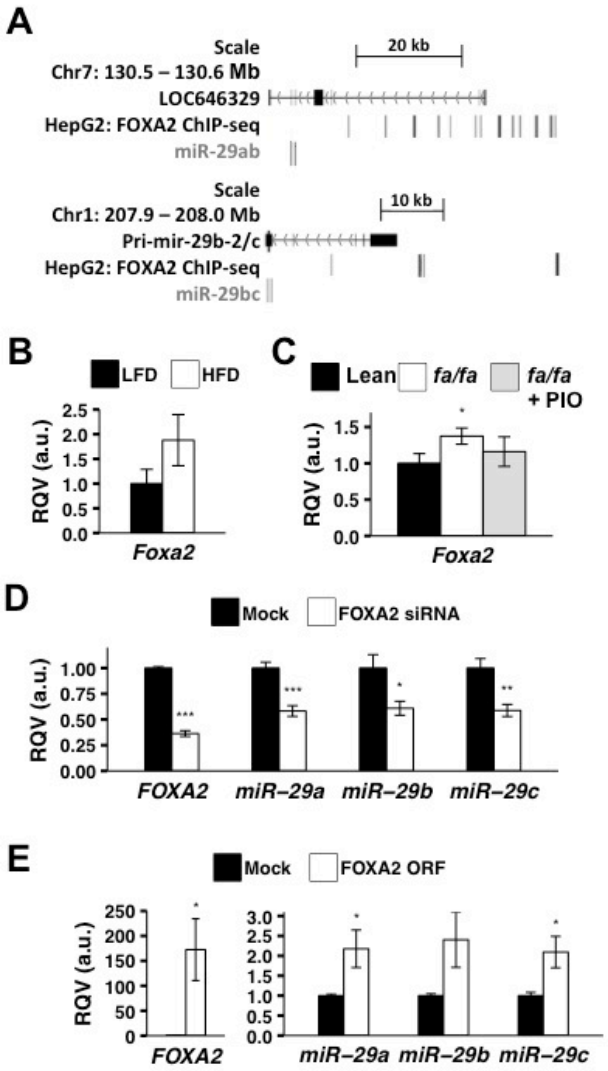

Figure 2.3. FOXA2 regulates miR-29 expression. (**A**) FOXA2 occupancy in HepG2 at the miR-29ab and miR-29b-2/c genomic loci are shown (based on ENCODE ChIP-seq data). LOC646329 represents the putative primary transcript of miR-29a and miR-29b-1 on chromosome 7 and Pri-miR-29b-2 represents the putative primary transcript of miR-29b-2 and miR-29c on chromosome 1. (**B**) Relative levels of Foxa2 mRNA in the livers of C57BL/6J female mice on HFD for 16 weeks (n = 3) and matched LFD for 16 weeks (n = 3) are shown. (**C**) Relative levels of Foxa2 mRNA in the livers of 16-week-old healthy male rats (n = 8), ZDF fa/fa male littermates (n = 11), and pioglitazone-treated (PIO) (4 weeks) ZDF fa/fa male rats (n = 6) are shown. (**D**) Effects of FOXA2-siRNA treatment (100 ηmol/L) in Huh7 cells on FOXA2 (mock, n = 14; siRNA, n = 13), miR-29a (mock, n = 12; siRNA, n = 12), and miR-29b and miR-29c (mock, n = 10; siRNA, n = 8) expression levels are shown. (**E**) Effects of FOXA2 open reading frame (ORF) overexpression plasmid (1 mg) in Huh7 cells on FOXA2 (mock, n = 6; plasmid, n = 5), miR-29a (mock, n = 6; plasmid, n = 5), miR-29b (mock, n = 5; plasmid, n = 4), and miR-29c (mock, n = 6; plasmid, n = 5) are shown. All transfections were conducted in triplicate and results were validated by at least two independent experiments. P-values were calculated according to the two-tailed unpaired Student t test. a.u., arbitrary unit. *$p < 0.05$; **$p < 0.01$; ***$p < 0.001$.

confidence hepatic target genes for Foxa2 from a published ChIP-seq study in mouse liver (Methods). We then determined, using our previously published method mirHub(Baran-Gale et al. 2013), that the Foxa2 mouse liver target gene set was significantly enriched for predicted miR-29 target sites (Figure 2.4A). Notably, we did not observe this enrichment among Foxa2 target genes in the mouse pancreatic islet, in which the Foxa2 regulatory network is re-wired relative to the liver(Hoffman et al. 2010) (Figure 2.4A). To evaluate further the predicted FOXA2-miR-29 feed-forward circuit, we experimentally tested three specific instances of the circuit with the genes *HMGCS2*, *ABHD5*, and *PPARGC1A*, which encode proteins that activate the enzymatic breakdown of fat in the liver(Vilà-Brau et al. 2011; Lord et al. 2012). The mRNA levels of all three genes in Huh7 cells were significantly ($p < 0.01$) increased by the miR-29a locked nucleic acid (LNA) inhibitor and significantly ($p < 0.05$) reduced by the miR-29a mimic (Figure 2.4B). Consistent with this observation, the protein levels of ABHD5 were also significantly ($p < 0.05$) up-regulated by the miR-29a LNA inhibitor after 48 hours (Figure 2.4C). Also, to determine whether miR-29 regulation of *HMGCS2* is mediated through the 3' UTR, we performed a reporter gene assay (Methods). Over-expression of the miR-29a mimic (100 ηM) in HEK293T cells significantly reduced ($p < 0.01$, ~65% loss) relative Firefly luciferase activity when the *HMGCS2* 3' UTR was inserted downstream of the *Firefly* reporter gene (Figure 2.4D). Moreover, targeted deletion (3 bp) of the predicted miR-29 target site in the *HMGCS2* 3' UTR substantially mitigated the repressive effect of miR-29 on *Firefly* activity (Figure 2.4D). Finally, siRNA-mediated knockdown of FOXA2 led to a significant ($p < 0.01$) decrease in the expression of *HMGCS2*, *ABHD5*, and *PPARGC1A* (Figure 2.4E). The latter observation suggests that FOXA2 is the primary driver of the expression levels of its target genes, whereas miR-29 serves as a feed-forward negative modulator (Figure 2.5).

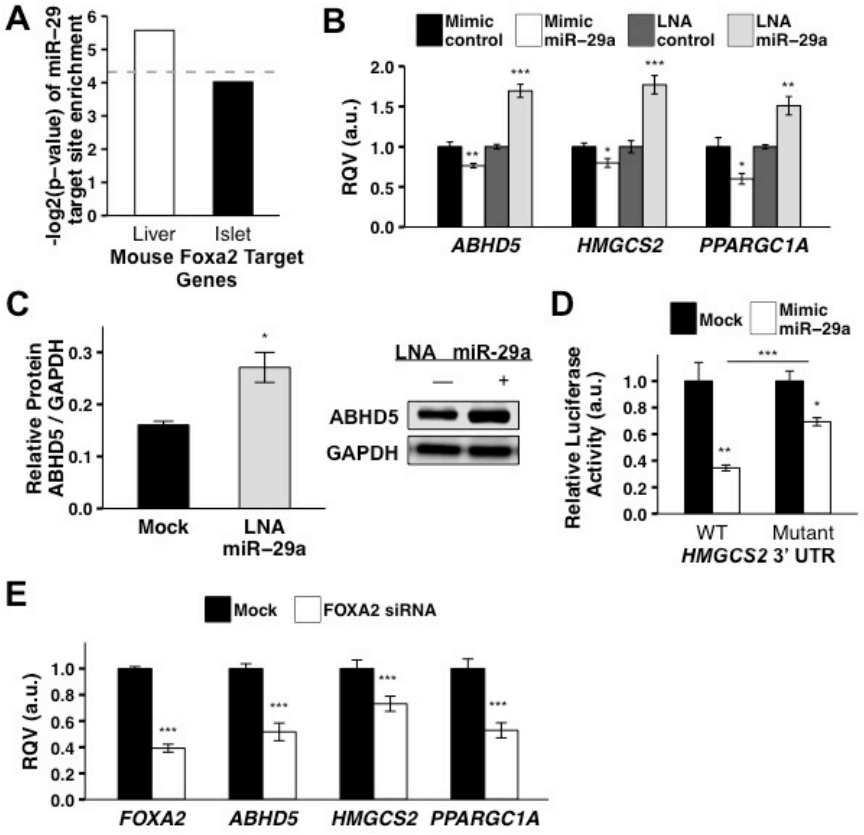

Figure 2.4. miR-29 fine-tunes FOXA2-mediated regulation of key lipid metabolism genes. (**A**) Significant enrichment of predicted miR-29 target sites among FOXA2-bound genes in mouse liver but not in mouse islet is shown. Dashed line reflects p = 0.05. (**B**) Effects of the miR- 29a mimic (10 ηmol/L) and the miR-29a LNA inhibitor (10 ηmol/L) in Huh7 cells on the mRNA levels of FOXA2-bound genes ABHD5 (mimic, n = 8; LNA, n = 6), HMGCS2 (mimic, n = 7; LNA, n = 7), and PPARGC1A (mimic, n = 7; LNA, n = 7) are shown. (**C**) Effect of the miR-29a inhibitor (LNA, 10 ηmol/L) in Huh7 cells on protein levels of ABHD5 is shown (mock, n = 3; LNA, n = 3). (**D**) Effects of the miR-29a mimic (100 ηmol/L) in HEK293T cells on the relative activity of Firefly reporter constructs containing either wild-type or mutated HMGCS2 3'UTR are shown. Firefly activity was normalized to Renilla activity. (**E**) Effects of FOXA2-siRNA treatment (100 nηol/L) in Huh7 cells on mRNA levels of ABHD5 (mock, n = 10; siRNA, n = 10), HMGCS2 (mock, n = 10; siRNA, n = 9), and PPARGC1A (mock, n = 8; siRNA, n = 4) are shown. P-values were calculated according to the two-tailed unpaired Student t test. a.u., arbitrary unit. *p < 0.05; **p < 0.01; ***p < 0.001.

Discussion

This study leveraged *in vivo, in vitro, and in silico* analyses to uncover a role for miR-29 as a potentially critical regulator of hepatic metabolic pathways. A prior study suggested that miR-29 is significantly elevated in the livers of the diabetic mouse model *db/db*(Pandey et al.

2011); however, to our knowledge this result had not been validated in other models. We showed in this study that liver miR-29 levels are elevated in two different animal models of metabolic dysfunction, and notably, are returned to normal levels upon treatment with an insulin sensitizer, Pioglitazone, in the ZDF diabetic rat. This finding signals the possibility that miRNAs could serve as tissue biomarkers of drug efficacy in type 2 diabetes.

Two recent miRNA profiling studies reported that type 2 diabetes might be associated with reduced levels of plasma miR-29(Zampetaki et al. 2010; Kong et al. 2011). We observe in this study that miR-29 is elevated in the liver of animals with insulin resistance and diabetes. The apparent inverse correlation between plasma and liver miR-29 levels in type 2 diabetes is intriguing. It is now widely appreciated that miRNAs are stably present in circulation and are transported by a variety of different types of extracellular vehicles (EVs), including exosomes and high-density lipoproteins(Arroyo et al. 2011; Creemers et al. 2012; Vickers and Remaley 2012; Boon and Vickers 2013; Turchinovich et al. 2013). Several studies have shown that numerous cell types secrete miRNAs, which can then be loaded onto EVs and delivered to recipient cells with functional integrity(Mittelbrunn et al. 2011; Vickers et al. 2011; Montecalvo et al. 2012). However, the mechanisms that regulate intercellular miRNA transfer remain poorly characterized and it represents a nascent but promising topic of research. Progress in this area will be critical for understanding why liver miR-29 is elevated but plasma miR-29 is reduced in type 2 diabetes. miR-29 is highly expressed in numerous metabolic tissues, including the

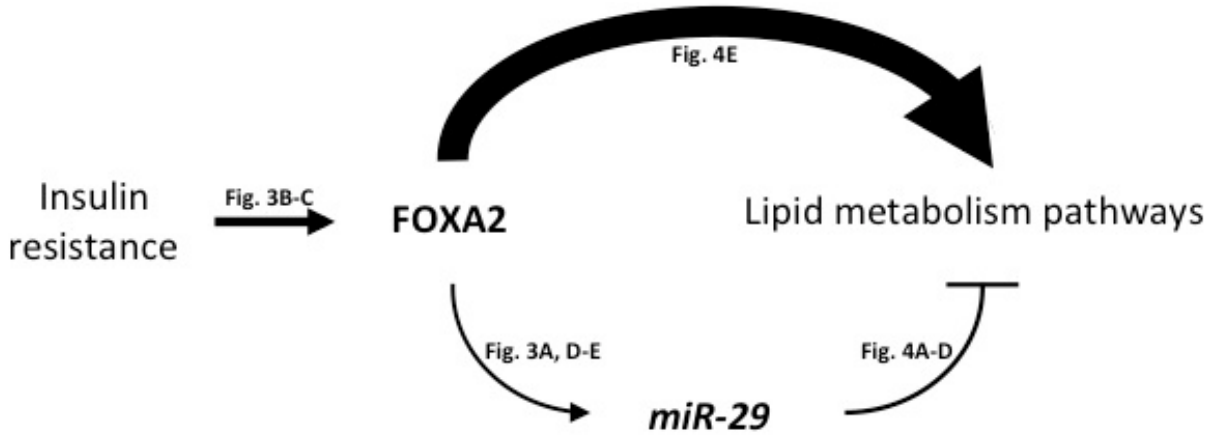

Figure 2.5. Schematic of the FOXA2:miR-29 regulatory circuit in the liver. A possible model of FOXA2:miR-29 circuitry in the liver is shown. In the insulin-resistant state, FOXA2 activity is upregulated, which in turn elevates miR-29 levels. FOXA2 drives the expression of genes involved in lipid metabolism, and miR-29 acts as a feed-forward fine-tuner of many of the same genes.

pancreatic islet(Baran-Gale et al. 2013; van de Bunt et al. 2013), and the relative contribution of each of these tissues to circulating miR-29 remains to be determined and merits further investigation.

We also demonstrated in this study that hepatic miR-29 expression is likely controlled at least in part by the insulin-regulated transcription factor, FOXA2, which contains >10 ChIP-seq derived binding sites in human hepatoma cells at the miR-29ab genomic locus on chromosome 7 and 4 binding sites at the miR-29bc genomic locus on chromosome 1. The evaluation of the combinatorial effect of these binding sites on miR-29 transcription is not trivial; however, it certainly warrants further investigation in order to more definitively establish direct FOXA2-mediated regulation of miR-29. Moreover, future studies *in vivo* should establish the extent to which FOXA2 controls miR-29 during hepatic insulin resistance.

Finally, we showed that miR-29 serves as a dampener of FOXA2-mediated activation of key lipid metabolism genes. For example, FOXA2 transcriptionally activates *HMGCS2*, which in

turn is directly repressed by miR-29. It has been postulated that such TF:miRNA regulatory circuits, termed incoherent feed-forward loops, are likely important for noise-buffering of gene expression(Tsang et al. 2007; Osella et al. 2011; Siciliano et al. 2013). Further detailed studies *in vivo* may help elucidate the physiological importance of the FOXA2:miR-29 regulatory circuit in lipid homeostasis.

Overall, this study strongly suggests that miR-29 merits further investigation as a candidate biomarker of metabolic status and drug efficacy, an etiological factor in type 2 diabetes, and a potentially important therapeutic target for a range of metabolic disorders. Follow-up studies in the Sethupathy laboratory using a locked nucleic acid (LNA) against miR-29 family *in vivo* resulted in reduced plasma cholesterol and liver fatty acid content, suggested a strong role for miR-29 on lipogenesis in mice(Kurtz et al. 2015). However, a significant change was not observed in plasma glucose levels upon treatment with miR-29 inhibitor, though plasma insulin levels were reduced(Kurtz et al. 2015). Importantly, these initial studies were conducted in mice, and will need to be repeated in other models such as non-human primates to better predict their effect in humans.

Current treatment modalities for type 2 diabetes include pharmacotherpeutics such as Metformin, PIO or Rosiglitazone. However, both PIO and rosiglitazone have severe counter indications, as they are linked to increased risk of heart failure related death(Ahmadian et al. 2013) and do not prevent diabetes-related complications. Treatment with Metformin may lead to increased weight gain and hypoglycemia, and many doctors choose to supplement Metformin treatment with second-line anti-diabetic drugs, some of the most effective of which are GLP-1 receptor agonists (Zinman et al. 2009; Reusch et al. 2014). GLP-1 is a hormone secreted by intestinal epithelial enteroendocrine cells (EECs). Interestingly, Roux-en-Y gastric bypass

surgery, which bypasses a large portion of the small intestine, has been shown to rapidly improve type 2 diabetes. This recovery is likely due at least in part to increased intestinal gluconeogenesis(Troy et al. 2008) and jejunal leptin activity(Rasmussen et al. 2014). While the majority of studies focus on liver, adipose, and pancreatic islets in type 2 diabetes progression (Figure 2.6), these bariatric surgery studies emphasize the importance of the intestine as a metabolic organ and mediator of metabolic disease warranting further investigation.

The intestine is understudied as a metabolic organ, and the field lacks understanding of miRNA expression and function in the intestine during health and disease. To move towards bridging this gap in understanding, the remaining chapters seek to first establish intestinal miRNAs as biomarkers of a GI disease (Chapter 3), identify functional roles for miRNAs in regulating intestinal physiology (Chapter 4), and finally evaluate how environmental factors regulate miRNA expression and function in the IE (Chapter 5).

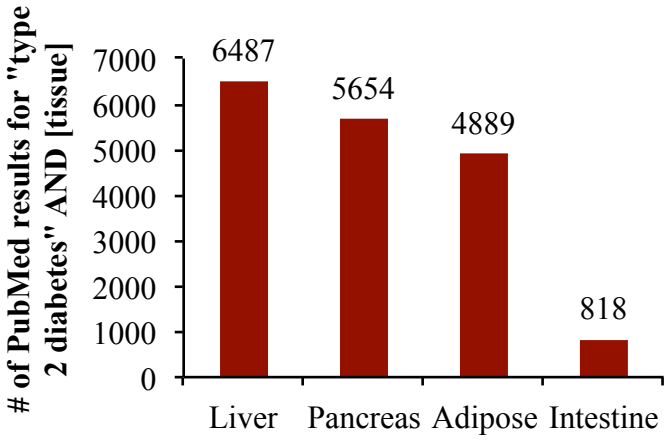

Figure 2.6. The intestine is an understudied metabolic organ. The number of PubMed search results are shown for the terms, “type 2 diabetes” AND [tissue]. Search was performed on 7/3/16.

CHAPTER 3 – MICRORNAS CLASSIFY DIFFERENT DISEASE BEHAVIOR PHENOTYPES OF CROHN'S DISEASE AND MAY HAVE PROGNOSTIC UTILITY*

Crohn's disease (CD) results from an aberrant immune response to the enteric microbiota in a genetically susceptible host. CD susceptibility genes identified through genome-wide association studies (GWAS) highlight mechanistic pathways. While many associated hits are found within innate immunity pathways, there are substantial overlap of GWAS hits for CD and type 1 and type 2 diabetes, including *CDKAL1*, *GCKR*, *THADA*, *IL2RA*, *IL10*, *PTPN2* and others(Lees et al. 2011), suggesting underlying common biology. Chronic inflammation is a risk factor for the development of type 2 diabetes(Dregan et al. 2014). Identifying biomarkers and potential therapeutic targets for CD and other chronic inflammatory diseases may provide insight into common disease pathogenesis and have substantial benefit for patients with metabolic diseases.

The innate immune system forms the first line of defense against pathogens and mediates mucosal responses to resident microbiota. Microbial recognition is initiated by pathogen-associated molecular patterns triggering extracellular receptors termed toll-like receptors or intracytoplasmic nucleotide-binding oligomerization domain-containing protein (NOD)-like

* Portions of this chapter previously appeared as a journal article in *Inflammatory Bowel Diseases*. The original citation is as follows: Peck, B. C. E., Weiser, M., Lee, S. E., Gipson, G. R., Iyer, V. B., Sartor, R. B., Herfarth, H. H., Long, M. D., Hansen, J. J., Isaacs, K. L., Trembath, D. G., Rahbar, R., Sadiq, T. S., Furey, T. S., Sethupathy, P., and Sheikh, S. Z. (2015) MicroRNAs Classify Different Disease Behavior Phenotypes of Crohn's Disease and May Have Prognostic Utility. *Inflammatory Bowel Diseases*. **21**, 2178–2187. http://doi.org/10.1097/MIB.0000000000000478

receptors. This leads to downstream signaling through pathways regulated by nuclear factor kappa-B, mitogen activated protein kinase, and interferons(Geremia et al. 2014).

A number of miRNAs have already been identified as regulators of pathways that underlie the pathogenesis of inflammatory bowel diseases (IBD), which includes CD and ulcerative colitis (UC). For example, miR-192, miR-122, miR-29 and miR-146a have been shown to target and repress *NOD2*, which has been implicated in CD(Brain et al. 2013; Y. Chen et al. 2013; Ghorpade et al. 2013; Chuang et al. 2014). Furthermore, a single nucleotide polymorphism (SNP), rs3135500, in the 3'UTR of *NOD2* weakens the miR-192 target site resulting in reduced inhibition of *NOD2*(Chuang et al. 2014). Another miRNA regulator of *NOD2* expression, miR-146a, has been shown to drive interleukin 6 (IL-6) and tumor necrosis factor (TNF) secretion in muramyl dipeptide (MDP) activated macrophages in experimental models of colitis(Ghorpade et al. 2013).

Recent studies have performed miRNA profiling in tissues of patients with IBD. Most of these studies used either microarray platforms(F. Wu et al. 2008; Fasseu et al. 2010; Takagi et al. 2010; F. Wu et al. 2010) or quantitative reverse transcriptase PCR (qRT-PCR)(Feng et al. 2012; Pekow et al. 2012; Z. Huang et al. 2014). These approaches are informative, but harbor at least three major limitations. First, they are limited to known miRNAs, and are therefore not sensitive to functionally distinct miRNA variants known as isomiRs. Second, they often cannot adequately distinguish among miRNAs in the same family that differ by only one or two nucleotides. Third, microarrays have low dynamic range, which mitigates the accuracy of differential miRNA expression analysis across samples, particularly for more lowly expressed miRNAs.

Small RNA-sequencing, while not without its own biases(Jayaprakash et al. 2011; Sorefan et al. 2012; Baran-Gale et al. 2013), ameliorates each of these three limitations. To our

knowledge, only one study has used this technology to investigate miRNAs in IBD(Lin, Cao, et al. 2013). In our study, we performed next-generation sequencing (NGS) of small RNAs (small RNA-seq) isolated from macroscopically non-inflamed colon tissue obtained from a set of extensively phenotyped patients with CD. We stratified the patients based on inflammatory, stricturing, or penetrating CD, and identified unique colonic miRNA signatures of each class. We also studied the effect of inflammation on miRNA expression through small RNA-seq of matched colon samples obtained from macroscopically inflamed regions from a subset of patients with CD. To determine disease-specificity of the inflammation effect, we used tissue samples from inflamed and non-inflamed regions of the colon in UC patients as controls. These studies revealed specific miRNAs that serve as colonic markers of distinct disease behaviors in CD. Furthermore, we reveal the potential prognostic utility of miRNAs in CD by demonstrating that miR-215 expression in index biopsies of well phenotyped patients with non-penetrating CD obtained at the time of diagnosis may predict progression to penetrating CD. Finally, using a statistical simulation strategy, we identified candidate miRNA drivers of the gene expression profiles associated with CD.

Research Design and Methods

Patient Population

Well-characterized CD patients from the adult IBD Center at University of North Carolina were included in this study. A total of 35 samples were submitted for small-RNA and

RNA-seq analyses (Supplemental Digital Content, Table 3.1[†]). For qRT-PCR validation, 15 Non-IBD controls as well as 20 CD and 6 UC patients were analyzed (Supplemental Digital Content, Table 3.2). In the prospective study, index biopsies from 10 NIBD control samples, 6 non-B3 CD patients, and 6 B3 patients were analyzed (Supplemental Digital Content, Table 3.3). This study received IRB approval at UNC Chapel Hill (Protocol #s 10-0355 & 15-0024).

Phenotyping

All data were collected by chart review and stored in a secured database. For the purpose of this study, phenotype was defined as all variables that were not genetic.

Clinical Phenotype

Clinical phenotypes included demographic and clinical variables: age, gender, disease duration, age at diagnosis, disease location, and type of disease behavior (Supplemental Digital Content, Table 3.4 & 3.5). B1: non-stricturing, non-penetrating, B2: stricturing, B3: penetrating/fistulizing. Stricturing disease was defined as the occurrence of constant luminal narrowing demonstrated by radiologic, endoscopic or surgical examination combined with pre-stenotic dilatation and/or obstructive signs or symptoms. Penetrating disease was defined as the presence of perianal, entero-enteric or entero-vesicular fistulae, intra-abdominal abscesses or intestinal perforation.

Identification of formalin-fixed, paraffin-embedded (FFPE) sections in patients with CD

We identified twelve adult patients followed at UNC's adult IBD clinic for inclusion into the study. Each patient was diagnosed at UNC with FFPE tissue available from a

[†] Supplemental Digital Content are available with the published version of the paper online at http://journals.lww.com/ibdjournal/Fulltext/2015/09000/MicroRNAs_Classify_Different_Disease_Behavior.20.aspx

macroscopically and microscopically quiescent section of the colon taken at the time of diagnosis (index biopsy). All 12 patients at time of diagnosis had a B1 CD phenotype. 6 of 12 patients as of 2015 had progressed to a B3 penetrating CD phenotype (5 with perianal fistulizing CD and 2 with intra-abdominal abscess secondary to CD affecting the terminal ileum). 6 of 12 patients remained in the B1 phenotype (2 of 6 with disease remission and 4 of 6 with active CD). Mucosal sections were identified by a pathologist (DGT) from each FFPE sample and scrolls were obtained to process for small RNA isolation (Supplemental Digital Content, Table 3.3, Supplemental Digital Content, Fig 3.1-2). Sections were selected for no or minimal chronic inflammation. The presence or absence of acute (active) and chronic inflammation was determined after review of each H&E stained slide. Activity was determined by the presence of histologic features of acute inflammation, including neutrophilic inflammation of crypt epithelium and crypt abscess formation. Chronicity was determined based upon the presence of features such as architectural distortion and basal lymphoplasmacytosis of the lamina propria. Degree of activity was determined based on the percentage of mucosa involved by active inflammation.

RNA isolation

RNA was isolated from fresh-frozen human colon tissues using the Qiagen RNeasy Mini Kit (Valencia, CA), which preserves both miRNA and mRNA content. This kit utilizes a column based DNase treatment to eliminate DNA contamination. miRNA was enriched from FFPE tissue samples using the Roche HighPure miRNA Isolation Kit (Penzberg, Germany, Supplemental Digital Content, Figure 3.2). RNA purity and integrity were assessed with Thermo Scientific Nanodrop 2000 (Waltham, MA) and Agilent 2100 Bioanalyzer (Santa Clara, CA), respectively.

Small RNA and mRNA-sequencing and expression analysis

Small RNA libraries were generated using Illumina TruSeq Small RNA Sample Preparation Kit (San Diego, CA). Single-end (50 bp) sequencing was performed on the Illumina HiSeq 2500 platform at the UNC High-Throughput Sequencing Facility (HTSF). Twelve libraries were randomly assigned to each sequencing lane. miRNAs and their isomiRs were annotated and quantified according to our previously described bioinformatics analysis pipeline(Baran-Gale et al. 2013). Sequencing quality and mapping statistics were compared across all samples (Supplemental Digital Content, Table 3.6). miRNAs with an expression level of 100 reads per million mapped (RPMM) in at least one sample were considered for differential expression analysis.

Libraries for RNA-seq were prepared using the Illumina TruSeq polyA+ Sample Prep Kit. Paired-end (50 bp) sequencing was carried out on the Illumina HiSeq 2500 platform at the UNC HTSF. Genotype data from the Illumina Immunochip was available for all samples with RNA-seq data. Genotype imputation was performed with MaCH-admix(E.Y. Liu et al. 2013), and custom genomes were created using genotype calls for all genotyped and imputed variants. RNA-seq reads were then aligned to personalized genomes using the "SNP-tolerant" GSNAP software(T.D. Wu and Nacu 2010). This alignment pipeline allows for elimination of mapping biases that arise from discrepancies in genetic variation between individual samples and a standard reference genome, at both homozygous and heterozygous sites. Sequencing quality and mapping statistics were compared across all samples (Supplemental Digital Content, Table 3.7). Differentially expressed (DE) genes in CD samples relative to NIBD samples were identified by unpaired Student's t-test after variance stabilizing transformation of the data (DESeq(Anders and Huber 2010)).

miRNAs and genes were considered significantly DE in CD relative to NIBD if they had a $\log_2$ (fold-change (FC)) ≥ +/- 1.0 at a p-value ≤ 0.05 by an unpaired two-tailed Students t-Test. Small RNA and mRNA-sequencing data were deposited in GEO (Accession #GSE66209).

Quantitative reverse transcriptase PCR

Total RNA was isolated from tissues using the Norgen Total RNA Purification kit (Thorold, Ontario, Canada). Fifty ηg RNA was used for reverse transcription with the Life Technologies TaqMan microRNA Reverse Transcription kit. miRNA qRT-PCR was performed using the TaqMan Universal PCR Master Mix per Life Technologies' protocol, on a BioRad Laboratories CFX96 Touch Real Time PCR Detection System (Richmond, CA). Reactions were performed in triplicate using *RNU48* as the normalizer.

miRhub analysis

Candidate master miRNA regulators were identified by miRhub(Baran-Gale et al. 2013; Kurtz et al. 2014), using the "non-network" mode and requiring a predicted target site to be conserved between human and at least one other species.

Results

Small RNA-sequencing reveals distinct miRNA signatures in the non-inflamed colon of CD patients with different disease behaviors

To characterize the small RNA transcriptome in different phenotypic classes of CD, we performed high-throughput sequencing of small RNA isolated from non-inflamed colon tissue from 21 patients and 14 NIBD controls (Methods). We obtained an average of ~18.5 million reads per sample, of which an average of ~75% were mapped to the human genome

(Supplemental Digital Content, Table 3.6). Individual miRNAs were annotated and quantified according to our previously described small RNA-seq analysis pipeline (Methods, GEO #GSE66209). We found that the expression levels of four miRNAs (miR-31-5p, miR-149-5p, miR-150-5p, and miR-375) were significantly altered ($\log_2$ (FC) > 1 or < -1, $p < 0.05$, two-tailed unpaired Student's t-test) in CD compared to NIBD controls (Figure 3.1A).

To identify miRNAs associated with specific CD phenotypes, we stratified the 21 patients according to their disease subclass (B1/non-stricturing, non-penetrating, n = 8; B2/stricturing, n = 6; B3/penetrating, n = 7) and compared miRNA profiles in each class with those of the NIBD control group. We found 9, 6, and 9 significantly ($\log_2$ (FC) > 1 or < -1, $p < 0.05$) DE miRNAs in the B1, B2, and B3 classes, respectively (Figure 3.1B-D, Supplemental Digital Content, Table 3.8). These included several 5'-end variants of canonical miRNAs (referred to as 5'-isomiRs), such as miR-375-3p+1, miR-143-3p-1, and miR-378a-3p+1, which have been shown to be functionally relevant and are only distinguishable from their canonical counterparts by sequencing-based analysis(Cloonan et al. 2011; Baran-Gale et al. 2013; Tan et al. 2014).

Strikingly, we found that the majority of the significantly DE miRNAs in each disease class were unique to that class (Figure 3.1). Specifically, 9/9, 4/6, and 7/9 miRNAs were exclusively DE compared to NIBD controls in B1, B2, and B3, respectively (Figure 3.1E). For example, miR-150-5p, which normally represses the immune response(Changchun Xiao et al. 2007), was significantly down-regulated only in the B1 disease class (Supplemental Digital Content, Figure 3.3). Also, miR-31-5p (up), miR-149-5p (down), miR-196b-5p (down), miR-215 (up), miR-223-3p (up), and miR-203 (down) were altered in B2 and/or B3, both of which exhibit fibrosis and penetrating/fistulizing phenotypes, but not in B1 (Figure 3.2). The down-regulation

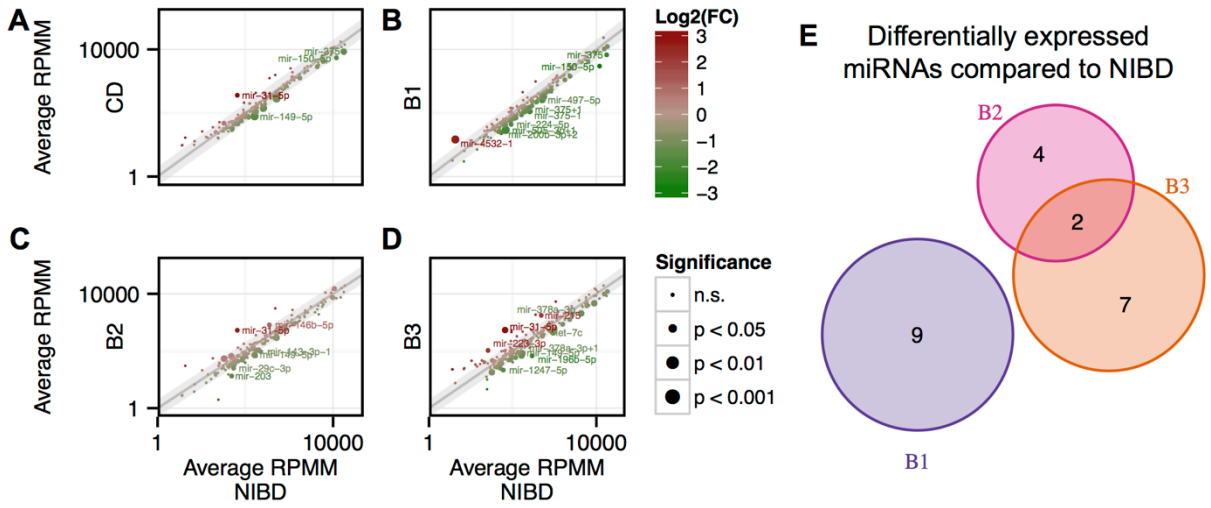

Figure 3.1. Colonic miRNAs are differentially expressed between Crohn's disease patients and controls. Scatter plots showing average miRNA expression as determined by small RNA-seq comparing (**A**) CD, (**B**) B1/non-stricturing, non-penetrating class, (**C**) B2/stricturing class, and (**D**) B3/penetrating class to NIBD patient samples. (**E**) Venn diagram showing overlap of significantly DE microRNAs relative to NIBD. Grey shaded region indicates $\log_2$ (FC) < 1 or > -1. Size of point indicates significance level as determined by a two-tailed unpaired Student's t-Test, while color indicates direction of change. miRNAs achieving significance and $\log_2$ (FC) of > 1 or < -1 change in expression are labeled and considered DE.

of miR-196(Kashiyama et al. 2012) and miR-203(Song et al. 2014), as well as the up-regulation of miR-192/215(Chung et al. 2010) and miR-223(Oglesby et al. 2013) have been associated with fibrosis in different tissues including kidney and skin. miR-31-5p and miR-149-5p were significantly DE in both B2 and B3 classes (Figure 3.2A, G). Although ileocolonic miR-31 levels were previously associated with CD(Olaru et al. 2011; Lin, Welker, et al. 2013), miR-149-5p has only been reported previously as a plasma marker of CD(Dalal and Kwon 2010; F. Wu et al. 2010).

To validate these findings, we performed qRT-PCR (Methods) for three miRNAs (miR-31-5p, miR-215, and miR-149-5p). We confirmed that all three were unchanged in B1 but DE in

both B2 and B3 (Figure 3.3). miR-31-5p was the most prominently up-regulated in both B2 (7.6-fold) and B3 (9.2-fold), whereas miR-215 was more modestly up-regulated in B3 (1.7-fold), and miR-149-5p was significantly down-regulated in both B2 (-3.6-fold) and B3 (-2.6-fold). Taken together, these results reveal distinct miRNA signatures associated with different CD disease classes. In particular, patients with B2/stricturing and/or B3/penetrating phenotypes exhibit a completely different colonic miRNA profile than patients without either of those conditions. To our knowledge, these findings are the first to demonstrate that molecular subtypes of CD stratify according to miRNA profiles.

Inflammation is not a primary driver of miR-31-5p, miR-215, and other CD-associated miRNAs

To determine whether the DE miRNAs are further dysregulated by active inflammation, we performed small RNA-seq on total RNA isolated from inflamed colon tissue from six individuals with CD, including at least one from each disease class (B1, n = 3; B2, n = 1; B3, n = 2), and compared the miRNA profiles with those of the patient-matched non-inflamed tissue (Supplemental Digital Content, Figure 3.4A, B; Supplemental Digital Content, Table 3.6, GEO #GSE66209). We found that none of the 22 miRNAs that were found to be significantly DE in the non-inflamed colon of B1, B2, or B3 classes of CD patients (Figure 3.1) were significantly altered in the matched inflamed tissue (Figure 3.4, Supplemental Digital Content, Figure 3.4A,C,D), although miR-149-5p did trend upward (Figure 3.4E). As a positive control, we compared miR-132 and miR-99b-5p, both of which are known to be associated with pro-inflammatory processes(Tserel et al. 2011; Maharshak et al. 2013), and found that they were indeed significantly elevated in inflamed relative to non-inflamed colon tissue (Supplemental Digital Content, Figure 3.4E & F). These findings suggest that the CD-associated miRNAs we

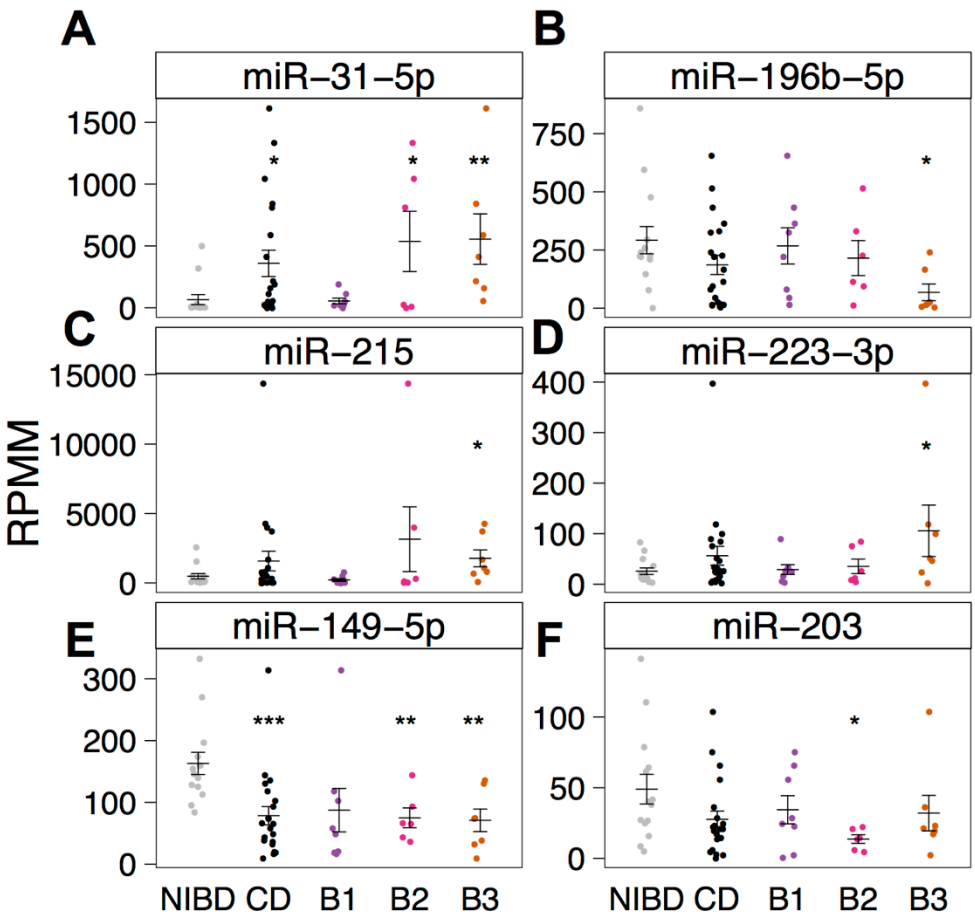

Figure 3.2. miRNAs are variably expressed across Crohn's disease subtypes. miRNA expression (RPMM) as determined by small RNA-sequencing is shown for (**A**) miR-31-5p, (**B**) miR-196b-5p, (**C**) miR-215, (**D**) miR-223-3p, (**E**) miR-149-5p, (**F**) miR-203, in NIBD (grey, n = 14) and CD (black, n = 21) patient samples. CD samples are further categorized as B1 (purple, n = 8), B2 (pink, n = 6), or B3 (orange, n = 7). Mean and standard error for each group are depicted using horizontal and vertical bars. Significance is determined using a two-tailed unpaired Student's t-Test comparing each group to NIBD samples, *$p < 0.05$, **$p < 0.01$, ***$p < 0.001$.

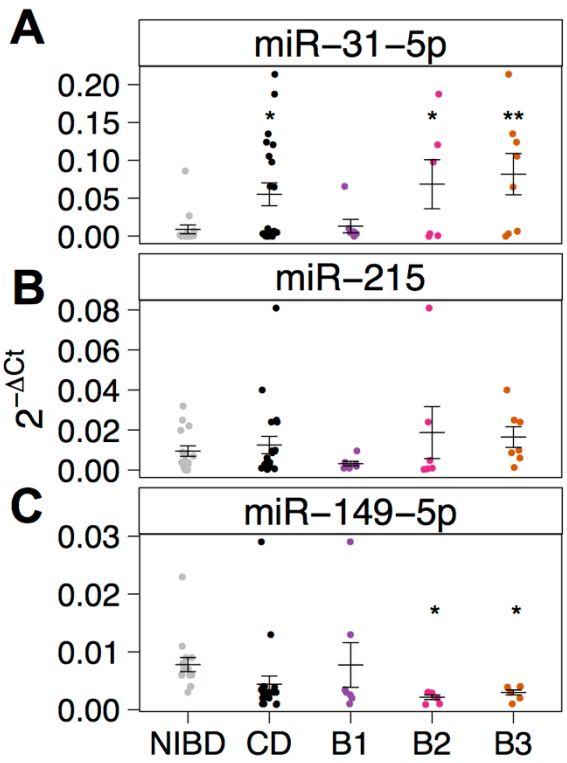

Figure 3.3. qRT-PCR confirms differential expression of four colonic miRNAs in Crohn's disease patients and controls. Relative miRNA expression levels ($2^{-\Delta Ct}$) as determined by qRT-PCR and normalized to *RNU48* are shown for (**A**) miR-31-5p, (**B**) miR-215, (**C**) miR-149-5p, in NIBD (n = 15, grey) and CD (n = 20, black) patient samples. CD samples are further categorized as B1 (purple, n = 7), B2 (pink, n = 6), or B3 (orange, n = 7). Mean and standard error for each group are depicted using horizontal and vertical bars. Significance is determined using a two-tailed unpaired Student's t-Test comparing each group to NIBD samples, *$p < 0.05$, **$p < 0.01$.

have identified are molecular markers of genetic predisposition to CD, as opposed to indicators of an acute inflammatory process.

We measured miR-31-5p by qRT-PCR in colon tissue with low-grade inflammation from patients with UC (n = 6) and found that the levels were not changed compared to colon tissue from normal controls (n = 15) (Figure 3.4G). Interestingly, miR-31-5p was 4.2-fold elevated in UC patient-matched inflamed tissue (Figure 3.4G), unlike what we observed in CD (Figure 3.4A).

Taken together, these findings indicate that while inflammation may modulate miR-31-5p in some disease contexts such as psoriasis(N. Xu et al. 2013) or even within the IBDs (UC, Figure 3.4G), biological processes other than inflammation are primarily responsible for the dysregulation of colonic miRNAs, such as miR-31-5p, miR-215, and miR-196b-5p, in CD.

miR-215 is a potential predictor of a penetrating disease phenotype in CD

To determine whether miR-31-5p, miR-149-5p, and miR-215 could predict the progression of a B1 CD phenotype to a B3 phenotype, we obtained from twelve patients FFPE colon tissue that was available from biopsies taken at the time of diagnosis at the UNC Hospital. All twelve patients were classified as B1-type CD at the time of diagnosis. Six out of the twelve patients subsequently developed a B3 phenotype ("B1→B3") whereas the remaining six did not ("B1→non-B3"). We performed qRT-PCR (Methods) for three miRNAs (miR-31-5p, miR-215, and miR-149-5p) on small RNAs enriched from the FFPE tissue. There was no statistical difference in expression of the miRNAs between the two groups (Figure 3.5A and Supplemental Digital Content, Figure 3.5A & B). However, a post-hoc analysis revealed that two of the patients (both in the B1→non-B3 group) were in complete clinical and mucosal remission, while the remainder had active disease. Adjusting for these two patients, we found that miR-215 was

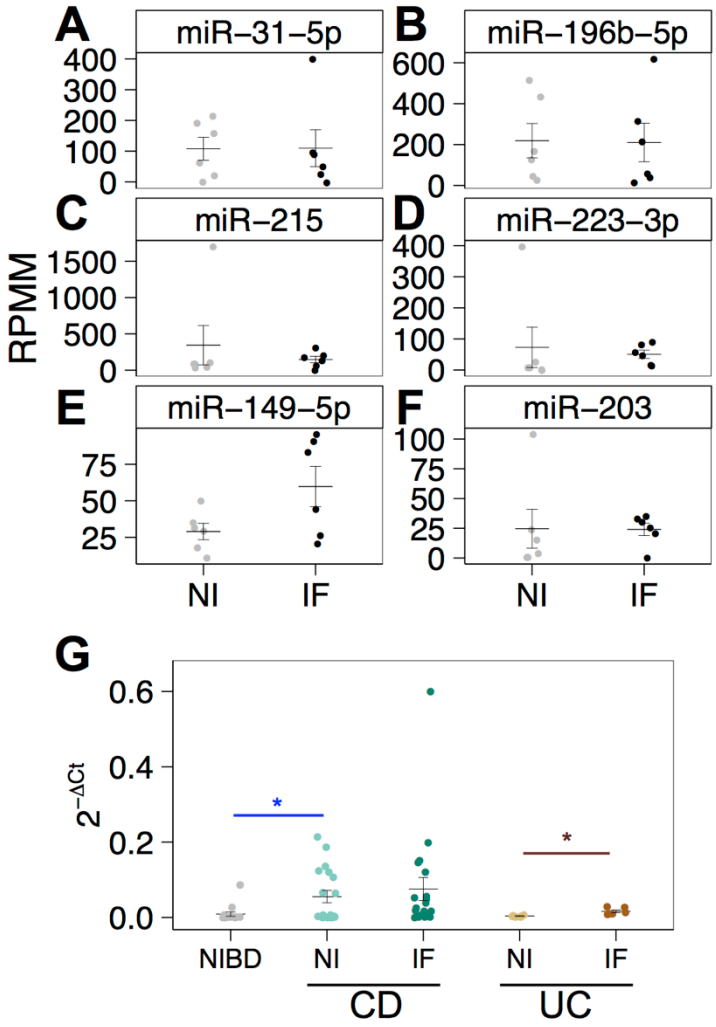

Figure 3.4. Differential expression of miRNAs is not dependent on inflammation status. miRNA expression (RPMM) as determined by small RNA-sequencing is shown for (**A**) miR-31-5p, (**B**) miR-196b-5p, (**C**) miR-215, (**D**) miR-223-3p, (**E**) miR-149-5p, (**F**) miR-203, in six matched non-inflamed (NI, grey) and inflamed CD samples (IF, black) patient samples. (**G**) Relative miR-31-5p expression levels ($2^{-\Delta Ct}$) as determined by qRT-PCR and normalized to *RNU48* are shown for samples from NIBD patients (n = 15), matched non-inflamed (NI) and inflamed (IF) CD patients (n = 19), and matched NI and IF UC patient samples (n = 6). Significance is determined using a two-tailed unpaired Student's t-Test comparing each group to NIBD (blue) samples or matched non-inflamed tissue (red with bar), *p < 0.05. Significance was not achieved by a two-tailed paired Student's t-Test comparing NI to IF in panels A-F.

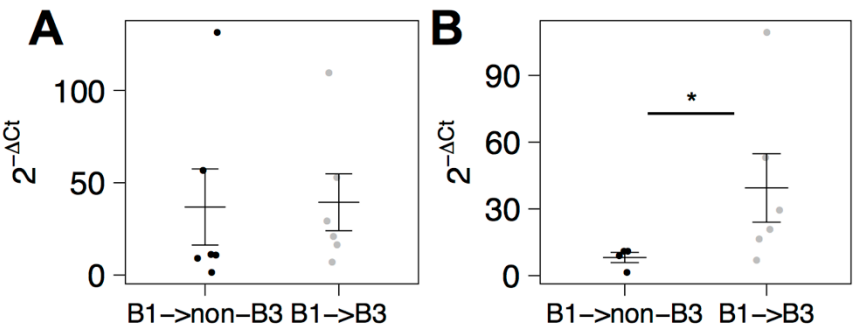

Figure 3.5. miR-215 may have prognostic utility. Relative miR-215 expression levels ($2^{-\Delta Ct}$) as determined by qRT-PCR and normalized to *RNU48* for B1 patient samples that (**A**) either progressed to a non-B3/penetrating disease (B1->non-B3, n = 6, black) or progressed to B3/penetrating disease (B1->B3, n = 6, grey). (**B**) Samples from Panel B were subcategorized to include only B1 samples from patients with active CD that did not progress to B3/penetrating disease (B1->non-B3, n = 4) or progressed to B3/penetrating disease (n = 6). Mean and standard error for each group are depicted using horizontal and vertical bars. Significance determined using a one-tailed, unpaired and unequal variance Student's t-Test comparing each group to B1->non-B3 samples, *$p < 0.05$.

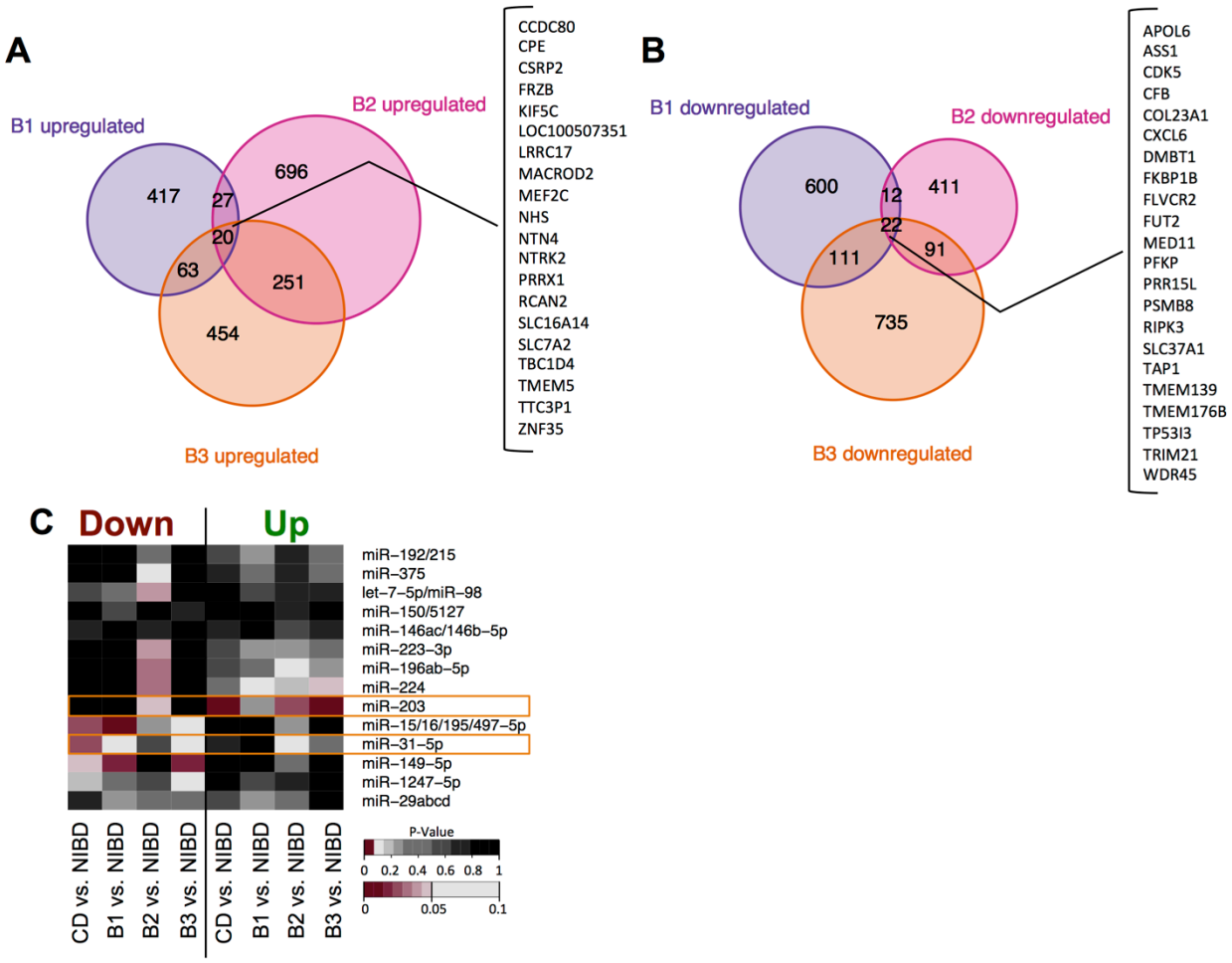

Figure 3.6. RNA-sequencing of matched RNA reveals commonly dysregulated genes across disease subtypes and potential master regulatory miRNAs. Venn diagram showing the number of differentially expressed genes ($p < 0.05$) that were (**A**) upregulated, or (**B**) downregulated, compared to NIBD controls in each of the CD subclasses. Genes that were significantly up- or down- regulated in all three classes respectively are shown on the right in the bracketed table. (**C**) Enrichment analysis for target sites of expressed miRNAs (RPMM > 100) in differentially expressed genes as determined by RNA-seq. On the x-axis, differentially expressed gene lists were divided into upregulated and downregulated genes for four comparisons: CD vs. NIBD, B1 vs. NIBD, B2 vs. NIBD, or B3 vs. NIBD. P-values less than 0.05 are shown in shades of red. Candidate master regulators are highlighted in orange boxes.

4.8-fold enriched in the B1→B3 group of patients relative to B1→non-B3 ($p = 0.049$, by one-tailed, unpaired & unequal variance Students t-Test, Figure 3.5B). To our knowledge this is the first description of using miRNAs to prospectively predict disease phenotype in CD.

Whole transcriptome analysis reveals that miR-31-5p and miR-203 are candidate drivers of the colonic gene expression profile in CD

To determine whether any of the miRNA markers of CD are also candidate master regulators of gene networks underlying disease pathogenesis, we first performed paired-end high-throughput sequencing of mRNAs isolated from the same colon tissue samples that were used for small RNA-sequencing studies (Methods). We obtained an average of ~29.4 million paired-end reads per sample, of which an average of ~70% mapped uniquely to the human genome (Methods, Supplemental Digital Content, Table 3.7). We used DESeq(Anders and Huber 2010) to identify DE genes in CD, as well as in each of B1, B2, and B3 phenotype classes, relative to the NIBD control group (Figure 3.6A & B). Similar to the results of the small RNA-seq analyses, there was very minimal overlap of DE genes between pairwise comparisons of B1, B2, and B3 classes (Figure 3.6A & B). These findings highlight the unique molecular identities of different disease behaviors of CD.

We next applied the miRhub algorithm(Baran-Gale et al. 2013; Kurtz et al. 2014), which determines whether the predicted regulatory effect of any miRNA on a set of DE genes is significantly greater than expected by chance (empirical $p < 0.05$). Only one significantly upregulated miRNA, miR-31-5p, was identified as a candidate master regulator of genes that are downregulated in CD (Figure 3.6C). Likewise, only one significantly down-regulated miRNA, miR-203, was identified as a candidate master regulator of genes that are up-regulated in CD (Figure 3.6).

Discussion

There is a rapidly expanding interest in evaluating the use of miRNAs as potential diagnostic markers of IBD. Most studies of miRNA expression in IBD have used qRT-PCR or microarrays to quantify miRNA abundance. Notable among these was the demonstration that miRNAs were DE in the sigmoid colons of patients with UC(F. Wu et al. 2008). A subsequent study demonstrated that none of the CD-associated miRNAs were altered in colon tissues from UC patients. Furthermore, miRNA expression in ileal CD was different than colonic CD(F. Wu et al. 2010). Inflammation was shown to alter the profiles of many of the implicated miRNAs, suggesting inflammation-dependent effects on miRNA expression. Our study is different in its unbiased, NGS-based approach to small RNAs. To our knowledge only one other study has employed small RNA-seq in patients with IBD(Lin, Welker, et al. 2013). This study, consistent with our findings, reported that miR-31 expression was increased in colon tissue from patients with CD. Although Lin *et al.* used tissues from patients with ischemic colitis and infectious colitis as controls, the effect of inflammation in the context of CD on miR-31 expression was not studied. miR-149 expression was found to be decreased in peripheral blood in patients with CD, but again, the effects of active CD versus inactive disease were not studied, making it difficult to interpret whether plasma miR-149 was truly a marker of genetic predisposition or a sequela of the inflammatory response. Using matched inflamed tissue from the same CD patients, we show that select groups of miRNAs, including miR-31, are aberrantly expressed in an inflammation-independent fashion in patients with CD. This effect was not seen in the inflammatory tissue obtained from patients with UC, suggesting the potential for the use of miR-31 as a marker of genetic predisposition for CD.

Perhaps most notably, our study is the first to demonstrate that miRNAs classify different

disease behaviors of CD. We identify a unique colonic miRNA profile for CD that is characterized by a penetrating (fistulas, perianal and intra-abdominal abscesses) inflammatory phenotype compared to a non-penetrating phenotype. Closer examination of the miRNAs uniquely altered in each disease behavior revealed pertinent altered biology in CD. For example, we found that miR-29c was uniquely downregulated in the B2 class, which is associated with stricturing secondary to fibrosis. The miR-29 miRNAs have long been established as potent repressors of fibrosis. The downregulation of miR-29c in B2 is consistent with the elevation in B2 of several extracellular matrix (ECM) genes, including *COL6A1*, *COL6A3*, *COL21A1*, and *ELN*. In fact, *ELN* is a validated target of miR-29 in several different cell types(Ott et al. 2011; P. Zhang et al. 2012). The downregulation of miR-29c in B2 likely leads to the increased expression of ECM genes, thereby contributing to the fibrotic phenotype. Also, miR-203 has been shown to regulate TNF-alpha, the major biological target in managing patients with CD(Primo et al. 2012). In our study, we found miR-203 to be downregulated in all classes of CD, but only significantly in the B2 class, which may contribute to elevated TNF-alpha levels seen in CD(Martínez-Borra et al. 2002). Importantly, we found that the degree of inflammation did not affect the expression of miR-203.

Our findings highlight the exciting potential of using a miRNA signature as a disease biomarker. Olaru *et al*. found that miR-224 and miR-31 were increased successively at each stage of IBD progression from non-inflamed to inflamed non-neoplastic, dysplastic and finally cancer(Olaru et al. 2011; Olaru et al. 2013). Zhang *et al*. found miR-31 to be dysregulated in IBD but not microscopic colitis(C. Zhang et al. 2014). miR-21 is also widely reported as dysregulated in UC and CD. Specifically, Ludwig *et al.* (2013) found that miR-21 was up-regulated in IBD-associated dysplastic lesions compared to active IBD patients(Ludwig et al.

2013). In our study, although highly expressed, there was no statistical difference in miR-21 expression between NIBD and CD tissue. These differences may be related to use of colonic tissue for our study compared to ileal mucosal samples as previously reported(Fasseu et al. 2010; F. Wu et al. 2010). However, subgroup analysis based on disease behavior did reveal that there is a trend towards higher miR-21 expression in B3 vs. NIBD (FC = 4.99, p = 0.14) that is not seen in B2 (FC = 1) or B1 (FC = 1.2) vs. NIBD. This highlights the importance of studying different disease classes of CD independently. Future studies, similar to ours but incorporating a larger patient cohort, will help make these molecular distinctions more evident. Other than miR-31, we did not see significant changes in colonic expression between CD and NIBD patients for miRNAs most frequently associated with UC, such as miR-126(Fasseu et al. 2010).

Our results reveal the importance of accounting for CD disease behavior in experimental design and data analysis in order to more sensitively capture potential diagnostic markers and therapeutic targets. Previous studies have been inconsistent in identifying miRNAs that may serve as biomarkers. Furthermore, no attempt has been made to use a miRNA signature as a potential prognostic marker of CD. By focusing on miRNAs that are highly expressed and demonstrate differences based on disease behavior, we have identified miRNAs with potential diagnostic and prognostic utility. miR-31 expression levels are similar between normal mucosal specimens from cecum, ascending, transverse, descending, sigmoid colon and rectum, making it a practical choice as a marker, given the frequency of colonoscopies and flexible sigmoidoscopes in patients with IBD(Olaru et al. 2011).

Our study focused on miRNA expression in the colon. Signatures in the small bowel are likely different and may add to the value of our study, particularly since it has been shown that inflammation does affect miRNA expression in the ileum(Z. Guo et al. 2015). miRNAs that we

found to be associated with a penetrating phenotype of CD (B3), including miR-31 and miR-215, are known to be increased in the terminal ileum compared to the colon(F. Wu et al. 2010). A future study design with samples also obtained from the ileum, incorporating a larger number of patients, may be able to pinpoint which miRNAs are associated with penetrating/fibrosing disease in the small intestine compared to perianal fistulizing disease in the colon.

Given the limitations of clinically phenotyping patients with CD, there is a need to develop molecular phenotypes that help predict disease behavior. Perhaps the most novel aspect of our study is the use of a new "prospective" patient cohort. By carefully selecting a group of patients with penetrating CD that on initial presentation lacked the presence of penetrating CD, we are able to identify a miRNA that may be predictive of this disease phenotype. Furthermore, the ability to test this in a FFPE sample block makes the application of our work a practical reality with potential for clinical use. There are many inherent difficulties in patient selection when conducting a prospective biomarker study. These include the availability of tissue at time of disease diagnosis, availability of detailed and carefully phenotyped patient's disease course, clinical follow-up, and accurate technology for analysis of FFPE samples. Despite these challenges and small sample numbers, the study yielded novel and intriguing results that merit detailed further investigation. Interestingly, post-hoc analysis of the B1→B3 group showed that miR-215 increased most in patients with a penetrating CD phenotype of the ileum (Supplemental Digital Content, Figure 3.6) compared to the patients with perianal fistulizing CD. Given the recent study showing that peripheral blood miRNAs can be used to distinguish active CD and UC from healthy controls, it will be interesting to test the potential of the select group of miRNAs that share a common systemic and colonic expression profile. Our findings demonstrate that miRNAs can be used to classify different CD disease behaviors and lay the groundwork to

study their clinical utility as prognostic markers of IBD.

To develop novel therapeutics for the treatment of IBD and other GI diseases, we must understand the role of miRNAs not only as biomarkers, but also as drivers of disease pathways. IBD is a complex disease involving immune cells, GI epithelia, metabolic networks, the mesenchyme, and diverse environmental factors(C. Li and Kuemmerle 2014). In combination, these factors mediate not only the progression and severity of disease, but also the response to treatment. This study investigated differences in miRNA expression from NI punch biopsies of CD and NIBD controls. This isolation method enriches for intestinal mucosa, which lacks inflammatory immune cells, suggesting that mucosal cell types (epithelia, mesenchyme, lymphatic and vasculature) likely drive differential expression of miR-215, miR-31, and miR-149 in CD. However, the functions of these miRNAs in the intestinal mucosa during intestinal homeostasis are still largely unknown. Identifying the cell type(s) of origin for these miRNAs altered in CD is an important next step.

CD is a chronic GI disease, and the IE undergoes constant and rapid renewal. For the IE to contribute to CD pathogenesis, there must be substantial changes to IE gene and miRNA expression. Our knowledge of the role of miRNAs during normal IE physiology is still quite limited, despite their well-established role in the regulation of proliferation and differentiation of other tissues and organ systems(Shenoy and Blelloch 2014). Understanding the role of miRNAs in normal intestinal epithelial homeostasis and their response to environmental stimuli will be vital next steps in developing miRNA therapeutics for CD and other GI diseases, including metabolic syndrome.

CHAPTER 4 – MIR-30 FAMILY CONTROLS PROLIFERATION AND DIFFERENTIATION OF INTESTINAL EPITHELIAL CELL MODELS BY DIRECTING A BROAD GENE EXPRESSION PROGRAM THAT INCLUDES SOX9 AND THE UBIQUITIN LIGASE PATHWAY [*]

To identify miRNAs potentially involved in intestinal epithelial homeostasis, we started by *in silico* prediction of miRNAs with putative target sites in *SOX9*, which encodes a transcription factor that is well known for its regulatory role in GI biology. Like other members of the SRY box family of transcription factors, SOX9 is tightly regulated by a complex network of transcriptional, post-transcriptional(S. Lee et al. 2014), and post-translational(She and W.-X. Yang 2015) modifiers. It is known to regulate proliferation and differentiation of diverse stem and progenitor cells, including but not limited to gonad(Kanai et al. 2005), chondrocyte(Mori Akiyama et al. 2003), neural crest(Nunn 2012), lung(Rockich et al. 2013), pancreas(Belo et al. 2013), and IE(Bastide et al. 2007; Belo et al. 2013; Rockich et al. 2013; Roche et al. 2015). The functional effect of Sox family members in general is frequently described as dosage dependent, with relative expression levels driving either cellular renewal or differentiation(Kamachi and Kondoh 2013; Sarkar and Hochedlinger 2013). Notably, varying levels of Sox9 have been shown to mark functionally distinct cell types of the mouse IE. Accordingly, a transgenic reporter mouse (Sox9-EGFP) has been developed to identify and isolate both differentiated cell types and

[*] This chapter previously appeared as a journal article in the *Journal of Biological Chemistry*. The original citation is as follows: Peck, B. C. E., Sincavage, J., Feinstein, S., Mah, A. T., Simmons, J. G., Lund, P. K., and Sethupathy, P. (2016) miR-30 family controls proliferation and differentiation of intestinal epithelial cell models by directing a broad gene expression program that includes SOX9 and the ubiquitin ligase pathway. *J. Biol. Chem.* http://doi.org/10.1074/jbc.M116.733733

actively cycling IESCs and progenitors based on the levels of cellular EGFP expression driven by the Sox9 promoter(Formeister et al. 2009; Gracz et al. 2010; Van Landeghem et al. 2012; Andres et al. 2013; Mah et al. 2014).

SOX9 is not uniquely expressed in IECs, and a few studies to date have assessed miRNA targeting of *SOX9* in other tissues. For example, miR-145 has been shown to target *SOX9* in various cancer subtypes(Dynoodt et al. 2013; C.-C. Yu et al. 2013) and chondrocytes(Martinez-Sanchez et al. 2012). Both miR-145 and miR-495 target *SOX9* in mesenchymal stem cells(B. Yang et al. 2011; S. Lee et al. 2014), and miR-101 targets *SOX9* in hepatocellular carcinoma(Y. Zhang et al. 2012). As both miRNA expression and mRNA 3'UTR usage can vary across cell types and conditions, these findings are not necessarily generalizable to the IE. To date no study has investigated miRNA-mediated regulation of *SOX9* in the context of IECs. More importantly, roles of specific miRNAs in the control of intestinal epithelial proliferation and differentiation are poorly characterized. In this study, we work toward bridging this knowledge gap using *in silico*, *in vitro*, and *in vivo* analyses.

Research Design and Methods

Animals

All animal studies were approved by the University of North Carolina at Chapel Hill's Institutional Animal Care and Use Committee (IACUC protocol #13-162). *Sox9-EGFP* female mice(Formeister et al. 2009; Gracz et al. 2010; Van Landeghem et al. 2012) on a CD1 background were fed a standard chow diet (Prolab RMH3000) *ad libitum*. Eleven week old mice were euthanized with a lethal dose of Nembutal (150 μg/gram of body weight) and were processed for jejunal IEC dissociation and fluorescence activated cell sorting.

IEC dissociation for flow cytometry and FACS

The small intestine was dissected and flushed with ice cold PBS to remove contents, then divided into 3 equal sections. The middle section was considered jejunum, and was prepared for FACS as previously described(Van Landeghem et al. 2012; Mah et al. 2014). IECs were sorted using a Mo-Flo XDP cell sorter (Beckman-Coulter, Fullerton, CA) at the University of North Carolina Flow Cytometry Core Facility using previously described gating parameters(Gracz et al. 2010; Van Landeghem et al. 2012; Mah et al. 2014). Cells that stained for CD31 (BioLegend, San Diego, CA), CD45 (BioLegend, San Diego, CA), and or Annexin-V (Life Technologies, Carlsbad, CA), were excluded prior to sorting. Following sorting, cells were pelleted by centrifugation and total RNA was isolated using the Norgen Total RNA kit (Norgen Biotek, Thorold, ON, Canada) as per the manufacturer's instructions. Nanodrop 2000 was used to quantify RNA.

Quantitative Reverse Transcription PCR (qRT-PCR)

Assays were performed in triplicate using either *U6 (*miRNA expression) or *RPS9 (*mRNA expression) as an internal control. All TaqMan assays were purchased from Applied Biosystems, and include: miR-30a (assay ID: 000417), miR-30b (assay ID: 000602), miR-30c (assay ID: 000419), miR-30d (assay ID: 000420), miR-30e (assay ID: 002223), miR-101a (assay ID: 002253), miR-101b (assay ID: 002531), miR-320a (assay ID: 002277), miR-145 (assay ID: 000467), *U6* (assay ID: 001973), *Sox9* (assay ID: Mm00448840_m1), *Rps9* (assay ID: Mm00850060_s1), *SOX9* (assay ID: Hs01001343_g1), *HES1 (*assay ID: Hs00172878_m1), *SI* (assay ID: Hs00356112_m1), and *RPS9* (assay ID: Hs02339424_g1).

Cell culture and transfections

Human intestinal epithelial cells (*HIECs*) were acquired from the Beaulieu laboratory(Perreault and Beaulieu 1996) and were cultured in OptiMEM 1 (Life Technologies) supplemented with 10% FBS (Life Technologies), 0.01 M HEPES (Life Technologies), and 5 ηg/mL hEGF (Invitrogen, Grand Island, NY). Cells were used between passages 20-30, and were maintained at 70% confluency. HIECs were seeded onto tissue culture-treated plates and transfected at 70% confluency with 3.25 μL/mL Lipofectamine 2000 (Life Technologies).

Caco-2 colon carcinoma cells were cultured in high glucose DMEM (Sigma-Aldrich, St. Louis, MO) supplemented with 10% FBS. Cells were used between passages 18 and 30, and were maintained at 70% confluency. Caco-2 cells were seeded onto tissue culture-treated plates and transfected at 70% confluency with 1.875 μL/mL Lipofectamine 3000 (Life Technologies).

Locked Nucleic Acids (LNAs) were purchased from Exiqon (Woburn, MA) including hsa-miR-101* (cat. 4101585-101), mmu-miR-30bcd (cat. 199900), and hsa-miR-320a (cat. 4101458-101). LNAs against mouse miR-30 family members are cross reactive with human miR-30 family.

For MG132 treatment studies, 6 μL of 10 mM MG132 (Z-Leu-Leu-Leu-al, Sigma-Aldrich, cat. C2211) or DMSO vehicle was added to each well of a 6-well plate for a final concentration of 25 μM MG132 at 68 hours post-transfection. Following a 4-hour treatment, cells were isolated for RNA and protein as described below.

Caco-2 differentiation

Similar to methods previously described(Basuroy et al. 2003; Andres et al. 2013; Gil-Zamorano et al. 2014), Caco-2 cells between passages 23 - 27 were grown on 100 mm tissue-culture treated plates (Corning cat. 430167). At 70% confluency, cells were transfected with 100

ηM LNA against miR-30bcd, miR-320a, or miR-101*. At 24 hours post-transfection, cells were trypsinized, and 2 x 10^5 cells were seeded onto transwell inserts (Costar #3460, Fisher Scientific). Reseeding onto the transwells following transfection was done to avoid differences in cell density due to cell death or changes in cell proliferation following transfection with each LNA. Differentiation was monitored every other day using transepithelial electric resistance (TER) beginning at 72 hours post-transfection. Cells were considered fully differentiated after 1 week following the beginning of the TER plateau(Briske-Anderson et al. 1997). Throughout differentiation, media was changed from both the top and bottom wells every other day following TER measurement. At 72 hours post-transfection, undifferentiated cells were harvested for RNA. At 21 days post-transfection, differentiated cells were harvested for RNA.

Western blot

Protein was isolated from cells, quantified, and run on a gel as previously described in Chapter 2(Kurtz et al. 2014). The membranes were blocked 1 hour in 5% milk, before being probed overnight at 4°C with SOX9 antibody (1:800, Abcam cat. ab26414). Secondary antibody was applied for 2 hours following wash steps at the following dilutions: goat α-rabbit (1:4000, Abcam ab97069). Precongugated β-actin-HRP (1:40,000, Sigma-Aldrich cat. A3854) was applied for 20 minutes and used as loading control. Western blot densitometry analysis was done using ImageJ(Rasband 2008).

RNA-sequencing

Total RNA from mock- and miR-30bcd LNA-treated HIECs was isolated at 24, 48, and 72 hours post-transfection. RNA quality was assessed using Agilent RNA Nano 6000 kit (Agilent Technologies, Inc, Santa Clara, CA) then run on a Bioanalyzer 2100 (Agilent). All

samples had high RNA integrity numbers (RINs), with RINs above 9.2 (with an average of 9.7). Samples were submitted to the UNC High Throughput Sequencing Facility (HTSF) for TruSeq Stranded Total RNA library preparation (Illumina, San Diego, CA) and paired-end 50 bp sequencing on a HiSeq 2000 (Illumina) multiplexing 6 samples per lane.

Bioinformatics

Following sequencing and demultiplexing by the UNC HTSF, reads were aligned to the hg19 genome using MapSplice(K. Wang et al. 2010), and transcripts quantified using RSEM(B. Li and Dewey 2011) by the UNC Bioinformatics Core Facility. Samples had an average of 119M reads, with 94.6% of reads uniquely mapping. Differential gene expression analysis was conducted using edgeR(Robinson et al. 2009). Genes with low expression (CPM < 10 in more than half the samples) were filtered out of our analysis. Gene counts were then TMM normalized and evaluated for differential gene expression. Raw sequencing data, as well as the raw and normalized counts tables are available through GEO (Accession # GSE79923).

Results

miR-30 is predicted to target SOX9 and is robustly expressed in the IE

We carried out a bioinformatic strategy using TargetScan6.2(Lewis et al. 2005; Grimson et al. 2007; Friedman et al. 2009; Garcia et al. 2011) to predict miRNA target sites in the *SOX9* 3'UTR that are conserved between mouse and human. We identified putative target sites for nine miRNA families. To narrow this list of possible miRNA regulators of *SOX9* in the IE, we analyzed the only dataset of publically available small RNA-sequencing data from mouse intestinal mucosa(McKenna et al. 2010). Only four miRNA families were expressed at a

minimum of 10 reads per million mapped (RPMM): miR-145, miR-101, miR-320, and miR-30 (Figure 4.1A). Of these, miR-30 has the strongest predicted base pairing with *SOX9*, consisting of an 8-mer seed as well as supplementary 3'-end pairing for two of the family members. Moreover, the miR-30 target site and flanking ~15 bases are highly conserved among most mammals including human, rodent, dog, opossum, and horse, as well as distant vertebrates such as lizard.

Because the intestinal mucosa includes diverse cell types not limited to epithelia, we next sought to evaluate the expression of the members of these four miRNA families across four main epithelial cell types. Specifically, we sorted functionally distinct IECs by fluorescence-activated cell sorting (FACS) from the jejunum of female conventionally raised *Sox9-EGFP* mice. This model allows for the isolation of four populations based on cellular EGFP, including EECs ($Sox9^{High}$), IESCs ($Sox9^{Low}$), transit amplifying cells ($Sox9^{Sublow}$), and differentiated enterocytes, Paneth and goblet cells ($Sox9^{Negative}$). We then performed RT-PCR for each of the four miRNA families across each IEC population. miR-101 and miR-145 were very lowly expressed, indeed barely detected, in any cell type of the IE (Figure 4.1B). It is worth noting that while miR-145 was reported to have robust expression in the McKenna *et al*. (2010) study of the entire intestinal mucosa, it was recently demonstrated that miR-145 is specific to mesenchymal cells in the intestine(Chivukula et al. 2014). By using FACS, we obtain a highly pure epithelial population, whereas the earlier McKenna *et al*. (2010) data was generated using an intestinal scraping method, which could lead to some mesenchymal, lymphatic, and/or vascular contamination. Based on these differences, we conclude that it is likely that both miR-145 and miR-101 are robustly expressed in a non-epithelial mucosal tissue, but not in IECs. In contrast, members of the miR-30 family and miR-320a showed robust expression in IECs (Figure 4.1B). Moreover,

only miR-30 family members exhibited differential expression across functionally distinct IECs, leading us to select this miRNA family for follow-up analyses.

Knockdown of miR-30 *in vitro* results in increased *SOX9* mRNA expression but decreased levels of SOX9 protein

To evaluate miR-30 regulation of *SOX9* in IECs, we knocked down miR-30 expression using LNAs complementary to miR-30b, miR-30c, and miR-30d (LNA30bcd) in human intestinal epithelial cells (HIECs). Upon knockdown of these miR-30 family members, we observed a significant increase in *SOX9* mRNA at 48 and 72 hours post-transfection (Figure 4.2A), which is consistent with alleviation of negative post-transcriptional regulation of *SOX9* by miR-30. However, we unexpectedly found that SOX9 protein was significantly down-regulated (Figure 4.2A & 4.2B). In fact, *SOX9* mRNA and protein expression were strongly inversely correlated (Pearson's $r = -0.93$, $p = 0.006$, Figure 4.2A) across three time points post-transfection with LNA30bcd. We confirmed that this inverse relationship between *SOX9* mRNA and protein exists in a second intestinal cell culture model, Caco-2 (Figure 4.2B), indicating that the finding is not unique to HIECs. To test for a direct relationship between miR-30 and the *SOX9* 3'UTR, we performed a luciferase reporter assay in Caco-2 cells. We observed increased relative luciferase activity in cells transfected with 100 ηM LNA30bcd (Figure 4.2D), consistent with direct targeting of *SOX9* by miR-30 that has been previously shown in cartilage(Chang et al. 2016). We hypothesized that the opposite effect of miR-30 inhibition on SOX9 mRNA and protein levels could be due to miR-30-mediated regulation of factors that modify SOX9 protein stability without affecting *SOX9* RNA levels, such as post-translational modifiers (Figure 4.2E).

Next-generation high-throughput RNA-sequencing reveals that miR-30 regulates genes enriched in the ubiquitin ligase pathway

To evaluate this hypothesis, we next sought to define the regulatory program that miR-30 directs in HIECs and to identify potential miR-30 targets that may be regulating SOX9 protein levels. Specifically, we performed next-generation high-throughput RNA-sequencing on total RNA isolated from mock- and LNA30bcd-transfected HIECs at three time points (see Methods). Following read alignment and transcript quantification, we identified DE genes using edgeR(Robinson et al. 2009). To avoid bias from lowly expressed genes, we filtered out genes that did not reach an expression threshold of 10 counts per million (CPM) in at least three of the samples. A total of 10,096 genes were included in our analysis. We first normalized gene counts using the generalized linear model (GLM) in edgeR in order to account for both the treatment and time variables in our experimental design. Samples were tightly clustered by treatment and time point according to multidimensional scaling, principal components, and hierarchical clustering analyses (Figure 4.3A, 4.3B, & 4.3C). Notably, cells treated with 100 ηM LNA30bcd at 24 hours post-transfection clustered with mock-transfected samples (Figure 4.3C).

However, cells treated with 100 ηM LNA30bcd at 48 and 72 hours post-transfection clustered into a distinct subclade, indicating that the regulatory effect of LNA30bcd was greatest at the later time points. Next, we performed differential expression analysis, and found that half of all genes (50.1%, or 5055) included in the analysis are significantly DE (FC ± 1.5 & FDR < 0.05) between mock- and LNA30bcd-transfected cells in at least one time point post-transfection (Figure 4.4A-C, Supplemental Table 4.1[†]). Notably, while *SOX9* was found to be upregulated as expected by LNA30bcd treatment at 72 hours post-transfection, it was certainly not the most

[†] Supplemental Table 4.1 & 4.2 are available with the published version of this article, online at http://www.jbc.org/content/early/2016/06/03/jbc.M116.733733/suppl/DC1

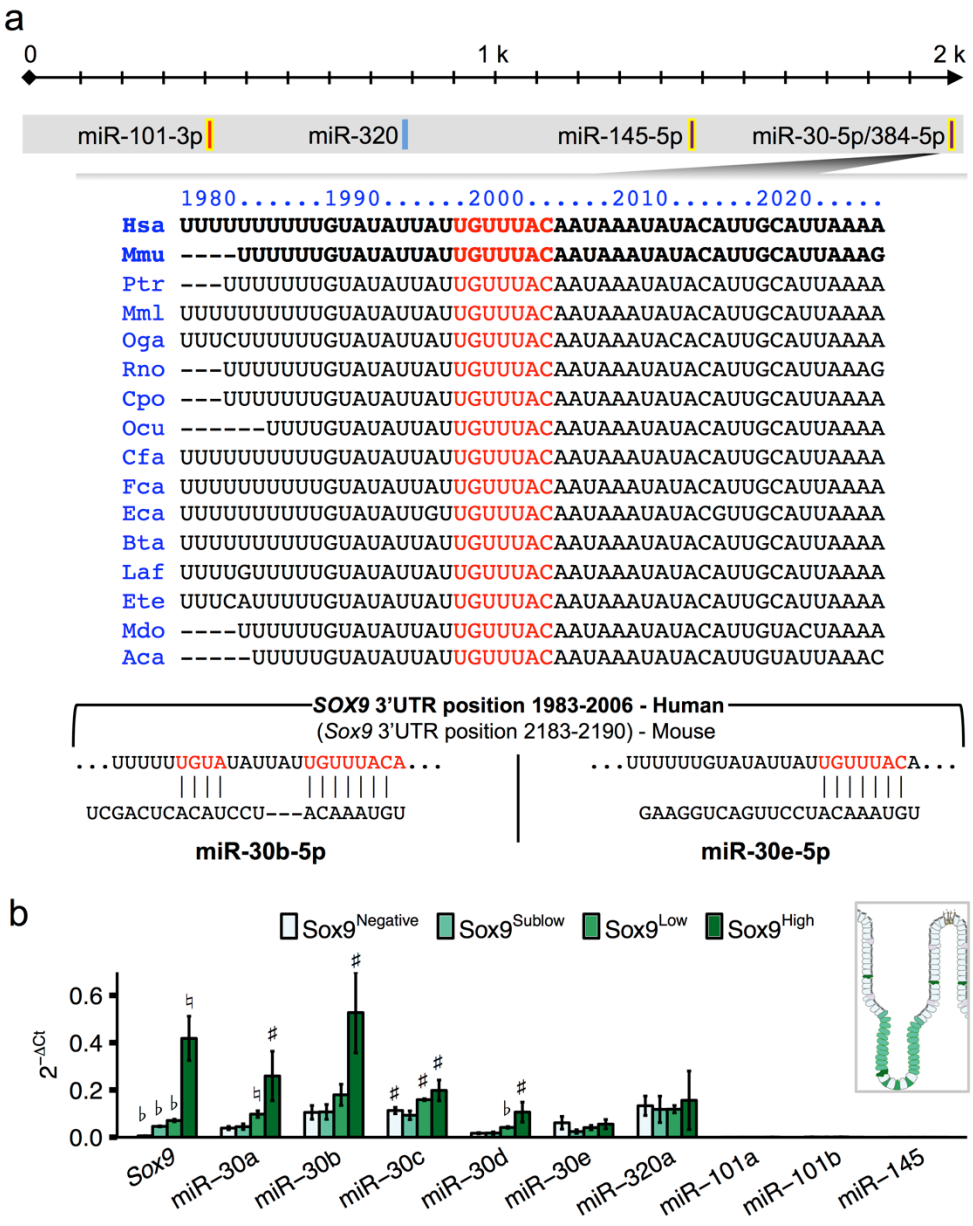

Figure 4.1. miR-30 is predicted to target the 3'UTR of *SOX9* and is differentially expressed across functionally distinct cell types of the intestinal epithelium. (**A**) Cartoon depicting the *SOX9* 3'UTR. miRNAs with predicted target sites conserved between mouse and human are labeled. Below, we show the conservation of the predicted miR-30 target site (red text) across various species (TargetScan6.2). miR-30b and miR-30e targeting are shown in detail with predicted base paring colored in red. (**B**) RT-PCR of *Sox9* and miRNAs with predicted target sites in the *Sox9* 3' UTR across functionally distinct mouse jejunal intestinal epithelial cells (n = 2-4). Significance determined by Students two-tailed paired t-test relative to non-sorted intestinal epithelial cells. $^{\flat}p < 0.001$, $^{\natural}p < 0.01$, $^{\#}p < 0.05$.

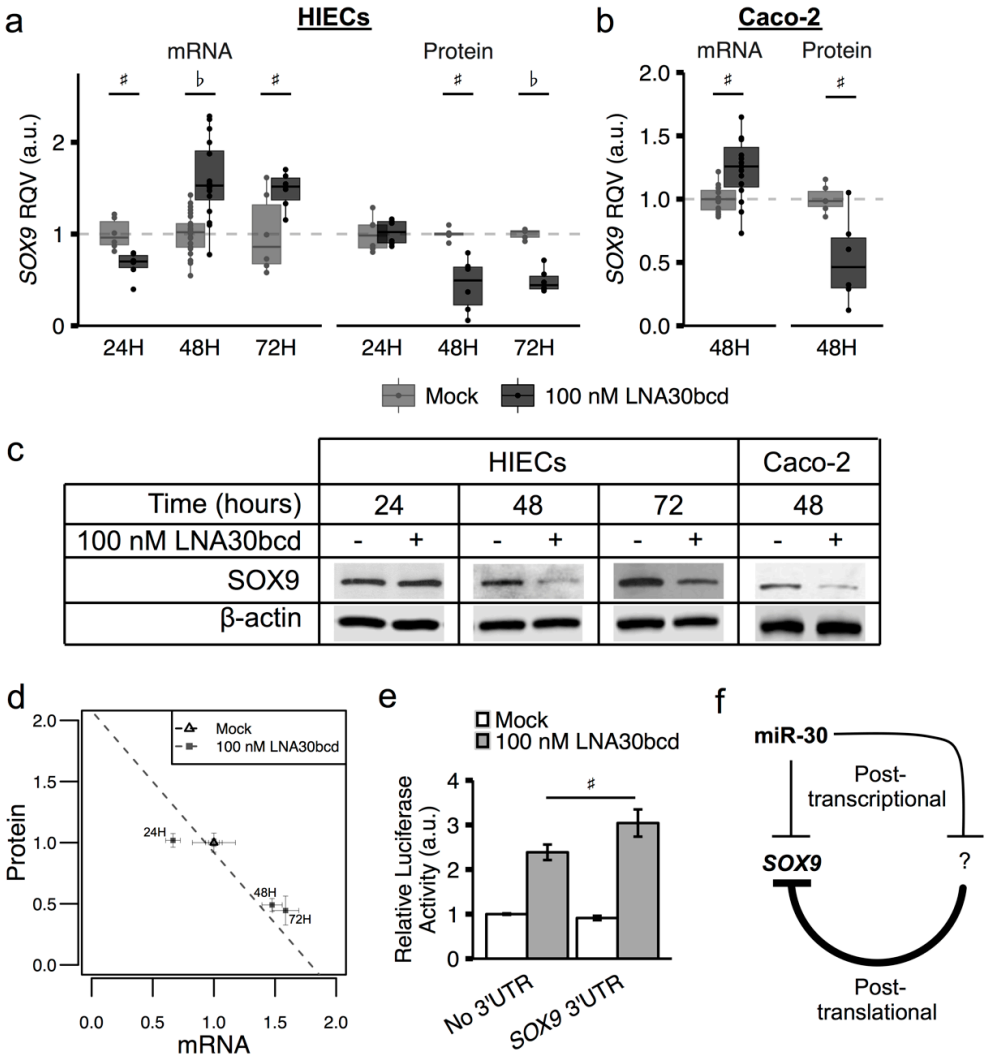

Figure 4.2. Knockdown of miR-30 increases *SOX9* mRNA and decreases SOX9 protein expression. (**A**) Relative quantitative value (RQV), across three time points, of *SOX9* mRNA by RT-PCR (left) and protein by Western blot densitometry (right) in HIECs upon either mock-transfection or 100 ηM LNA30bcd-transfection. (**B**) RQV of *SOX9* mRNA by RT-PCR (left) and protein by Western blot densitometry (right) in Caco-2 cells upon mock transfection or 100 ηM LNA30bcd transfection after 48 hours (mock and 100 ηM LNA30bcd mRNA n = 15 each, protein n = 6 each). (**C**) Images of representative western blots are shown for the protein expression data shown in panels (**A & B**). (**D**) Correlation of mean RQVs of SOX9 mRNA and protein across time points and transfection conditions. (**E**) Relative firefly luciferase activity in Caco-2 cells at 48 hours after transfection with plasmids encoding both firefly (with and without the *SOX9* 3'UTR) and renilla luciferase genes. Caco-2 cells were subjected to either mock co-transfection or 100 ηM LNA30bcd co-transfection (n = 10-11 each). (**F**) Model of miR-30 regulation of SOX9 in the intestinal epithelium. For panels (**A & B**), a standard box-and-whisker plot is shown, with shaded box indicating interquartile range (IQR), thick horizontal line showing median, and extending whiskers showing maximum and minimum points within 1.5*IQR. Actual data points are plotted as filled circles superimposed on their respective box-and-whisker plots.

robustly or significantly altered gene (Figure 4.4D).

To evaluate the efficacy of our knockdown, we performed analysis with miRhub(Baran-Gale et al. 2013; Kurtz et al. 2014; Peck et al. 2015), which tests for miRNA target site enrichment among specific genes of interest. We found that both highly conserved and species-specific predicted miR-30 targets sites were significantly enriched ($p < 0.05$) in genes upregulated at both 48 and 72 hours post-transfection, but as expected not in down-regulated genes (Figure 4.4E). At 24 hours post-transfection, predicted miR-30 target sites were not enriched. Together, these data suggest that our knockdown of miR-30 using LNA30bcd was specific and highly effective in HIECs, particularly in the later time points of our study.

To identify genes that might act as post-translational regulators of SOX9 protein in response to LNA30bcd treatment, we performed Gene Ontology (GO) Molecular Function enrichment analysis(Ashburner et al. 2000; Gene Ontology Consortium 2015) using Enrichr(E.Y. Chen et al. 2013) on genes with predicted miR-30 target sites that were significantly upregulated ($FC > 1.5$ & $FDR < 0.05$) relative to mock-treated cells at each time point (see Supplemental Table 4.2 for gene lists). Only three terms were identified as being significantly enriched (adjusted p-Value < 0.05; Figure 4.5A & 4.5B) at any time point in the upregulated gene sets. Interestingly, these included 'ubiquitin-protein transferase activity' and 'ligase activity.' Ubiquitin ligase mediated regulation of SOX9 has been shown previously in chondrocytes(Hattori et al. 2013), and therefore is consistent with our hypothesis that miR-30 may regulate SOX9 protein levels indirectly through control of post-translational modifiers of SOX9.

To evaluate whether miR-30 influences ubiquitin ligase mediated degradation of SOX9 protein, we subjected Caco-2 cells to either mock or LNA30bcd transfection and then treated

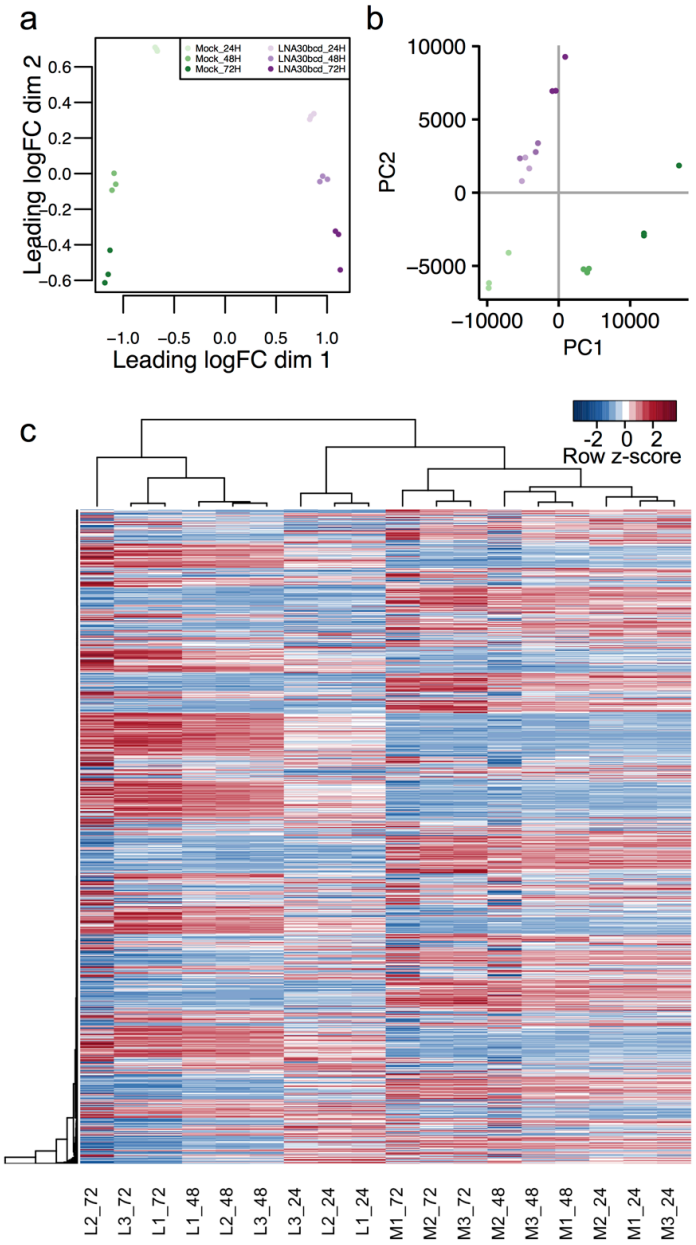

Figure 4.3. Next-generation high-throughput RNA-sequencing of LNA30bcd treated HIECs (**A**) Multi-dimensional scaling plot of normalized reads (counts per million or CPM > 10 in 3+ samples) in HIECs subjected to either mock-transfection or 100 ηM LNA30bcd-transfection at 24 hours (24H), 48 hours, (48H) and 72 hours (72H) post-transfection, n = 3 each. (**B**) Principal components analysis of normalized reads (CPM > 10 in 3+ samples) across all time points and transfection conditions. (**C**) Heat map showing all genes with CPM > 10 in 3+ samples (n = 10,096). Samples are hierarchically clustered by Euclidean distance. For each column, samples are listed along the bottom, with the first letter indicating mock (M) or 100 ηM LNA30bcd (L) treated HIECs, followed by the replicate number (1-3), and the time point post-transfection (24, 48, or 72 hours).

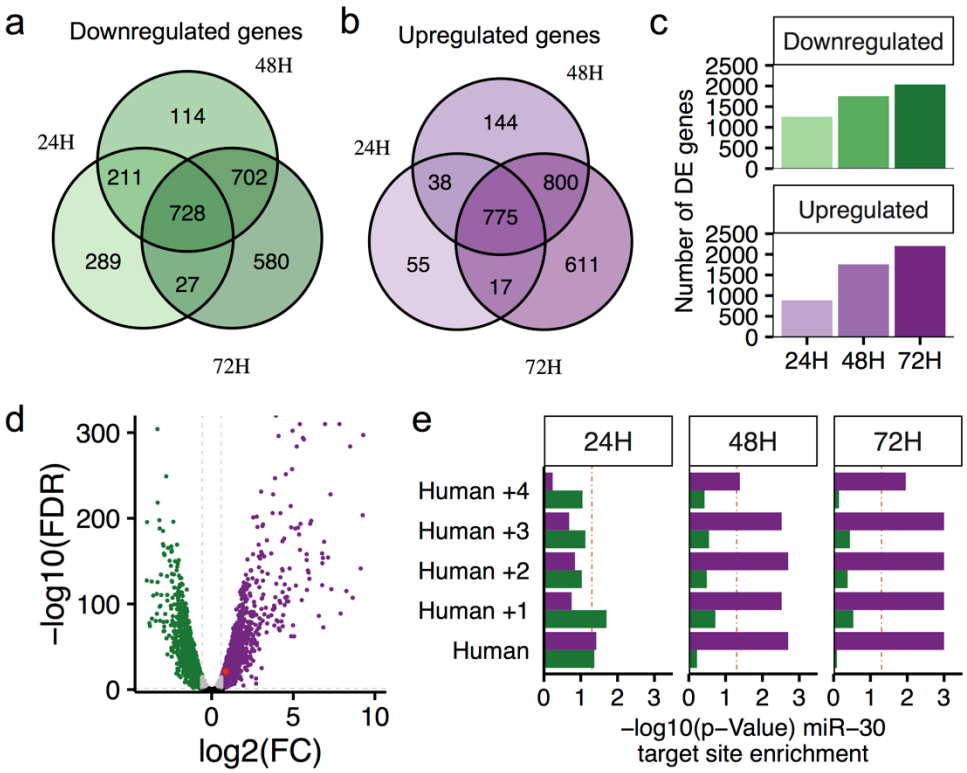

Figure 4.4. LNA30bcd-treated HIECs undergo robust changes in gene expression over a three-day time course. (A) Venn diagram s showing significantly down-regulated genes (fold-change or FC < -1.5, FDR < 0.05) across time points in HIECs after 100 ηM LNA30bcd transfection compared to mock transfection. (**B**) Venn diagram showing significantly up-regulated genes (FC > 1.5, FDR < 0.05) across time points in HIECs after 100 ηM LNA30bcd transfection compared to mock transfection. (**C**) Bar graph showing the number of significantly downregulated and upregulated genes across time points. (**D**) Volcano plot showing differentially expressed genes at 72H. Red dot shows *SOX9*. Horizontal dashed line shows p = 0.05, and vertical dashed lines indicate FC = -1.5 and 1.5. (**E**) Results of miRhub analysis to test for enrichment of predicted miR-30 target sites in significantly upregulated (purple) and downregulated (green) genes at each time point. Our analysis was run human-centric. Each row indicates the conservation of the miRNA target site on the gene list, with "Human" indicating a site found in human genes, while "Human+1" indicates a site found in human genes and conserved in one additional species, and so on. Vertical dashed line (red) indicates empirical p = 0.05.

them with vehicle or MG132, a potent proteasome inhibitor. We found that MG132 treatment for 4 hours was sufficient to rescue SOX9 protein expression following LNA30bcd treatment (Figure 4.5C). This suggests that miR-30 is able to regulate SOX9 protein expression through post-transcriptional regulation of ubiquitin ligases (Figure 4.5D).

miR-30 promotes IEC proliferation and inhibits IEC differentiation

Based on previous work, altered levels of SOX9 are expected to lead to changes in the balance between proliferation and differentiation(Bastide et al. 2007; Belo et al. 2013; Shi et al. 2013). Therefore, given the strong regulatory effect of miR-30 on SOX9 protein, we hypothesized that treatment of HIECs with LNA30bcd would affect this balance as well. Notably, we found by analysis of the RNA-seq data in the HIECs that the expression of genes previously associated with regulation of proliferative balance in the IE (Figure 4.6A), including *CTNNB1*(Mologni et al. 2010), *DLL4*(He et al. 2015), and *LGR4*(Mustata et al. 2011), were significantly reduced. Consistent with this observation, we found that knockdown of miR-30 significantly reduces HIEC proliferation, as measured by H^3-thymidine uptake (Figure 4.6B). At 48 hours post-transfection, HIECs showed a 65% reduction in H^3-thymidine uptake after treatment with 100 ηM of LNA30bcd ($p < 0.001$; Figure 4.6B).

Given the reduced proliferation and reduced expression of proliferative markers, we hypothesized that treatment with LNA30bcd may promote differentiation of IECs. We evaluated differential expression of genes known for their role in regulating differentiation in the IE using the RNA-seq data. Interestingly, we observed a 5-fold increase in *HES1* expression in HIECs transfected with 100 ηM LNA30bcd (Figure 4.6B). *HES1* is an early marker of enterocyte differentiation in the IE(Noah et al. 2011). The Caco-2 cell line is one of very few cell models that will spontaneously differentiate into small intestinal enterocyte-like cells and express key

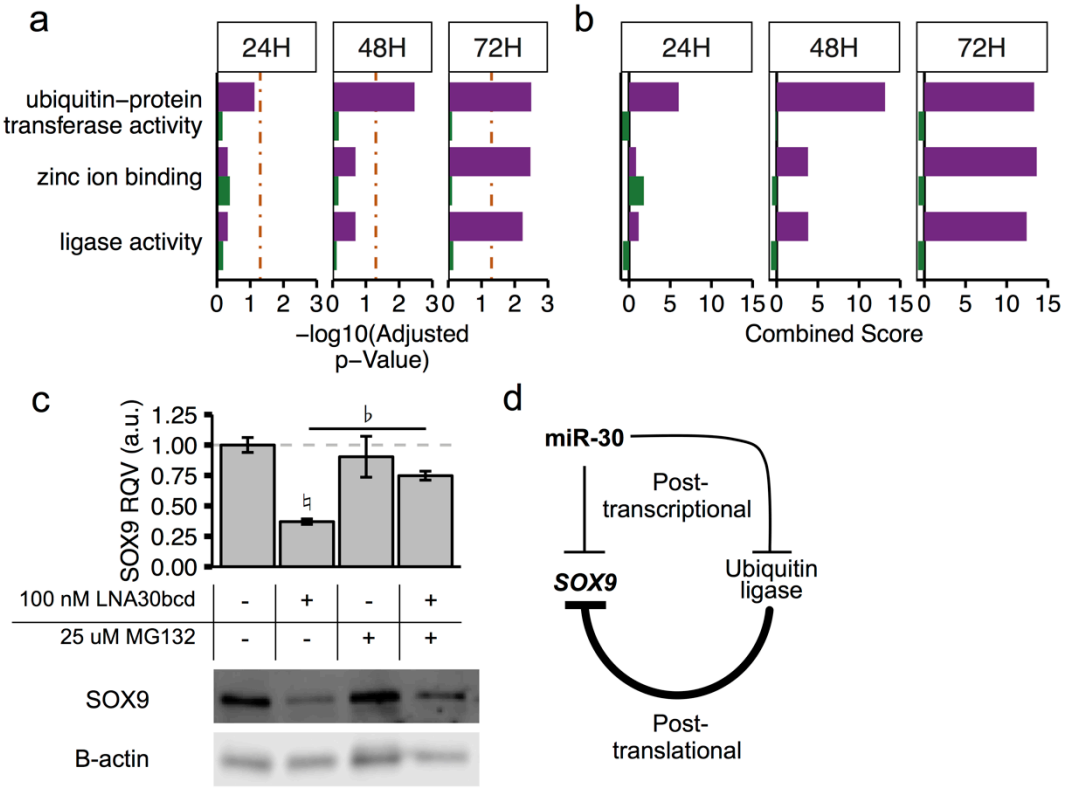

Figure 4.5. miR-30 target genes in intestinal epithelial cells are over-represented in the ubiquitin ligase pathway. (**A & B**) Gene Ontology Molecular Function enrichment analysis using Enrichr identifies three terms as enriched in the upregulated gene lists across time points. p-value (**A**) and combined scores (**B**) are shown for upregulated (purple) and downregulated (green) gene lists. (**C**) Relative SOX9 protein expression in Caco-2 cells subject to mock transfection (n = 2 each) or 100 ηM LNA30bcd transfection (n = 3 each) at 72 hours post-transfection following 4 hours of treatment with either 25 μM MG132 or vehicle (DMSO). Below, representative western blot. (**D**) Cartoon showing model of miR-30 regulation of SOX9 mRNA and protein expression levels.

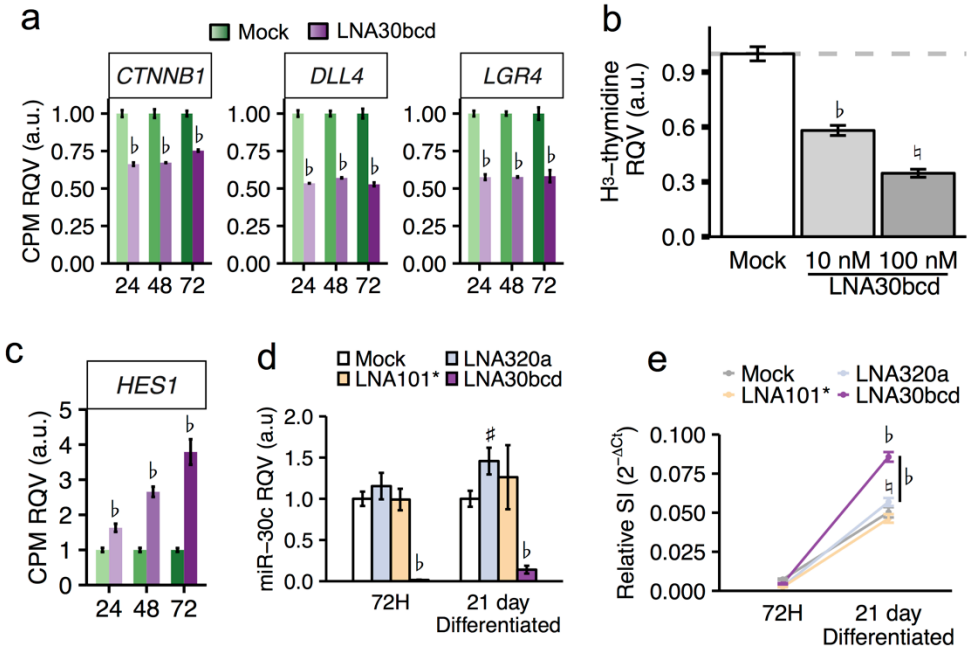

Figure 4.6. miR-30 promotes proliferation and inhibits enterocyte differentiation. (**A**) Relative quantitative value (RQV) of mean counts per million (CPM) of markers of proliferation in 100 ηM LNA30bcd treated HIECs across time points. Significance determined by using edgeR generalized linear model (GLM) accounting for treatment and time. ♭False Discovery Rate (FDR) < 0.001, ♮FDR < 0.01, ♯FDR < 0.05. (**B**) RQV of H^3-thyimidine incorporation in HIECs subjected to mock transfection or LNA30bcd transfection (10 ηM or 100 ηM) at 48 hours post-transfection (n = 12 each). Significance determined by two-tailed unpaired Student's t-test. ♭p < 0.001, ♮p < 0.01, ♯p < 0.05. (**C**) RQV of mean CPM of Hairy and Enhancer of Split 1 (*HES1*) in 100 ηM LNA30bcd-treated HIECs across time points (n = 3 each). Significance determined by GLM accounting for treatment and time. ♭FDR < 0.001, ♮FDR < 0.01, ♯FDR < 0.05. (**D**) RQV of miR-30c by RT-PCR in Caco-2 cells at 72 hours and 21 days after either mock transfection (72H n = 9, 21 days n = 6), 100 ηM LNA30bcd transfection (72H n = 9, 21 days n = 6), 100 ηM LNA101* (72H n = 6, 21 days n = 3), or 100 ηM LNA320a (72H n = 9, 21 days n = 6). Significance determined using two-tailed unpaired Students t-test. ♭p < 0.001, ♮p < 0.01, ♯p < 0.05. (**E**) RQV of Sucrase Isomaltase (*SI*) by RT-PCR in in Caco-2 cells at 72 hours and 21 days after either mock transfection (72H n = 9, 21 days n = 8), 100 ηM LNA30bcd (72H n = 9, 21 days n = 9), 100 ηM LNA101* (72H n = 6, 21 days n = 6), or 100 ηM LNA320a (72H n = 9, 21 days n = 9). Significance determined using two-tailed unpaired Students t-test. ♭p < 0.001, ♮p < 0.01, ♯p < 0.05.

markers of mature enterocytes upon reaching confluency(Van Beers et al. 1995; Borchardt 2011). To test whether miR-30 regulates enterocyte differentiation of IECs, we transfected Caco-2 cells with 100 ηM LNA30bcd, and allowed the cells to differentiate on transwell membranes (see Methods). With a single transfection of LNA30bcd, we observed significant and sustained knockdown of miR-30 levels for 21 days, the latest time point measured (Figure 4.6D). At 21 days post-transfection, we also observed that Caco-2 cells transfected with LNA30bcd expressed significantly higher levels of sucrose isomaltase (*SI*), a classic marker of differentiated enterocytes(Zweibaum et al. 1983), compared to mock transfected cells or those transfected with LNAs against other miRNAs (Figure 6E). Taken together, our data suggest that miR-30 normally acts to promote proliferation and inhibit enterocyte differentiation in the IE through a broad regulatory program that includes the proteasome pathway.

Discussion

In this study, we sought to investigate miRNA control of intestinal epithelial proliferation and differentiation. Our starting point was to identify miRNAs that might regulate SOX9, a key transcription factor in intestinal epithelial homeostasis. We focused on miR-30 because it has a *SOX9* target site that is broadly conserved across vertebrates, including human and rodent, and it is robustly and variably expressed among stem, progenitor, and differentiated cell types of the IE. Upon knockdown of miR-30 in two intestinal-relevant cell lines, we unexpectedly found inverse effects on SOX9 mRNA and protein expression. We performed next-generation high-throughput RNA-sequencing and found that the upregulated genes with predicted miR-30 target sites were most significantly enriched for ubiquitin ligases. Post-translation regulation of SOX9 by UBE3A has been described previously(Hattori et al. 2013). Moreover, UBE3A does have a predicted miR-30 target site, and is upregulated in LNA30bcd-treated HIECS. However, the

predicted miR-30 target site in *UBE3A* is human specific. It is therefore possible that the inverse relationship between *SOX9* mRNA and protein in response to LNA30bcd treatment is human specific. More research will be needed to identify the specific miR-30-directed ubiquitin ligase protein that acts on SOX9 protein in IECs.

Knockdown of the miR-30 family in HIECs and Caco-2 cells resulted in reduced proliferation and enhanced enterocyte differentiation. This finding is consistent with the relatively higher expression levels of miR-30 in proliferating subpopulations, such as the progenitors, compared to non-proliferating enterocytes (Figure 4.1B). Previous literature investigating the role of miR-30 suggests a dosage and cell type-specific response on proliferation. While increased proliferation has been seen in many cancer cells in response to reduced miR-30 levels, studies have found knockdown of miR-30 result in decreased proliferation(Agrawal et al. 2009). In terms of differentiation, the miR-30 family has been shown to regulate myogenic and osteoblastic differentiation. Upregulation of miR-30 family members in myoblasts promotes differentiation(Guess et al. 2015). Alternatively, knockdown of miR-30 in an osteoblast precursor cell line promotes differentiation(T. Wu et al. 2012). Our results, and those of previous studies, emphasize the importance of conducting cell type-specific analyses on miRNA regulatory networks. Moreover, further research is warranted to evaluate miR-30 regulatory networks in the IE *in vivo*.

More broadly, our RNA-sequencing revealed a complex and widespread network of genes influenced by knockdown of a single miRNA family. Through time-course mRNA profiling following knockdown of a single miRNA family, we found that the effect of treatment with LNA30bcd on miR-30 target genes was only beginning to emerge at 24 hours, evident at 48 hours, and very robust at 72 hours post-transfection. Most studies using LNAs against target

miRNAs evaluate knockdown and gene expression changes at a single time point post-transfection. It is clear from our data that there are highly variable effects of miRNA knockdown across a span of only two days, emphasizing the importance of evaluating multiple time points following treatment with LNAs. In Caco-2 cells we observed significant knockdown of miR-30 even 21 days following a single transfection with LNA30bcd; therefore, it would of interest to evaluate gene expression at this time point to determine whether the effects on miR-30 target genes are still robust. Detailed time-course studies may help elucidate the short-term and long-term effects of LNA treatment, which has relevance both for experimental design and for therapeutic development.

Our analyses provide new evidence that miR-30 plays a significant role in regulating proliferation and differentiation in the IE. Further analyses *in vivo* (mouse) or through *ex vivo* culture systems (mouse or human) are warranted to extend the definition of miR-30's function across distinct cell types of the IE in health and disease. This study represents one of the very first to investigate the regulatory activity of a specific miRNA in IECs using a highly interdisciplinary strategy, and therefore provides a blueprint for similar studies of other miRNAs.

Importantly, given the heterogeneity of cell types within the IE, other miRNAs are also likely to be important regulators of IEC function, and many may have cell type-specific functions. However, there is a dearth of information regarding miRNA expression in distinct cell populations of the IE. In 2010, McKenna *et al*. published the only small RNA-sequencing data from mouse intestine(McKenna et al. 2010), which motivated some of the follow-up studies in this chapter; however, McKenna *et al*. investigated whole mucosa and did not assay functionally distinct IEC types separately. Understanding the expression of miRNAs across cell types of the IE and in response to environmental stimuli would lay the groundwork for understanding their

functions in the context of health and disease. Moreover this knowledge would fill a vital knowledge gap in the development of therapeutics toward the treatment of GI diseases.

CHAPTER 5 – MICRORNA PROFILING IN INTESTINAL EPITHELIAL SUBPOPULATIONS AND FUNCTIONAL STUDIES IN ENTEROIDS IDENTIFY GUT MICROBIOTA-RESPONSIVE MIR-375 AS A CANDIDATE REGULATOR OF STEM CELL PROLIFERATION[1]

The IE is a single layer of cells exposed to the intestinal lumen, and is composed of multiple cell types including the proliferative IESCs and progenitor cells (also known as transit amplifying cells), as well as differentiated absorptive enterocytes and secretory goblet, Paneth, and EECs (Figure 5.1A). IESCs divide to yield more rapidly proliferating progenitors that give rise to all of the other IEC types and drive continuous renewal of the IE every ~3-5 days(Creamer et al. 1961). Proper renewal facilitates important intestinal epithelial functions including barrier integrity to protect against invasion of harmful toxins present in the intestinal lumen, nutrient digestion and absorption, and the production of hormones that regulate systemic energy homeostasis. These physiological processes are mediated in part by interactions with resident microbiota(Velasquez-Manoff 2015). Studies using GF animals have demonstrated that gut microbiota influence intestinal barrier function, nutrient absorption, proliferation, differentiation, cellular signaling, and migration(Jaladanki and J.Y. Wang 2011; Everard and Cani 2014). However, the molecular factors and mechanisms underlying microbiota-mediated control of IEC functions, particularly IESC proliferation, are unknown.

[1] Portions of this chapter will be submitted for publication in a peer-reviewed journal. The full manuscript is available on the preprint server, bioRxiv. See: Peck, B. C., Mah, A. T., Pitman, W. A., Ding, S., Lund, P. K., and Sethupathy, P. (2016) Functional transcriptomics in diverse intestinal epithelial cell types reveals robust gut microbial sensitivity of microRNAs in intestinal stem cells. *bioRxiv*. http://dx.doi.org/10.1101/087882.

microRNAs (miRNAs) have emerged as critical regulatory factors of many biological processes in numerous tissues and are known to confer phenotypic robustness in response to environmental stimuli. However, less is known about miRNA expression and function in the IE when compared to most other tissues. Recently, however, miRNAs were implicated in the regulation of IEC physiology. McKenna *et al*. (2010) demonstrated in mice that the IEC-specific knockout of *Dicer1*, an essential enzyme for canonical miRNA biogenesis, results in altered IEC proliferation, differentiation, nutrient absorption, and impaired barrier function, indicating that miRNAs are likely important modulators of intestinal homeostasis(McKenna et al. 2010). Furthermore, the presence of microbiota in the gut has been shown to alter miRNA expression profiles in intestinal macrophages(D. Wang et al. 2012), as well as in whole intestine tissue(Dalmasso et al. 2011; Archambaud et al. 2013). Understanding the mechanisms by which microbiota regulate miRNA expression in IESCs and other IEC subtypes will elucidate a critical molecular network that controls intestinal homeostasis and, given the heightened interest in miRNA-based therapies, may offer novel therapeutic strategies in the treatment of GI diseases associated with altered IESC function. However, to our knowledge no study to date has investigated miRNA expression and activity across the functionally distinct IEC subtypes, and cell type-specific effects of microbiota on miRNAs is completely unknown. We hypothesized that each IEC subtype has a distinct miRNA profile, and that miRNAs respond to gut microbiota in a cell type-specific manner in order to control function and overall homeostasis of the IE.

Research Design and Methods

Animals

The University of North Carolina at Chapel Hill's Institutional Animal Care and Use Committee approved all animal studies. The original source (GENSAT Brain Atlas Project) and

maintenance of *Sox9-EGFP* mice have been described elsewhere(Formeister et al. 2009; Gracz et al. 2010; Van Landeghem et al. 2012). Sox9-EGFP mice on a C57BL/6J background were generated by the P. Kay Lund Laboratory by crossing Sox9-EGFP mice on a CD1 background wih a C57Bl/6J mice for 10 generations. Germ-free (GF) animals were generated at the UNC Gnotobiotic Core Facility. Four pairs of female GF littermates were used in these experiments at 8-10 weeks of age. A single sex, female, was selected for these initial experiments for a number of reasons, including cost. This sex was selected because experiments in the Sethupathy lab have previously focused on female mice, and comparability across experiments in the lab and the power to determine differential miRNA expression was of paramount. Future studies will evaluate males. Each littermate pair came from separate litters born between April and July 2015. GF mice were housed with animals of the same sex from the same litter, on Envigo 7070C Tekland Diamond Dry Cellulose bedding. Four age-matched, conventionally-raised Sox9-EGFP animals and wild-type C56BL/6J animals were included as controls in each individual FACS experiment. Crypt culture studies were performed using female conventionally-raised C56BL/6J and GF Sox9-EGFP animals. For HFD experiments, conventionally-raised Sox9-EGFP animals on a C57BL/6J background were maintained beginning at 8 weeks of age on either a 45% kcal from fat HFD (Research Diets #D12451) or normal chow diet (ProLab RMH 3000). Animals were monitored for weight gain each week. Fasting blood glucose was taken from HFD and chow-fed animals after 16 weeks on diet. Animals were sacrificed and IECs isolated for FACS after 20 weeks on diet. Conventionally-raised mice were bedded on Andersons irradiated ¼ inch Bed-O'cobs laboratory animal bedding.

Conventionalization (CV)

For each littermate pair, 0.2 - 0.7 g of fresh fecal pellets were collected on separate days

from multiple animals across 6-8 cages in the conventionally-raised Sox9-EGFP animal colony housed at UNC and were frozen at -80°C until reconstitution. Less than one hour before conventionalization, the fecal sample was thawed on ice and then reconstituted at 1 g/10 mL cold PBS under anaerobic conditions. The fecal slurry was passed through a 100-μm filter to remove debris and 1 mL was aliquoted into a fresh microcentrifuge tube. For each littermate pair, one GF animal was conventionalized using prepared fecal slurry and administered by oral gavage at 10 μL/g body weight. To ensure conventionalization, whiskers and anus were swabbed and the remaining slurry was painted onto several pieces of food left on the bottom of the animal's cage. Conventionalized animals were housed individually throughout the duration of conventionalization with access to food and water ad libitum. Conventionalized mice were bedded on Andersons irradiated ¼ inch Bed-O'cobs laboratory animal bedding.

IEC isolation and fluorescence-activated cell sorting (FACS)

After a two-week conventionalization period, both the CV and GF animals were anesthetized using isofluorane, then euthanized by cervical dislocation. The small intestine was removed and divided into 3 equal sections. The proximal and distal 10 cm were considered duodenum and ileum, respectively. The middle section was considered jejunum and used for all studies. Jejunum was flushed with ice cold PBS to remove contents, and total IEC were prepared for FACS as previously described(Van Landeghem et al. 2012) in Chapter 4. Conventionally-raised age-matched Sox9-EGFP animals were included in each individual sorting experiment and used to set Sox9-EGFP gates. Sox9-EGFP cells were sorted based on Sox9-EGFP intensity directly into RNA lysis buffer (Norgen Biotek, Thorold, ON, Canada). Additionally, non-sorted IECs (NS) were collected for each animal, except one conventionalized mouse (CV314), which did not have enough remaining sample to isolate a NS IEC population. NS IECs were purified by

FACS to exclude non-epithelial and dying cells, but were not sorted based on Sox9-EGFP intensity. Due to the density of cells, $Sox9^{Neg}$ cells were sorted into cell culture media, then pelleted following sorting by centrifugation. Total RNA was isolated using either the Norgen Total RNA kit (for $Sox9^{Neg}$ & NS IECs) or the Norgen Single-Cell RNA Purification kit, which has a smaller column (for low cell number populations including $Sox9^{High}$, $Sox9^{Low}$, $Sox9^{Sublow}$) as per the manufacturer's instructions. Nanodrop 2000 was used to quantify RNA.

mRNA library preparation and sequencing

mRNA-sequencing libraries were prepared from 10 ng total RNA using the Clonetech SMARTer Ultra Low Input library preparation kit combined with Nextera XT DNA sample preparation kit (Illumina) by the UNC High Throughput Sequencing Core Facility (as per the Clonetech sample preparation guide). Four libraries were randomly pooled per lane and sequenced 100 bp single-end on a HiSeq2000 platform at the UNC High Throughput Sequencing Core Facility. Seven bases were trimmed from the beginning of each read using Trimmomatic (v0.36)(Bolger et al. 2014) to eliminate remaining SMART adapter sequences, then reads were aligned to the UCSC mouse transcriptome (mm10) using Salmon (v0.5.1)(Patro et al. 2015)in quasi-mapping-based mode. Transcript counts were then imported into R (v3.1.2), and filtered using edgeR (v3.8.6)(Robinson et al. 2009) to include transcripts with expression of greater than 10 counts per million (CPM) in 4 or more samples. Counts were normalized and differential expression of genes quantified using edgeR. Raw sequencing data as well as counts are available through GEO (Accession #GSE81126).

Small RNA library preparation and sequencing

The small RNA-sequencing was done at the Genome Sequencing Facility of Greehey

Children's Cancer Research Institute at University of Texas Health Science Center at San Antonio. Libraries were prepared using an average of 50 ng of total RNA using the TriLink CleanTag Small RNA Ligation kit (TriLink Biotechnologies, San Diego, CA) and suggested library preparation method. Six to seven libraries were pooled per lane, and were sequenced single-end 50x on the HiSeq2000 platform. One GF Sox9^{Sublow} sample failed during sequencing. However, for the remaining samples, we received an average of 26.5 million reads per sample (range 6.2 - 42.5).

Bioinformatics

Sequencing quality was extremely high as assessed using FASTQC. Reads were trimmed and aligned to the mouse genome (mm9) as previously described(Baran-Gale et al. 2013), with the following modification: only contigs with greater than one read alignment were passed into the Shrimp alignment pipeline. An average of 58.9% of reads mapped to the mouse genome across samples. Due to the large number of reads mapping throughout the genome in the NS IEC sample from mouse CV315, Shrimp failed to align this sample, and it was eliminated from further analysis. Raw sequencing data and miRNA quantification tables for all samples can be accessed through GEO record GSE81126. Annotated miRNAs with a reads per million mapped (RPMM) expression threshold of greater than 100 in at least one sample were used in further analyses. Spearman correlation was determined for all samples, and the correlation matrix was hierarchically clustered using the complete linkage method. One aberrant CV Sox9^{Sublow} sample was identified on the basis of poor clustering by PCA and hierarchical clustering analyses, and was removed from subsequent analyses.

Enteroid culture

Jejunum was isolated and flushed with cold PBS (Gibco cat. 14190-144, ThermoFisher Scientific, Waltham, MA), opened, and divided into 6 cm sections. Sections were placed in cold high-glucose DMEM and rocked to remove excess fecal matter. Each section was then placed in 3 mM EDTA (cat 46-034-Cl, Corning, Corning, NY) diluted in PBS and rocked at 4º C for 15 minutes. The luminal side of the tissue was gently scraped to remove villi and placed into fresh 3 mM EDTA/PBS and rocked an additional 30 minutes at 4º C. Sections were shaken for 2 minutes in ice cold PBS to remove crypts, then filtered through a 70 μm cell strainer and counted. For each well, 400 crypts were resuspended into 10 μL of Reduced Growth Factor Matrigel (cat. 356230, BD Biosciences, Franklin Lakes, NJ) supplemented with PBS or an equal volume of 500 ηM miRCURY LNA Power Inhibitor against miR-375-3p (cat # 4101397, Exiqon, Woburn, MA) or Negative Control A (cat # 199006, Exiqon). Advanced DMEM/F12 (Gibco, ThermoFisher) supplemented with GlutaMAX (Gibco cat. 35050-061, ThermoFisher), Pen/Strep (Gibco cat. 15140, ThermoFisher), HEPES (Gibco cat 15630-080, ThermoFisher), N2 supplement (Gibco cat. 17502-048, ThermoFisher), 1 ηg/μL EGF (cat. 2028-EG, R&D Systems, Minneapolis, MN), 2 ηg/μL Noggin (cat # 250-38, PeproTech, Rocky Hill, NJ), 10 ηg/μL murine R-spondin (cat # 3474-RS-050, R&D Systems), and Y27632 (cat. ALX-270-333-M025, Enzo Life Sciences, Farmingdale, NY) was added. Enteroids were counted at Day 1 and bud formation assessed at Day 4 and Day 8 using an Olympus IX83 Inverted Microscope fixed with a live imaging incubator. Media supplemented with 250 ηM LNA or PBS was changed at Day 4, and growth factors supplemented every other day. Enteroids were harvested at Day 8 and RNA was isolated using the Norgen Total RNA isolation kits as per manufacturers instructions. For whole mount staining, enteroids were fixed in 2% PFA, permeabilized and then stained using

antibodies against PCNA (ab29, 1:500, Abcam, Cambridge, MA) and Ki67 (ab15580, 1:250, Abcam). Nuclear staining was done using Hoechst 33342 (cat. H3570, ThermoFisher). Confocal imaging was performed at the UNC Microscopy Core Facility on a Zeiss CLSM 710 Spectral Confocal Laser Scanning Microscope.

Validation of miRNA expression levels

miRNA expression in the CV and GF animals was validated by qRT-PCR using Taqman assays (Applied Biosystems, Foster City, CA). Relative quantitative value (RQV) is determined relative to control gene *U6*.

Linear Model

The model covariates include cell type, *T*; condition, *C*; littermate pair, *P*; and sequencing group, *G*; as well as an interaction term between cell type and condition (1).

$$Y_{miR} = \beta_0 + \beta_T\chi_T + \beta_C\chi_C + \beta_{Interaction}\chi_T * \chi_C + \beta_P\chi_P + \beta_G\chi_G + \varepsilon_{miR} \quad (1)$$

To determine significance, a multiple testing correction (False Discovery Rate) was performed on p-values for each covariate across all miRNAs.

Results

GF animals have fewer stem and more EECs

To evaluate miRNA expression and response to microbiota in functionally distinct IEC subpopulations, we used the well-characterized Sox9-EGFP transgenic mouse model, which permits the isolation and analysis of four IEC populations using FACS based on differing levels of cellular EGFP intensity (Figure 5.1C). These are $Sox9^{Low}$ (actively cycling IESCs), $Sox9^{Sublow}$ (progenitor cells), $Sox9^{Neg}$ (mostly differentiated enterocytes as well as goblet cells and Paneth

cells), and Sox9^{High} (primarily EECs as well as reserve/quiescent stem cells)(Formeister et al. 2009; Gracz et al. 2010; Van Landeghem et al. 2012; Andres et al. 2013; Mah et al. 2014). To assess the effect of microbiota on these distinct IEC populations, we used four pairs of GF Sox9-EGFP littermates. One littermate from each pair was randomly selected at 8 to 10 weeks of age for conventionalization. Following a two-week conventionalization (see Methods), IECs were collected from GF and CV littermates and FACS isolated based on Sox9-EGFP intensity. Special care was taken to gate out cellular debris, dead and dying cells, immune cells, and multiplets. Additionally, a strict gating scheme was used to avoid ambiguity between cell populations. No statistical difference between CV and GF animals was observed for spleen weight, small intestine length, or colon length, even when accounting for animal body weight (Figure 5.2A-D). However, there was a statistical difference in body and liver weight (Figure 5.2E-F). Although GF and CV animals exhibit similar percentages of Sox9-EGFP populations, there is a notable trend toward more Sox9^{High} ($p = 0.056$, two-tailed, paired Student's t-Test) and less Sox9^{Low} ($p = 0.14$, two-tailed, paired Student's t-Test) cells in GF vs. CV animals (Figure 5.1D). Reduced numbers of actively proliferating cells have been observed in GF animals previously(Sommer and Bäckhed 2013).

Conventionalized IESCs show enrichment for genes involved in proliferation.

To determine whether the gene expression profile in Sox9^{Low} cells (which we will refer to as IESCs for simplicity) from GF mice is consistent with reduced proliferation, we isolated total RNA from GF and CV IESCs and performed high-throughput RNA- sequencing. Of the ~12.2k genes that met our inclusion criteria (see Methods), we found 138 genes to be significantly elevated in CV IESCs, and 552 genes to be significantly elevated in GF IESCs (Figure 5.3A). Gene Ontology Biological Process(Ashburner et al. 2000; Gene Ontology Consortium 2015)

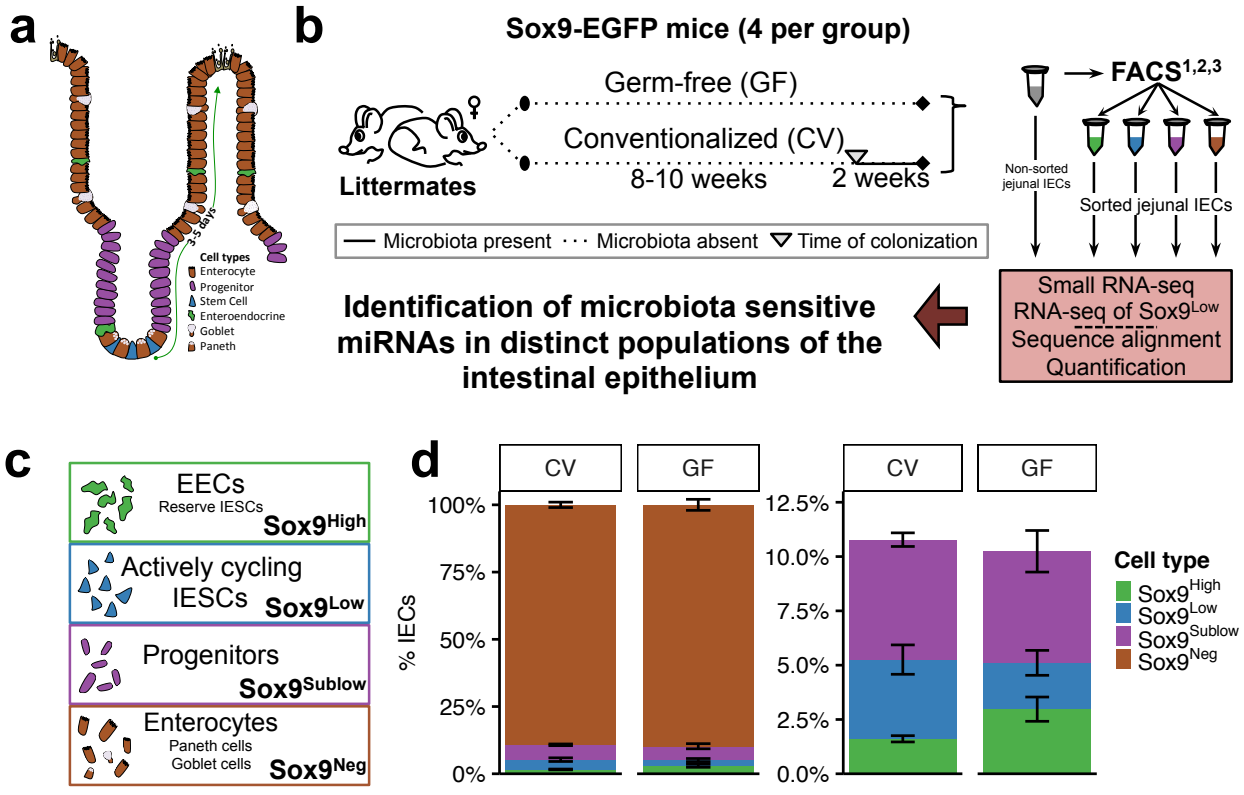

Figure 5.1. The Sox9-EGFP mouse model can be used to define cell type-specific responses to microbiota. (**A**) Cartoon showing location and types of intestinal epithelial cells (IECs). (**B**) Diagram of the experimental design. (**C**) IEC subtypes found in each Sox9-EGFP sort. (**D**) Mean percentage of each IEC subtype sorted from jejunal IEC from GF (GF) and conventionalized (CV) animals (n = 4 each). Error bars depict standard error of the mean.

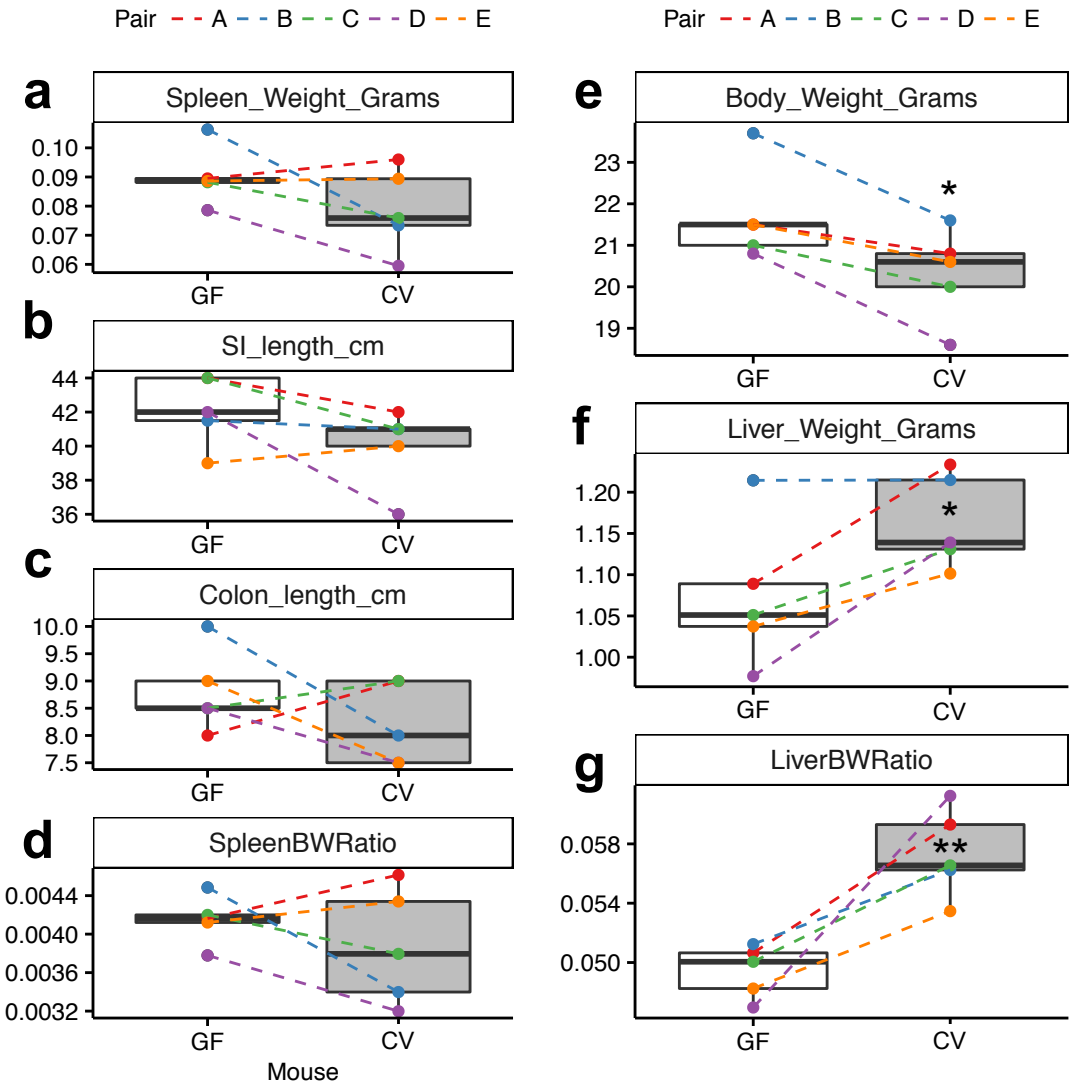

Figure 5.2. Biological data from conventionalized (CV) and GF (GF) animals. **(A)** Weight in grams of the spleen, (**B**) length of small intestine (SI) in centimeters (cm), (**C**) length of colon in cm, (**D**) ratio of spleen to body weight in grams, (**E**) body weight in grams, (**F**) liver weight in grams, and (**G**) ratio of liver to body weight, are shown for GF (white filled) and CV animals (grey filled). Littermate pairs are shown in the same color. Note, due to FACS machine failure, Pair B was not included in FACS, small or RNA-sequencing analyses. Data are shown in standard box-and-whisker plots with median displayed as thick horizontal line, shaded region depicting the interquartile range (IQR), and whiskers extending to the maximum and minimum data points that fall within 1.5*IQR. * $p < 0.05$, ** $p < 0.01$.

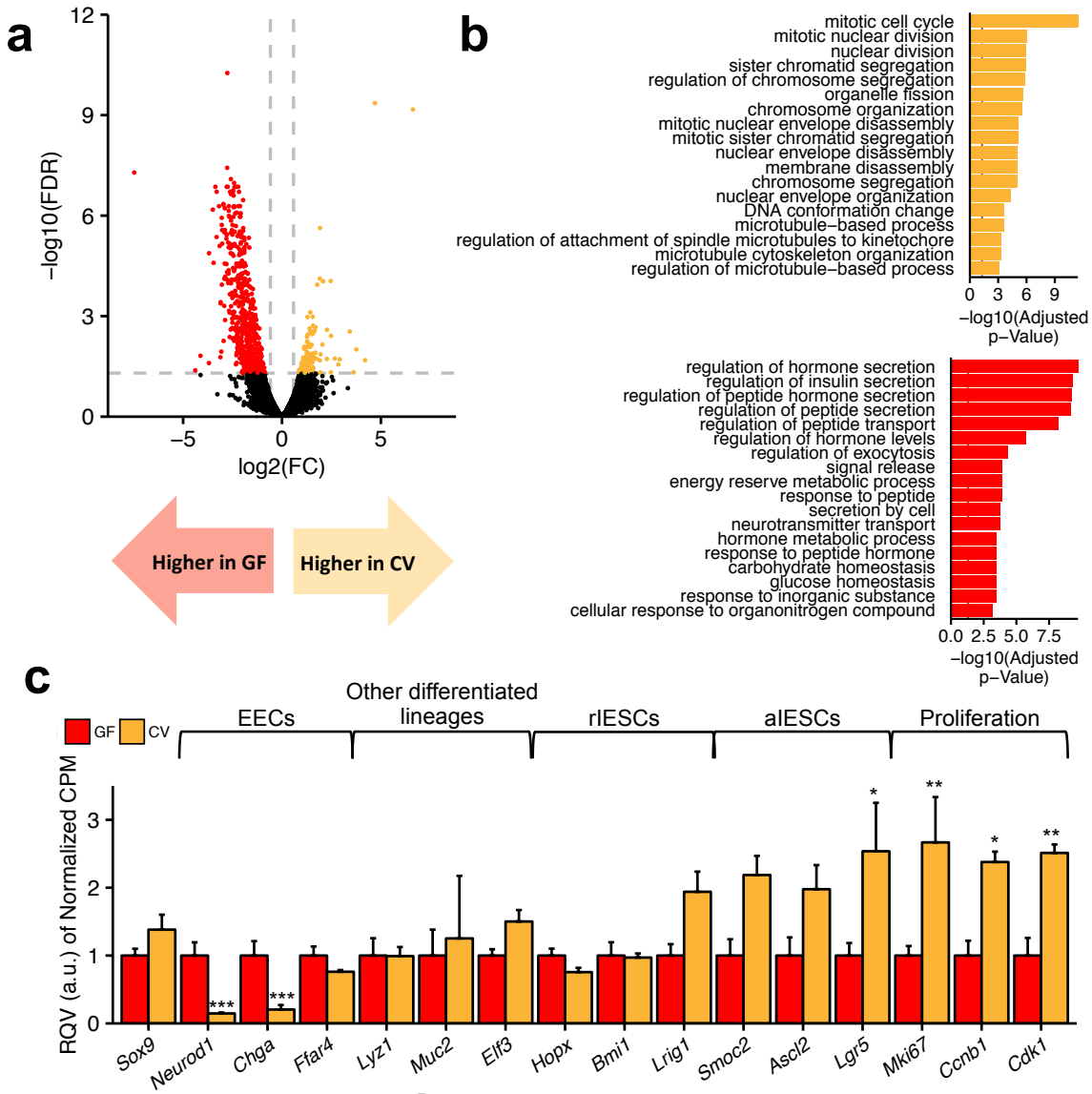

Figure 5.3. RNA-seq of the Sox9^{Low} population from GF and conventionalized animals. (**A**)Volcano plot showing differentially expressed genes in Sox9^{Low} intestinal epithelial stem cells (IESCs) between GF (GF) and conventionalized (CV) mice. Horizontal dashed grey line indicates a False Discovery Rate (FDR) of 0.05. Vertical dashed grey lines indicate fold change (FC) > 1.5 or < -1.5. Significantly changed genes are colored in orange and red, representing genes that at enriched in CV or GF IESCs, respectively. (**B**) Top Enrichr Gene Ontology Biological Process enrichment terms for genes significantly upregulated in CV (top) or GF (bottom) IESCs. (**C**) Relative quantitative values (RQV), which is in arbitrary units (a.u), of normalized counts per million (CPM) for selected genes in CV and GF IESCs (n = 4 animals per condition). Genes selected include *Sox9*; genes known as markers for enteroendocrine (EEC) cell types; other differentiated lineages, including Paneth cells (*Lyz*), goblet cells (*Muc2*), enterocytes (*Elf3*); reserve/quiescent IESCs (rIESCs); actively cycling IESCs (aIESCs); as well as other markers of proliferation. Significance was determined using edgeR differential expression analyses, combined with multiple testing correction, and is denoted as follows: * FDR < 0.05, ** FDR < 0.01, *** FDR < 0.001. Error bars depict standard error of the mean.

enrichment analysis using Enrichr(E.Y. Chen et al. 2013) revealed that genes elevated in CV IESCs are most significantly over-represented in pathways related to proliferation such as 'mitotic cell cycle' and 'nuclear division' (Figure 5.3B). The genes elevated in GF IESCs genes were associated with processes related to hormone secretion and transport (Figure 5.3B). Consistent with these findings, we observed that established markers of proliferation (*Ccnb1*, *Cdk1*, and *Mki67*) are significantly up-regulated in CV IESCs (Figure 5.3C), whereas several, but not all, classic markers of EECs (*Neurod1* and *Chga*) are significantly up-regulated in GF IESCs (Figure 5.3C). Interestingly, *Lgr5* a known marker of actively cycling IESCs is upregulated in CV IESCs, however, given that this gene codes for a receptor protein that signals to the Wnt pathway, it is possible that the upregulation is due to increased Wnt activity upon conventionalization. Known markers of reserve (quiescent) stem cells were not significantly different between CV and GF $Sox9^{Low}$ cells (Figure 5.3C), nor were markers for Paneth cells (*Lyz*), goblet cells (*Muc2*), or enterocytes (*Elf3*). These data confirm that the $Sox9^{Low}$ cells are indeed enriched for IESCs and that CV IESCs harbor a gene signature consistent with increased proliferative capacity. We therefore moved forward with small RNA- sequencing of each of the functionally distinct IEC subpopulations.

Small RNA-sequencing of each IEC population reveals cell type-specific expression of miRNAs

Total RNA was isolated from the four sorted populations from each animal, as well as from non-sorted IECs (NS IECs; NS IECs were purified by FACS, but not sorted based on Sox9-EGFP intensity). Small RNA-sequencing was performed in two batches, each of which contained small RNA libraries from sorted and unsorted IECs from two GF animals and two CV animals. miRNAs and their isomiRs were aligned and quantified using miRquant, our previously

described method (see Methods for details)(Baran-Gale et al. 2013). To test our hypothesis that miRNAs are DE among functionally distinct IEC subtypes, we evaluated miRNAs with an expression level of at least 100 reads per million mapped (RPMM) in one or more samples. We showed that miRNA expression profiles are sufficient to cluster most samples by their respective cell types regardless of GF/CV status (Figure 5.4A). For example, $Sox9^{Neg}$ cells and NS IECs are tightly clustered, which is expected given that NS IECs are composed of 85-90% $Sox9^{Neg}$ cells. However, we found that the only exception is the $Sox9^{Low}$ IESC population, which segregates into two different clusters based on the GF/CV condition (Figure 5.4A). Specifically, GF $Sox9^{Low}$ cells exhibit a miRNA profile that more closely resembles that of $Sox9^{High}$ cells (EECs) than CV $Sox9^{Low}$ cells. GF or CV status was not sufficient to segregate any other IEC subtype into distinct clades, which indicates that IESCs are particularly sensitive to the presence or absence of microbiota. Importantly, similar results were seen when clustering samples using reads per million mapped to miRNAs (RPMMM) as our normalization (Figure 5.5).

miRNA	Cell type	Fold enrichment
miR-194-1-3p	$Sox9^{Neg}$	4.59
miR-194-1-3p+1	$Sox9^{Neg}$	4.20
miR-194-1-5p	$Sox9^{Neg}$	3.16
miR-194-1-5p+1	$Sox9^{Neg}$	3.54
miR-194-2-5p+1	$Sox9^{Neg}$	2.02
miR-215-3p	$Sox9^{Neg}$	3.87
miR-215-5p	$Sox9^{Neg}$	2.26
miR-215-5p+1	$Sox9^{Neg}$	2.48
miR-215-5p+5	$Sox9^{Neg}$	2.46
miR-139-3p	$Sox9^{High}$	2.90
miR-182-5p	$Sox9^{High}$	3.54
miR-183-5p	$Sox9^{High}$	3.43
miR-183-5p+1	$Sox9^{High}$	3.92
miR-200b-3p+1	$Sox9^{High}$	2.09
miR-3107-5p	$Sox9^{High}$	3.23
miR-340-5p	$Sox9^{High}$	2.35
miR-486-5p	$Sox9^{High}$	3.23
miR-672-5p	$Sox9^{High}$	6.18
miR-122-5p	$Sox9^{Sublow}$	3.95

Table 5.1. miRNAs enriched at least 2-fold in one intestinal epithelial cell (IEC) subtype relative to all others studied. The 'fold enrichment' is the ratio of mean expression in the listed cell type over that of the next highest expressed population.

To investigate differential expression of miRNAs across the distinct IEC subtypes, we performed hierarchical clustering of the

top 100 most highly expressed miRNAs across all of the sorted populations (Figure 5.4B). Many miRNAs were uniquely enriched in one IEC subtype relative to all others (>2-fold more highly expressed than any other cell type; Table 5.1). For example, we found that miR-215 and miR-194 are robustly enriched in $Sox9^{Neg}$ cells, which consist primarily of enterocytes. Both of these miRNAs are processed from a single primary miRNA transcript on Chr1 and were previously shown to be induced by HNF4α during differentiation of Caco-2 colon carcinoma cells(Hino et al. 2008). Six miRNAs are enriched in $Sox9^{High}$ cells (EECs and reserve stem cells), including miR-182-5p and miR-183-5p (Table 5.1), which are also generated from a single primary miRNA transcript. Consistent with enrichment in a subpopulation of cells composed largely of EECs, miR-182 has been shown to have important functions in other endocrine cells, specifically, pancreatic beta cells(Melkman-Zehavi et al. 2011). miR-122-5p is the only miRNA enriched in $Sox9^{Sublow}$ cells. In the liver, miR-122-5p has been identified as a negative regulator of proliferation(Bandiera et al. 2015). Unexpectedly, we did not find any miRNAs enriched in the $Sox9^{Low}$ IESCs; however, this population demonstrated the most robust miRNA changes in response to microbial presence (Figure 5.4 & 5.6).

To evaluate the cell type-specific responses to microbiota and to account for batch and littermate effects, we used a linear modeling approach (see Methods). We found that no miRNA is significantly altered by microbiota in every cell type, but 44 miRNAs are significantly altered by microbiota in at least one cell type (Figure 5.6), which underscores the highly cell type-specific miRNA response to microbiota.

miR-375 is robustly and DE in IESCs of GF and conventionalized mice

Of these 44 miRNAs, only two are altered in differentiated cell types: miR-215-5p and miR-184-3p, which are upregulated in $Sox9^{Neg}$ (primarily enterocytes) and downregulated in

Sox9^{High} (EECs) in response to conventionalization. miR-184-3p is a prominent negative regulator of insulin secretion in the endocrine pancreas(Tattikota et al. 2015), but to our knowledge has not been reported in EECs previously. In contrast, we found seventeen miRNAs to be significantly altered by conventionalization in the Sox9^{Sublow} progenitor population, all of which are upregulated. Moreover, thirty-three miRNAs are significantly altered by the presence of microbiota in the Sox9^{Low} IESC population (Figure 5.6). Twenty-five of these are uniquely changed in the Sox9^{Low} population, while eight others are also significantly changed in either Sox9^{Sublow} or Sox9^{High} cells. miR-375-3p is ~2-fold (FDR = 0.04) reduced in CV IESCs compared to GF IESCs and is the most highly expressed of the 33 microbiota-sensitive miRNAs in IESCs (Figure 5.7A). Notably, miR-375-3p is 2.2- and 8-fold more highly expressed than the next-most significant microbiota-sensitive miRNA in the CV and GF IESC populations, respectively (Figure 5.7A). We also found that its isomiR, miR-375-3p-1, is significantly downregulated in IESCs upon conventionalization (FC = -1.85, FDR = 0.03; Figure 5.7A). qRT-PCR in Sox9^{Low} cells confirmed that the miR-375-3p family is significantly downregulated by conventionalization (FC = -3.85, p = 0.03; Figure 5.7B).

Knockdown of miR-375 in *ex vivo* enteroids results in increased proliferation

To test the functional effect of miR-375-3p downregulation, we knocked down miR-375-3p by gymnosis of locked nucleic acid (LNA) inhibitors (Figure 5.8)(Stein et al. 2009; Knudsen et al. 2015) in *ex vivo* enteroid cultures derived from intestinal crypts of GF mice (Figure 5.9). *Ex vivo* enteroid culture systems have been shown to maintain *in vivo* cellular composition and molecular gene expression profiles over time(Grün et al. 2015). Gymnosis allows for the knockdown of mRNA and miRNAs using complementary LNAs without the use of often toxic transfection reagents(Stein et al. 2009; Knudsen et al. 2015). We achieved a ~700-fold

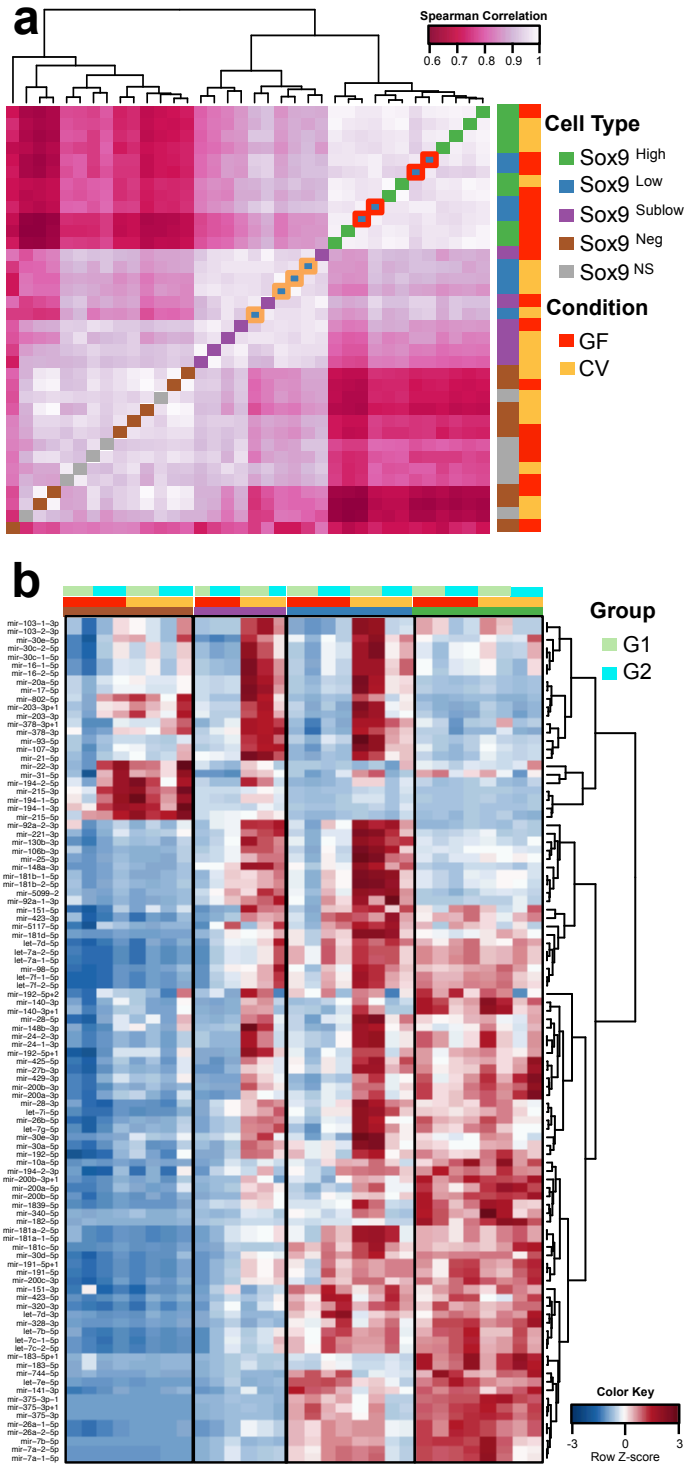

Figure 5.4. miRNAs in the intestinal epithelium show cell type-specific expression and responses to microbiota. (**A**) Hierarchical clustering of samples by global miRNA expression (including only miRNAs with reads per million mapped [RPMM] > 100 in 1+ samples). (**B**) Hierarchical clustering of the top 100 most highly expressed miRNAs across sorted intestinal epithelial cell (IEC) subtypes. Color bars denote cell type, condition, and sequencing group (G1 or G2).

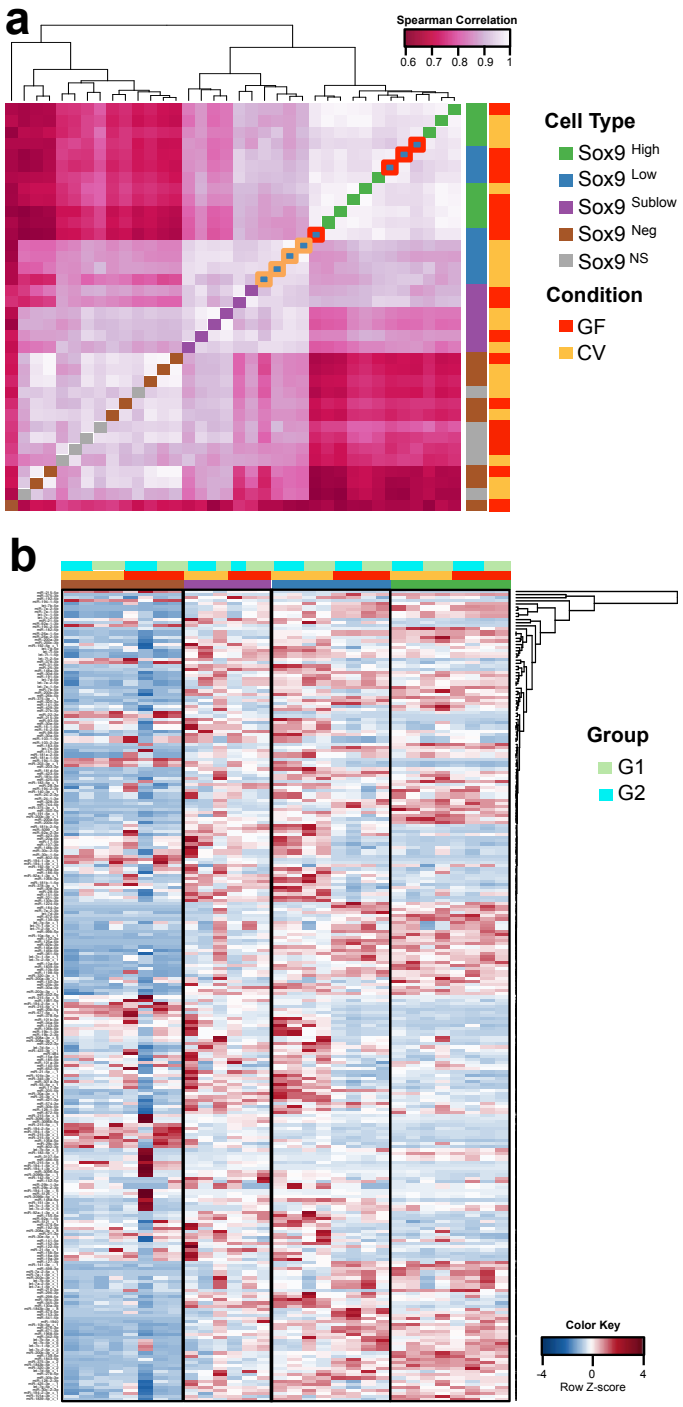

Figure 5.5. Similar clustering of CVGF samples is seen using RPMMM normalization. (A) Hierarchical clustering of samples by global miRNA expression (including only miRNAs with reads per million mapped to miRNAs [RPMMM] > 100 in 1+ samples). (**B**) Hierarchical clustering of the top 100 most highly expressed miRNAs across sorted intestinal epithelial cell (IEC) subtypes. Color bars denote cell type, condition, and sequencing group (G1 or G2).

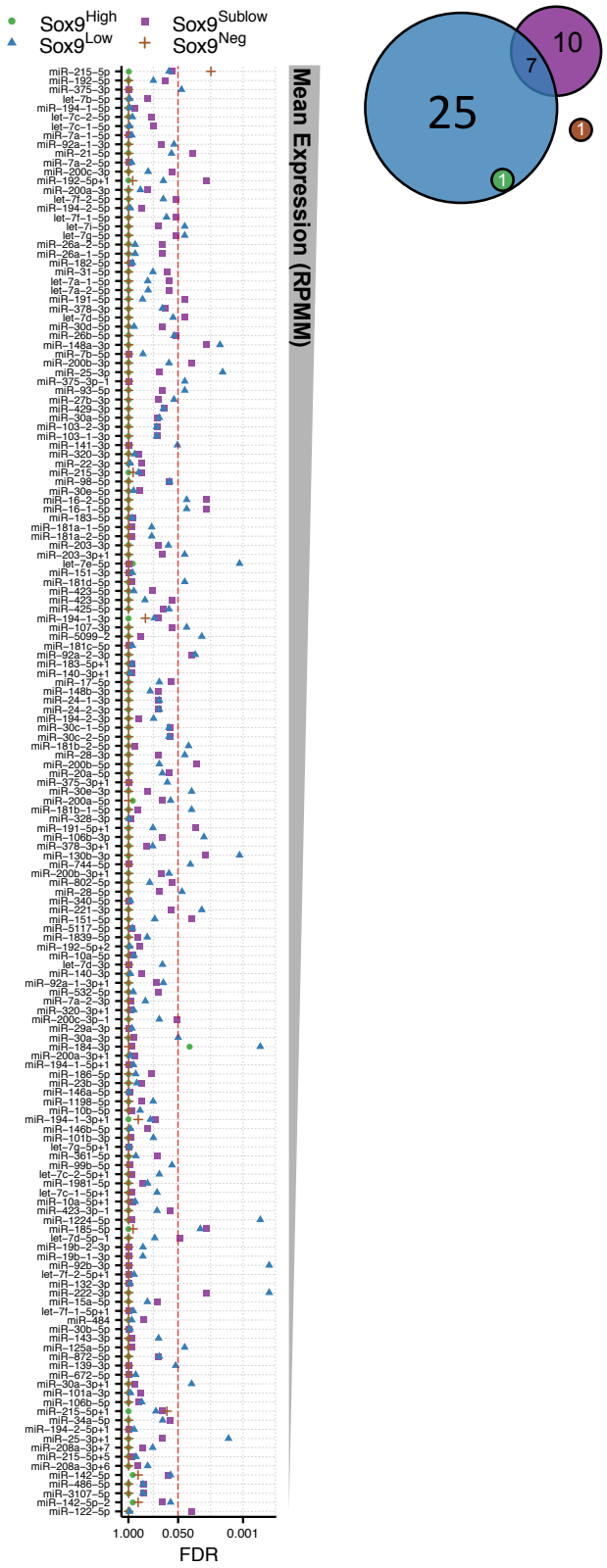

Figure 5.6. Cell type-specific response of miRNAs in response to conventionalization revealed through linear modeling analysis. (**A**) A linear model was used to account for the following covariates: cell type, condition, sequencing batch, and littermate pair. For each

miRNA that met an expression threshold of reads per million mapped (RPMM) > 100 in 1+ samples, the False Discovery Rate (FDR) multiple testing correction of the cell type*condition covariate interaction p-value is plotted. miRNAs are ordered by average expression across all intestinal epithelial cells (IEC) subtypes, and vertical red dashed line indicates FDR = 0.05. Cell type is signified by color and shape. (**B**) Venn diagram showing the number of significantly altered miRNAs in each IEC subtype between GF and CV mice. Cell type is signified by color scheme provided in panel (**A**).

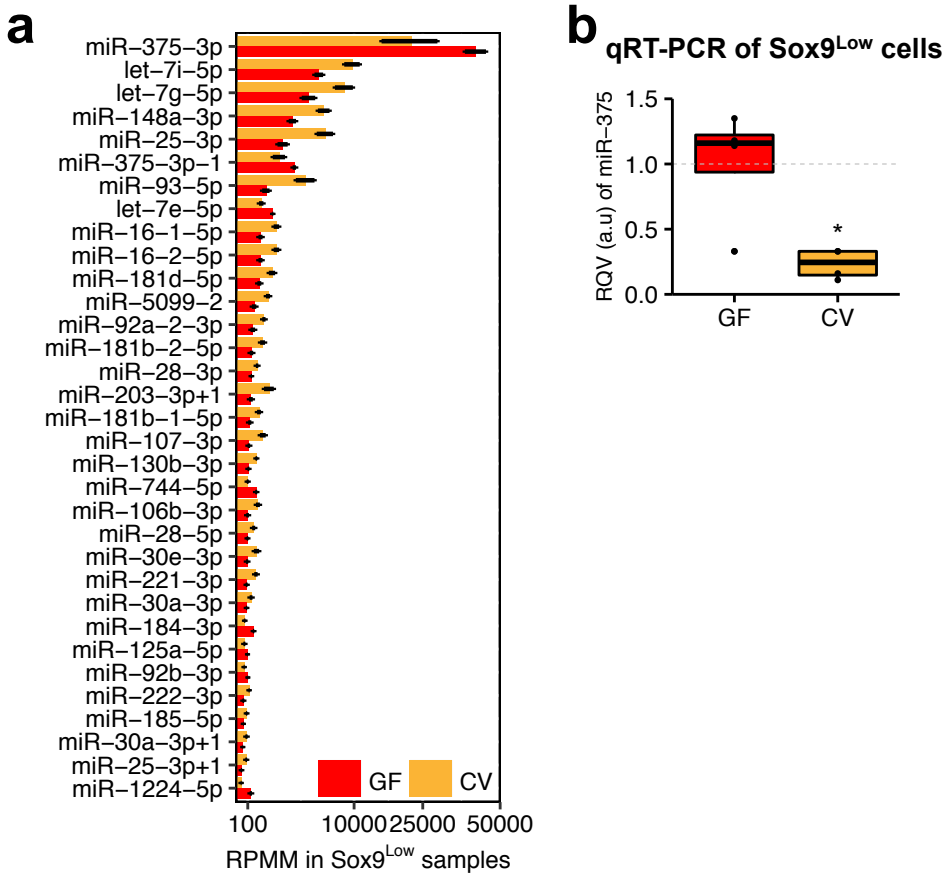

Figure 5.7. miR-375-3p is highly expressed in Sox9^{Low} intestinal epithelial stem cells and is significantly downregulated upon conventionalization. (**A**) Mean relative expression in reads per million mapped (RPMM) of miRNAs (n = 33) that were significantly altered (FDR < 0.05; n = 4) in the Sox9^{Low} population in response to conventionalization. Y-axis is shown on a square root scale. Error bars depict standard error of the mean. (**B**) qRT-PCR confirming miR-375 is reduced upon conventionalization (n = 4 for each condition). Data are shown in a standard box-and-whisker plot with median displayed as thick horizontal line, shaded region depicting the interquartile range (IQR), and whiskers extending to the maximum and minimum data points that fall within 1.5*IQR. * $p < 0.05$, two-tailed Student's t-Test.

knockdown of miR-375-3p at day 8 in enteroids treated with an LNA complementary to miR-375-3p (LNA-375; Figure 5.9A). At both day 4 and 8, LNA-375-treated enteroids from GF Sox9-EGFP mice exhibited dramatically increased budding, a marker of IESC proliferative capacity(Fuller et al. 2012; Seiler et al. 2015), relative to mock and LNA-Scramble-treated enteroids (Figure 5.9B & 5.9C). Consistent with this finding, whole mount staining of the enteroids also showed increased PCNA and Ki67 staining upon knockdown of miR-375-3p (Figure 5.9D). These data indicate that miR-375-3p is a potent regulator of IESC proliferation and that microbiota may regulate IESC renewal in part via modulation of miR-375-3p (Figure 5.10).

HFD induces robust changes in IESC gene expression but minimal changes in miRNA expression across Sox9-EGFP populations

To evaluate the role of diet in regulating miRNA expression of distinct cell types of the IE, we performed FACS on IECs from Sox9-EGFP mice following a 20-week HFD. Mice on a HFD doubled in body weight (Figure 5.11A) and had elevated blood glucose (Figure 5.11B), and a decreased liver to body weight ratio (Figure 5.11C). No difference was seen in spleen weight between HFD and chow animals when body weight increase was taken into account. By RNA-sequencing, HFD IESCs were enriched for genes (n = 50 genes) involved in the positive regulation of lipid catabolism (data not shown, GO Biological Process enrichment analysis adjusted p-Value = 0.011), and had enrichment for PPARD binding sites (ENCODE and ChEA Consensus TFs from ChIP-X, adjusted p-Value = 0.02). The latter point is consistent with recent reports showing PPARD being activated in Lgr5+ cells of HFD- treated mice and implicated as contributing to the development of colon cancer(Beyaz et al. 2016). Downregulated genes (n = 462) were enriched for those involved in the regulation of hormone secretion and transport,

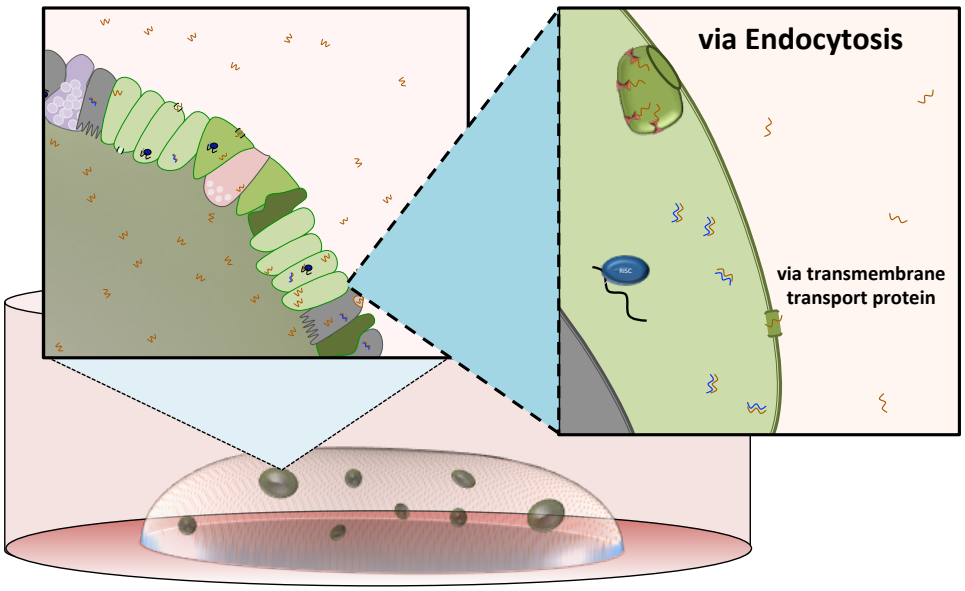

Figure 5.8. Schematic of miRNA knockdown in enteroids using gymnosis. Crypts are embedded in reduced growth factor BD Matrigel supplemented with 500 ηM locked nucleic acid (LNA) complementary to a specific miRNA dissolved in PBS. Target miRNAs are inhibited by the LNA, which is taken up via gymnosis, a term coined by the Troels Koch laboratory in 2009(Stein et al. 2009), to describe a transfection method that uses no carrier reagent. Instead, naked LNA are taken up by cells via endocytosis following binding to receptor molecules, or possibly taken up through a nucleic acid transport protein. The precise mechanisms by which gymnosis occurs are still under investigation.

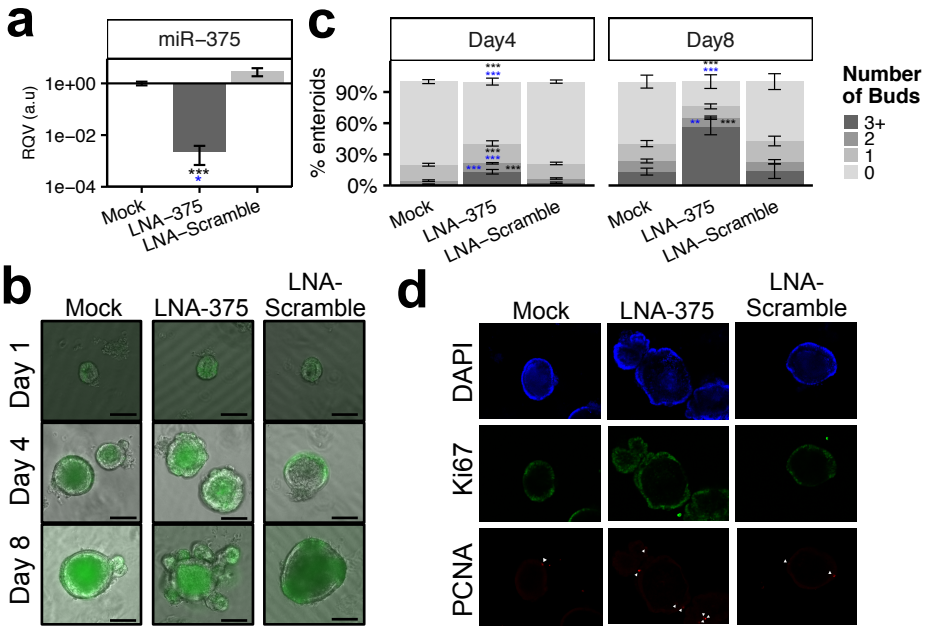

Figure 5.9. *Ex vivo* knockdown of miR-375 in enteroids results in increased proliferation. Crypts were isolated from female GF (GF) Sox9-EGFP mice, (**A**) Relative quantitative values (RQVs) are shown for miR-375-3p in mock-, LNA-375-, and LNA-Scramble-treated enteroids at Day 8 as measured by qRT-PCR relative to *U6* expression. (**B**) Representative images of 20X magnified enteroids at Day 1, Day 4, and Day 8, following mock, LNA-375, or LNA-Scramble uptake by gymnosis. Sox9-EGFP expression (green) is overlaid on the bright field images. (**C**) Mean percent of GF enteroids with 0, 1, 2, or 3+ buds at Day 4 and Day 8 following mock (n = 12), LNA-375 (Day 4 n = 12, Day 8 n = 11), or LNA-Scramble (Day 4 n = 12, Day 8 n = 9) uptake by gymnosis. (**D**) 10X confocal images of whole mount enteroids stained for PCNA, Ki67, and nuclei. White arrows indicate cells within the enteroid that stained for PCNA. Experiments were performed in duplicate. The 'n' refers to number of wells, which were seeded with ~400 crypts at Day 0. Significance was determined using a Student's two-tailed unpaired t-Test relative to mock (black asterisks) or LNA-Scramble (blue asterisks). * $p < 0.05$, ** $p < 0.01$, *** $p < 0.001$. Error bars depict standard error of the mean.

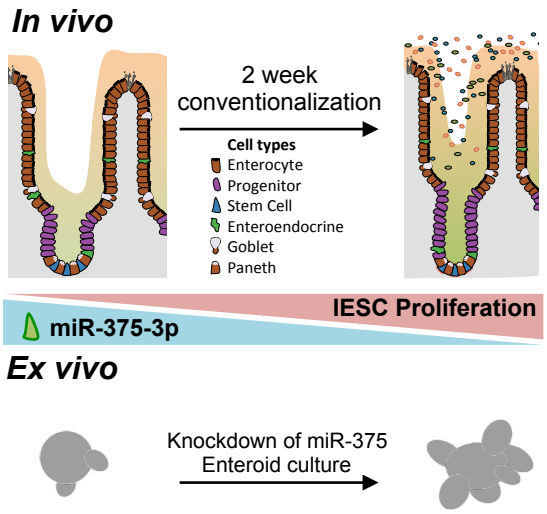

Figure 5.10. Current working model of miR-375-3p mediation of the effects of microbiota on intestinal epithelial stem cell (IESC) proliferation. Previous research shows increased intestinal epithelial proliferation upon conventionalization of GF (GF) mice. We found that miR-375-3p is downregulated in IESCs upon conventionalization, and that *ex vivo* knockdown of miR-375-3p results in increased proliferative capacity.

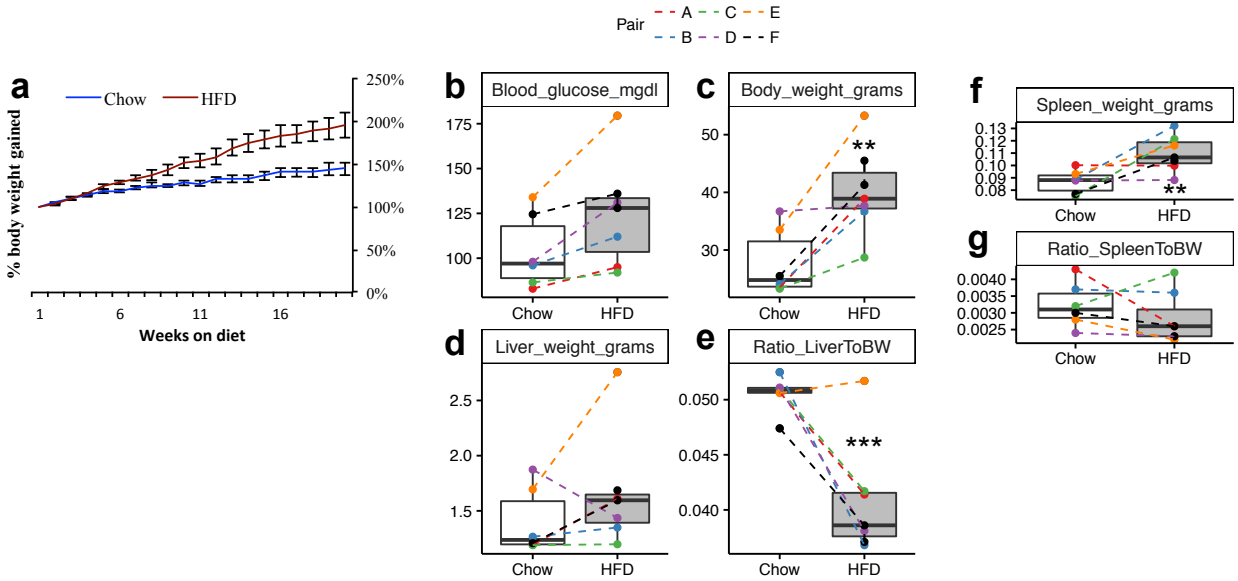

Figure 5.11. Mice on a 20-week high-fat diet show increased weight gain, blood glucose, and liver weight. (**A**) Weight gain as a percentage of starting weight are shown for animals on a high-fat diet (HFD) or chow diet. Groups were significantly different after 5 weeks on diet. (**B**) Fasting blood glucose levels for animals on a chow or HFD are shown at 16-weeks, p = 0.08**.** (**C**) Body weight in grams, (**D**) liver weight in grams, (**E**) ratio of liver to body weight, (**F**) spleen weight in grams, and (**G**) ratio of spleen to body weight. Littermate pairs are shown in color. Note, due to FACS machine failure, pair C & D, and one HFD animal from pair F were not included in small or RNA-sequencing analyses. Data are shown in standard box-and-whisker plots with median displayed as thick horizontal line, shaded region depicting the interquartile range (IQR), and whiskers extending to the maximum and minimum data points that fall within 1.5*IQR.* p < 0.05, ** p < 0.01.

insulin secretion, and glucose homeostasis (GO Biological Process enrichment analysis adjusted p-Value < 0.001). Interestingly, downregulated genes were also enriched for hemostasis and blood coagulation terms, and cellular response to cytokines (GO Biological Process enrichment analysis adjusted p-Value < 0.05). These terms are consistent with the known effects of long-term HFD, which has been shown to impair the function of small intestine (SI) hormone-secreting EECs(Richards et al. 2016) and induce intestinal inflammation{Ding:2010eg}.

Small RNA-sequencing analysis of HFD Sox9-EGFP sorted populations revealed tight clustering by cell type, however, no population segregated by dietary condition (data not shown). Importantly, these samples did cluster with like cell types in CV and GF animals (Figure 5.12). Although a linear modeling analysis revealed no miRNAs significantly changed between HFD and chow-fed animals in any cell population, using either RPMM or RPMMM normalization, 15 miRNAs were significantly changed (FDR < 0.05) between HFD and chow IESCs by t-Test in the RPMM data. These include members or isomiRs of the let-7, miR-215, miR-192, miR-30, and miR-148 families.

Discussion

In this study, we have shown that miRNAs are responsive to the presence of gut microbiota in a cell type-specific manner. Microbiota exert the strongest effect on host miRNA expression in the $Sox9^{Low}$ population, which is highly enriched in IESCs. Subpopulation analysis was necessary to identify this effect, as IESCs make up only 1-3% of all IEC types. miR-375-3p was identified as significantly downregulated in the IESC population in response to microbiota, and follow-up experiments *ex vivo* demonstrated miR-375-mediated control of IESC expansion and proliferation, thereby providing a mechanism by which microbiota may regulate these processes *in vivo*. miR-375-3p has been associated previously with the regulation of proliferation and differentiation in several tissues(Y. Wang et al. 2013; Yan et al. 2013; Knudsen et al. 2015). It is predicted to target many members of the Wnt/β-catenin and Hippo signaling pathways, but so far has only been shown to inhibit Frizzled-8(Y. Wang et al. 2013) and Yap1(Z.-W. Zhang et al. 2013). miR-375-3p has been knocked down systemically in mice, and while the authors did not study intestinal proliferation, they observed an increased rate of intestinal transit(Nezami et al. 2014). miR-375-3p is best studied in the context of pancreatic endocrine cell differentiation

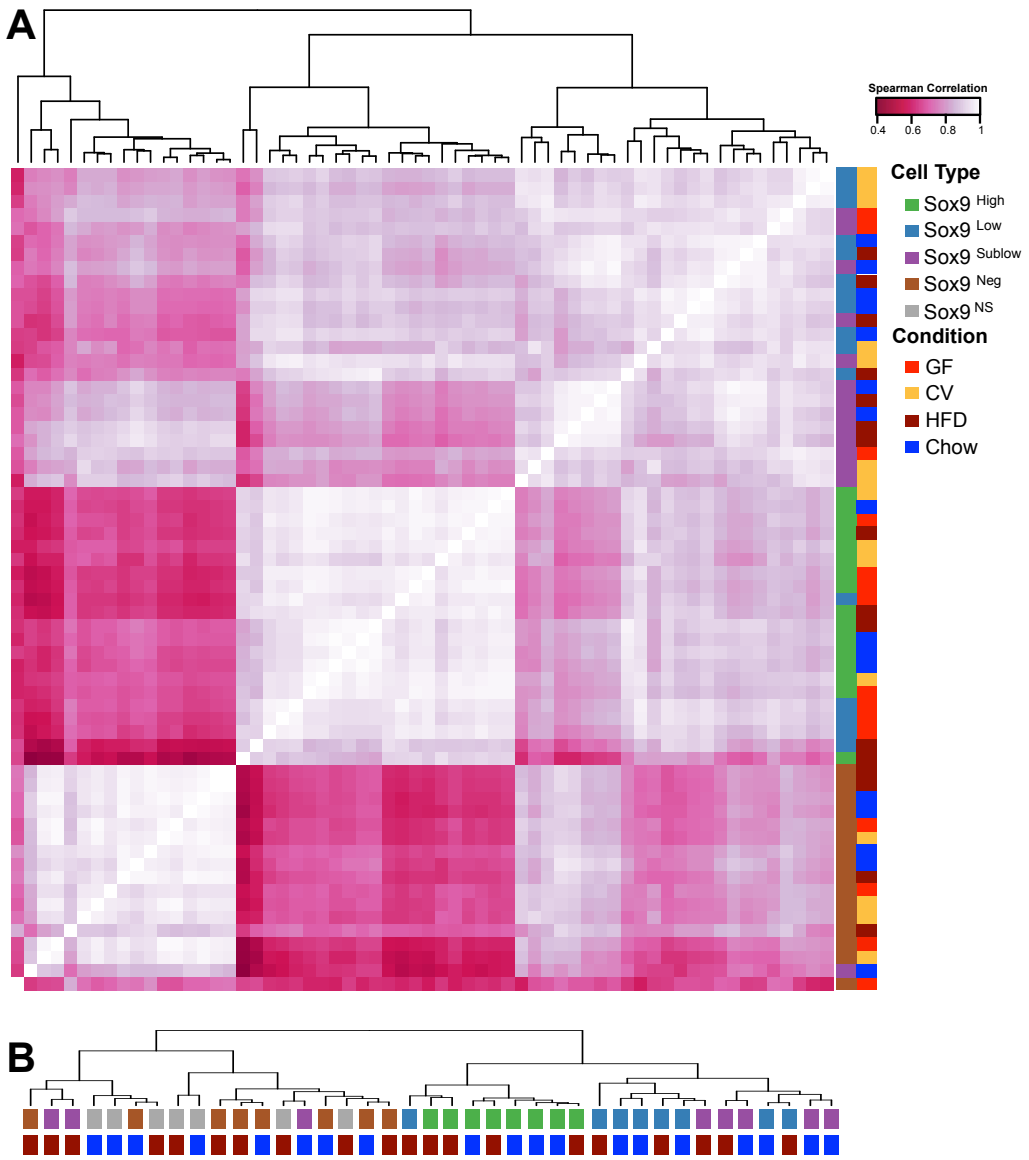

Figure 5.12. Global miRNA expression profile is sufficient to cluster HFD, CV, and GF samples by cell type. (**A**) Hierarchical clustering of all samples, and of (**B**) HFD and Chow samples alone, by global miRNA expression (including only miRNAs with reads per million mapped to miRNAs [RPMMM] > 100 in 1+ samples). Color bars denote cell type and condition.

and function(Poy et al. 2004; Poy et al. 2009; Nathan et al. 2015), although more recently, Knudsen at al. (2015) identified a role for miR-375-3p in regulating EEC differentiation(Knudsen et al. 2015). We found that miR-375-3p is robustly expressed in both IESCs and EECs; however, we observed that miR-375-3p is responsive to microbiota only in IESCs but not in EECs. This observation might suggest cell type-specific microbial signaling pathways and cell type-specific roles for miR-375-3p.

An important added value of our study is the first ever map of miRNA expression across different IEC subtypes, and the cell type-specific influence of microbiota on miRNA expression. We also provide evidence that IESC microbiota-sensitive miR-375-3p influences IEC proliferation, most likely through physiological maintenance of actively cycling IESC. Of course many questions still remain, including how microbiota influence miRNA expression in IESCs. This phenomenon may be explained by direct and/or indirect mechanisms. Regarding direct mechanisms, although thus far bacteria have only been found to reside within the crypts of the caecum and colon, where microbial density is highest(Pédron et al. 2012), it nevertheless remains a possibility that bacteria residing within the jejunal crypt may directly influence miRNAs in the stem cell subpopulation. Indirect mechanisms are also possible, such as changes in the microenvironment (metabolites and bacterial endotoxins) or through indirect signaling by immune or mesenchymal cells, which were not profiled in this study. Though outside the scope of this analysis, further research is certainly warranted to investigate the interesting relationship between host miRNAs and resident microbiota.

An unexpected finding was that GF IESCs ($Sox9^{Low}$) have a miRNA expression profile more similar to that of $Sox9^{High}$ cells. Interestingly, our RNA-sequencing data of IESCs also showed enrichment for markers of EECs in the GF mice. One possibility is that $Sox9^{Low}$ cells are

primed for the EEC lineage in the absence of microbial influence. Alternatively, one of the caveats of the Sox9-EGFP model is that while the $Sox9^{High}$ population consists primarily of EECs, it also includes a small population of reserve or quiescent stem cells(Roche et al. 2015). It is therefore possible that microbiota influence the maintenance of reserve stem cells in addition to their role in regulating actively cycling IESCs through miR-375-3p. Though outside the scope of this study, more research, including single cell analyses, will need to be conducted to delineate more precisely the differences between GF and CV IESCs, as well as to determine which miRNAs are involved in the maintenance of active and quiescent IESC states.

It is also important to note that each segment of the IE has distinct physiological roles and differing magnitudes of microbial load. Our study only examined changes in response to microbiota in IECs from the jejunum. In the future we would like to assess differences in cell type-specific responses to microbiota along the length of the intestine. Conventionalization is a gradual process in mice. Our study examined a signle time point post- conventionalization of young GF mice. Experimental variation in age at conventionalization and timepoint post-conventionalization are important future directions toward fully understanding the role of microbiota in regulating stem cell function. Additionally, it would be interesting to investigate cell type-specific responses to microbiota in other populations not sorted herein, including goblet and Paneth cell populations. These cell types do not express Sox9-EGFP, and are rare cell populations in the $Sox9^{Neg}$ fraction, which comprise primarily enterocytes. Nevertheless, Paneth and goblet cells may experience robust changes in response to microbial presence, based on their known functions. While our current focus is on the Sox9-EGFP model, which precluded examining these populations, they deserve attention in future work.

Perhaps the most surprising finding in these studies is that we did not see robust changes

in miRNA expression in any population in response to a long-term HFD. It is possible that significant changes in miRNA expression may be found in other regions of the intestine, or at different time points on a HFD. While not as robust as the changes observed in CV compared to GF animals, the HFD data do support the idea that IESCs are very responsive to environmental stimuli. Given that microbiota are known to change in response to a HFD, it is worth investigating when this change occurs and whether particular species are involved in altering IESC miRNA expression. It is possible that the changes in microbiota contributed to the altered miRNA expression in HFD-fed animals. However, many more studies will need to be conducted to better understand the relevant time points and changes that occur at the axis of microbiota, miRNA, and diet. Future evaluations of the GE data for HFD, CV, and GF animals include TF-binding enrichment analysis and miRhub(Baran-Gale et al. 2013) analyses. Nevertheless, this study represents the first to our knowledge to evaluate the effect of diet and microbiota on miRNA expression in distinct cell populations of the mouse jejunum.

In summary, we provide novel evidence about the miRNA landscape in four distinct cell populations from the IE, and demonstrate that miRNA profiles are highly different across the IEC subtypes, and also that miRNAs respond to the presence of microbiota in a highly cell type-specific manner. We investigate one IESC microbiota-sensitive miRNA, miR-375-3p, and show that its downregulation results in significantly increased proliferative capacity, providing one possible mechanism by which microbiota regulate proliferation of IESCs *in vivo*. The data provided herein progresses the field, and offers the scientific community a valuable resource through which researchers can initiate novel studies into miRNAs and microbiota-mediated regulation of intestinal physiology, homeostasis, and disease pathogenesis.

CHAPTER 6 – DISCUSSION, CONCLUSIONS, & FUTURE DIRECTIONS

In this dissertation, I have evaluated miRNAs as biomarkers of metabolic and intestinal disease, drivers of physiological processes in the liver and IE, and responders to environmental stimuli in a cell type-specific manner in the IE. Both the liver and intestine are highly relevant metabolic organ systems, which when dysregulated contribute to the development of many metabolic disorders including obesity and type 2 diabetes. In evaluating the roles of miRNAs in these processes, I have set the groundwork for future research to identify potential miRNA therapeutic targets toward the treatment of a wide range of metabolic and GI diseases.

The research presented in Chapter 2 evaluated hepatic targets of one miRNA, miR-29, that is not only upregulated in the plasma of type 2 diabetics, but also in the plasma and liver of several animal models of metabolic disease. My pathway analysis identified a potential mechanism of miR-29's action in fine-tuning hepatic lipid metabolism driven by modulating FOXA2, which is dysregulated in the liver of type 2 diabetics, spawned several follow-up studies in the lab to investigate the use of anti-miR-29 treatment in alleviating insulin resistance and hypercholesterolemia *in vivo*(Kurtz et al. 2015). While these pre-clinical trials in mice hold great promise, understanding the dynamics of miR-29's dysregulation in humans, as well as the off-target effects of systemic delivery of miR-29 inhibitors in primates are important next steps toward vetting miR-29's potential as a metabolic disease therapeutic. These early findings also inspired my own research objectives to focus more on the intestine, which is the primary site of

nutrient absorption, response to diet, and interaction with components of the gut microbiota, all of which are altered during metabolic disease pathogenesis. The intestine is highly understudied relative to other major metabolic organs despite its clear importance and likely role in early metabolic disease progression.

The limited understanding of miRNA expression and relevance in the intestine posed a certain challenge. I began by focusing on identifying potential colonic miRNA biomarkers of CD (Chapter 3), which is an inflammatory intestinal disease that puts patients at risk for the development of both type 2 diabetes and cancer. Given the elevated risk and common GWAS associated genes, it is possible that there are common underlying intestinal processes dysregulated during disease pathogenesis further motivating my study.

Our adult CD patients showed extreme heterogeneity between patient phenotypes, gene, and miRNA expression, which complicated our analysis. Perhaps unsurprisingly, given the diversity of phenotypes found across CD patients, we found that miRNAs do not necessarily segregate CD vs. Non-IBD patients, but instead miRNAs more robustly distinguish subtypes of CD, which indicate multiple pathways leading to the various forms of CD. In investigating enrichment for miRNA target sites in DE genes within distinct subtypes of CD, we identified several putative master regulatory miRNAs, including miR-31, which suggest a key role for these miRNAs in driving disease pathogenesis. Further analysis of these miRNAs and our potential prognostic markers of CD are ongoing in the lab. Importantly, a larger cohort may improve power and clarity of the associations we identified and would strengthen our resolve to evaluate the functional effects of these miRNAs *in vitro*, *ex vivo*, and *in vivo*. Further characterization of the cohort we do have, including drug history and environmental risk factors (like smoking and diet) may also help strengthen our model, as would evaluating other small

regulatory RNAs identified by sequencing but not evaluated in our study. Functional characterization of the DE miRNAs in intestinal culture models would also be beneficial, as it would inform us as to the possible effect their dysregulation has on disease phenotype and progression. In on-going follow-up studies to identify potential prognostic indicators of disease progression and response to treatment in the lab, we have initiated a large-scale study of pediatric CD patients using index biopsies, which are collected at diagnosis before treatment begins, which we hope will reduce noise and improve power. Our hope is to use the knowledge gained from these studies to better treat pediatric patients and prevent or reverse disease progression.

In Chapter 3, we confirmed that intestinal miRNAs are dysregulated during disease, strengthening evidence for a key role for them as potential drivers of disease pathogenesis. To evaluate whether miRNAs were important in regulating key intestinal epithelial physiological processes, I sought to identify and characterize key miRNA networks in the IE in Chapter 4. We began by evaluating conserved miRNA target sites of *SOX9*, a well-established transcriptional regulator of proliferation and differentiation in the IE. Our *in silico* analyses led us to focus on miR-30, which we went on to show plays a key role in regulating both proliferative and enterocytic differentiation pathways. Surprisingly, our data suggests that this role is not exclusively through the regulation of *SOX9*, but a much broader GRN. While this is an important finding in the field of intestinal biology, our findings also have profound implications for miRNA biology. Specifically, we found that miR-30 targets *SOX9* to upregulate mRNA expression. But, through a larger inhibitory network involving ubiquitin ligases, miR-30 knockdown actually has a net-negative effect on SOX9 protein expression. Understanding transcriptional control of miR-30 in the IE is of particular interest in the future.

Our data show that miR-30 expression is positively correlated with *Sox9* across distinct cell types of the mouse IE. Understanding the co-regulatory relationship, as well as the identities of other positively correlated miRNAs, would advance the field of intestinal biology. Our study involved a deep sequencing time course of HIECs following knockdown of miR-30. Further analysis of this information-rich dataset could provide insight on the dynamics of miRNA:GRNs. As most studies aimed at identifying potential miRNA therapeutic targets focus on only a few genes or pathways, this data set may hold keys to understanding the extent to 'off-target' effects following miRNA knockdown within tightly controlled culture conditions. miR-30 has been identified as a regulator of hepatic lipogenesis and recent studies have delivered systemic miR-30 mimic to assess the potential of these therapeutic approaches in the treatment of hypercholesterolemia and atherosclerosis(Irani et al. 2016); however, few analyses to assess the potential 'off-target' effects of mimic delivery on the intestine or the effect of delivery mode (oral compared to intravenous) have been conducted. For miRNAs, like miR-30, with significant roles in intestinal proliferation and differentiation, care in analyzing the effect of treatment on the IE is critical to avoid triggering the development of intestinal lesions or physiological disorders.

miRNAs are well-known to regulate large GRNs through inhibitory post-transcriptional regulation. Nevertheless, it is likely that miRNA target mRNA and protein expression are positively correlated in some cases, such as was seen with miR-30 and *SOX9* in the IE. However, as we show in Chapter 4, regulation of gene expression relies on more than just the transcriptional and post-transcriptional regulators, emphasizing the importance of studies evaluating mRNA, miRNA, and protein dynamics together. Our study also confirms an important role for miRNAs in regulating key IE processes. However, given the variety of functionally-distinct cell types in the intestine, a finer understanding of cell type-specific miRNA

expression in the IE is needed to begin to understand fully their roles in responding to environmental cues and regulating gene expression.

In Chapter 5, not only do I provide the first ever map of the IE miRNA landscape, but also show that IECs have unique miRNA expression profiles across functionally distinct cell populations of the IE. Further, I show that miRNAs respond to the presence of microbiota in a highly cell type-specific manner. To my knowledge, my study also provides the first ever gene expression profile of GF and conventionalized IESCs. Consistent with the increased rate of IE proliferation and migration seen in CV animals(Khoury et al. 1969; Savage et al. 1981), our CV IESCs showed enrichment for genes involved in cell cycle. GF IESC were enriched for genes involved in hormone production and secretion, which is also consistent with reports of GF animals having increased numbers of EECs and circulating hormones(Uribe et al. 1994). Further functional characterization of GF and CV IESCs in the context of the Sox9-EGFP mouse model is an important next step to validate the model and assess the effect of microbiota on IESCs. Our identification of miR-375 as a microbiota-responsive miRNA in IESCs provides a mechanism for both proliferative and hormonal differences seen between CV and GF animals, as knockdown of miR-375 *ex vivo* increased proliferation, and a recent study by Knudsen *et al*. showed miR-375 is an important regulator of EEC differentiation. Yet, many questions remain. These include the precise mechanism by which miR-375 exerts its pro-proliferative influence and the mode by which microbial presence influences the expression of miR-375 and other DE miRNAs. miR-375 is predicted to target many genes, including *Fzd8*, *Klf4*, *Klf5*, and *Yap1*, in the Wnt/β-catenin, Hippo, and other proliferation-associated signaling pathways. However, due to IESCs rarity in enteroid culture, demonstrating direct targeting of these genes by miR-375 in IESCs has proven

difficult. Further knockdown studies *ex vivo* followed by FACS to isolate IESCs may help confirm these targets and identify others.

Identifying the mechanisms by which microbiota influence miRNA expression in IESCs is a complex task. The influence exerted by microbiota could be direct, such as through a TLR ligand binding. However, there are several possible indirect mechanisms including IESC or non-epithelial cell sensing of metabolites, which may impact IESCs possibly through cytokine-directed signaling. Additionally, IESCs may sample luminal contents or uptake/sense bacterial-derived metabolites that induce changes in IESC miRNA expression. Isolating the key mechanism(s) will require further analyses of GF Sox9-EFGP animals and *ex vivo* culture systems using modified colonization studies or injection strategies with heat-killed and live monocultures. As a first step, analyzing the matched jejunal contents using DNA-sequencing will allow us to better model and predict which microbial species influence IESC miRNA expression.

It is very likely that many miRNAs are involved in regulating these intestinal physiological processes in response to microbiota. As stem cells are implicated in the development of colorectal carcinoma, and are vital drivers of tissue repair following injury including that induced by IBD(Moossavi et al. 2013), further research into microbiota- and diet-sensitive IESC miRNAs and the precise role of the DE miRNAs in regulating IESC function are important next steps. Toward this goal, functional evaluations of the miRNAs that were deemed significantly enriched using miRhub will help us identify master miRNA drivers of microbial influence. For example, in preliminary analyses miR-34 and miR-25 target sites were significantly enriched in genes downregulated in IESCs of CV mice, and miR-24 targets were enriched in genes downregulated in HFD IESCs. Functional studies of these miRNAs *ex vivo* are warranted. Importantly, we can also begin evaluating the mechanisms of miRNA changes in

IESCs by evaluating their transcriptional drivers. Enrichment analyses of TF binding sites in DE gene and miRNA promoter regions will help identify additional drivers of microbiota-responsive gene networks. These networks can be further evaluated using assays *in vitro* and *ex vivo*.

An important technique for the field relevant to these follow-up studies is also described in Chapter 5, which is the use of gymnosis to knockdown gene expression in *ex vivo* enteroids. Other methods to knockdown gene expression in enteroids rely on time-consuming, costly, and low-efficiency viral transduction, electroporation, or transfection. Using no transfection reagent, and affordable LNA technology, we show effective knockdown of miRNA expression in enteroids for just the second time(Knudsen et al. 2015). Ongoing work in the lab aims to further characterize this technique to knockdown miRNA and gene expression in enteroids, which may then be further extrapolated for use in other organoid model systems. For example, next steps include evaluating the knockdown efficiency in specific cell populations of the IE including IESCs and EECs, and determining the concentration and half-life of LNAs in this culture system. Understanding the mechanisms behind this technique holds great promise for the broader scientific and medical community.

Finally, there is still a substantial amount that we do not know about miRNAs and other non-coding RNAs in the IE and their role in maintaining homeostasis or contributing to metabolic disease pathogenesis. Using a large array of approaches spanning functional genomics, molecular biology, bioinformatics, physiology, and stem cell biology I have begun to address some of the most pertinent questions. These include whether known biomarkers of metabolic disease have functional significance or whether miRNAs can be used as biomarkers of disease severity, progression, and as prognostic indicators of GI disease. I have asked how key environmental stimuli like the presence or absence of microbiota, or dietary stimuli, affect

distinct cell populations of the IE. I have found that miRNAs in the adult actively cycling IE stem cell population are the most microbiota-sensitive cell population in the IE. This information has a profound impact on how we must now think about the IE and its constant exposure to microbiota, frequent encounters with anti-microbial agents, and ever-changing dietary stimuli. As the stem cell population is long-lived in the IE, and changes in miRNA expression can affect proliferation and differentiation of IECs, DE miRNAs in IESCs could have a prolonged influence on IE physiology and thereby disease progression. Understanding the role of miRNAs in maintaining metabolic homeostasis in the IE is a key objective toward substantially improving current therapeutic options for the treatment of GI and metabolic diseases.

From a broader perspective, my study has profiled the changes in miRNA expression in response to microbial presence and a single dietary perturbation in a single mouse strain and in a single sex. The effect of host-genetic variation on miRNA responses to microbiota across the IE has not been evaluated, but is of great interest both biologically and from a precision medicine-perspective, as is understanding the relationship between diet and microbiota, which would influence bioavailability and presence of certain metabolites and microbial species. Toward the development of effective therapeutics for the treatment of GI and metabolic diseases, understanding the interaction and relationship between dietary macromolecules, specific microbial species, and IESC miRNA expression based on host-genotype is a vital, but long-term goal for which my research lays the ground work.

This dissertation, and the accompanying published journal articles and publicly released next-generation high-throughput sequencing datasets provide substantial groundwork from which the scientific community can build upon for years to come.

REFERENCES

Abrams GD. 1977. Microbial effects on mucosal structure and function. Am J Clin Nutr 30:1880–1886.

Agrawal R, Tran U, Wessely O. 2009. The miR-30 miRNA family regulates Xenopus pronephros development and targets the transcription factor Xlim1/Lhx1. Development 136:3927–3936.

Aguilar M, Bhuket T, Torres S, Liu B, Wong RJ. 2015. Prevalence of the metabolic syndrome in the United States, 2003-2012. JAMA 313:1973–1974.

Ahmadian M, Suh JM, Hah N, Liddle C, Atkins AR, Downes M, Evans RM. 2013. PPARγ signaling and metabolism: the good, the bad and the future. Nat Med 19:557–566.

Aidy El S, Merrifield CA, Derrien M, van Baarlen P, Hooiveld G, Levenez F, Doré J, Dekker J, Holmes E, Claus SP, et al. 2013. The gut microbiota elicits a profound metabolic reorientation in the mouse jejunal mucosa during conventionalisation. Gut 62:1306–1314.

Aidy El S, van Baarlen P, Derrien M, Lindenbergh-Kortleve DJ, Hooiveld G, Levenez F, Doré J, Dekker J, Samsom JN, Nieuwenhuis EES, et al. 2012. Temporal and spatial interplay of microbiota and intestinal mucosa drive establishment of immune homeostasis in conventionalized mice. Mucosal Immunol 5:567–579.

Al-Daghri NM, Clerici M, Al-Attas O, Forni D, Alokail MS, Alkharfy KM, Sabico S, Mohammed AK, Cagliani R, Sironi M. 2013. A nonsense polymorphism (R392X) in TLR5 protects from obesity but predisposes to diabetes. J. Immunol. 190:3716–3720.

Anders S, Huber W. 2010. Differential expression analysis for sequence count data. Genome Biol. 11:R106.

Andres SF, Simmons JG, Mah AT, Santoro MA, Van Landeghem L, Lund PK. 2013. Insulin receptor isoform switching in intestinal stem cells, progenitors, differentiated lineages and tumors: evidence that IR-B limits proliferation. J. Cell. Sci. 126:5645–5656.

Arantes RME, Nogueira AMMF. 1997. Distribution of enteroglucagon- and peptide YY-immunoreactive cells in the intestinal mucosa of GF and conventional mice. Cell and Tissue Research 290:61.

Archambaud C, Sismeiro O, Toedling J, Soubigou G, Bécavin C, Lechat P, Lebreton A, Ciaudo C, Cossart P. 2013. The intestinal microbiota interferes with the microRNA response upon oral Listeria infection. mBio 4:e00707–13.

Aron-Wisnewsky J, Clément K. 2016. The gut microbiome, diet, and links to cardiometabolic and chronic disorders. Nat Rev Nephrol 12:169–181.

Arroyo JD, Chevillet JR, Kroh EM, Ruf IK, Pritchard CC, Gibson DF, Mitchell PS, Bennett CF, Pogosova-Agadjanyan EL, Stirewalt DL, et al. 2011. Argonaute2 complexes carry a population

of circulating microRNAs independent of vesicles in human plasma. PNAS 108:5003–5008.

Arumugam M, Raes J, Pelletier E, Le Paslier D, Yamada T, Mende DR, Fernandes GR, Tap J, Bruls T, Batto J-M, et al. 2011. Enterotypes of the human gut microbiome. Nature 473:174–180.

Ashburner M, Ball CA, Blake JA, Botstein D, Butler H, Cherry JM, Davis AP, Dolinski K, Dwight SS, Eppig JT, et al. 2000. Gene ontology: tool for the unification of biology. The Gene Ontology Consortium. Nat. Genet. 25:25–29.

Bagge A, Clausen TR, Larsen S, Ladefoged M, Rosenstierne MW, Larsen L, Vang O, Nielsen JH, Dalgaard LT. 2012. MicroRNA-29a is up-regulated in beta-cells by glucose and decreases glucose-stimulated insulin secretion. Biochem. Biophys. Res. Commun. 426:266–272.

Bandiera S, Pfeffer S, Baumert TF, Zeisel MB. 2015. miR-122--a key factor and therapeutic target in liver disease. J. Hepatol. 62:448–457.

Baran-Gale J, Fannin EE, Kurtz CL, Sethupathy P. 2013. Beta cell 5'-shifted isomiRs are candidate regulatory hubs in type 2 diabetes. PLoS ONE 8:e73240.

Bartel DP. 2009. MicroRNAs: target recognition and regulatory functions. Cell 136:215–233.

Bastide P, Darido C, Pannequin J, Kist R, Robine S, Marty-Double C, Bibeau F, Scherer G, Joubert D, Hollande F, et al. 2007. Sox9 regulates cell proliferation and is required for Paneth cell differentiation in the intestinal epithelium. The Journal of Cell Biology 178:635–648.

Basuroy S, Sheth P, Kuppuswamy D, Balasubramanian S, Ray RM, Rao RK. 2003. Expression of kinase-inactive c-Src delays oxidative stress-induced disassembly and accelerates calcium-mediated reassembly of tight junctions in the Caco-2 cell monolayer. J Biol Chem 278:11916–11924.

Becker S, Oelschlaeger TA, Wullaert A, Pasparakis M, Wehkamp J, Stange EF, Gersemann M. 2013. Bacteria regulate intestinal epithelial cell differentiation factors both in vitro and in vivo. PLoS ONE 8:e55620.

Beg MS, Brenner A, Sachdev J, Ejadi S, Borad M, Kang Y-K, Lim H, Kim T-Y, Bader A, Stoudemire J, et al. 2015. Abstract C43: Safety, tolerability, and clinical activity of MRX34, the first-in-class liposomal miR-34 mimic, in patients with advanced solid tumors. Mol Cancer Ther 14:C43.

Belo J, Krishnamurthy M, Oakie A, Wang R. 2013. The role of SOX9 transcription factor in pancreatic and duodenal development. Stem Cells and Development 22:2935–2943.

Beyaz S, Mana MD, Roper J, Kedrin D, Saadatpour A, Hong S-J, Bauer-Rowe KE, Xifaras ME, Akkad A, Arias E, et al. 2016. High-fat diet enhances stemness and tumorigenicity of intestinal progenitors. Nature 531:53–58.

Bhajun R, Guyon L, Gidrol X. 2016. MicroRNA degeneracy and pluripotentiality within a Lavallière-tie architecture confers robustness to gene expression networks. Cell. Mol. Life Sci.

73:2821–2827.

Biton M, Levin A, Slyper M, Alkalay I, Horwitz E, Mor H, Kredo-Russo S, Avnit-Sagi T, Cojocaru G, Zreik F, Bentwich Z, Poy MN, Artis D, Walker MD, Hornstein E, Pikarsky E, Ben-Neriah Y. 2011. Epithelial microRNAs regulate gut mucosal immunity via epithelium-T cell crosstalk. Nat Immunol 12:239–246.

Bolger AM, Lohse M, Usadel B. 2014. Trimmomatic: a flexible trimmer for Illumina sequence data. Bioinformatics 30:2114–2120.

Bonamichi-Santos R, Aun MV, Agondi RC, Kalil J, Giavina-Bianchi P. 2015. Microbiome and asthma: What have experimental models already taught us? J Immunol Res 2015:614758.

Boon RA, Vickers KC. 2013. Intercellular transport of microRNAs. Arteriosclerosis, Thrombosis, and Vascular Biology 33:186–192.

Borchardt RT. 2011. Hidalgo, I. J., Raub, T. J., and Borchardt, R. T.: Characterization of the human colon carcinoma cell line (Caco-2) as a model system for intestinal epithelial permeability, Gastroenterology, 96, 736-749, 1989--the backstory. AAPS J 13:323–327.

Brain O, Owens BMJ, Pichulik T, Allan P, Khatamzas E, Leslie A, Steevels T, Sharma S, Mayer A, Catuneanu AM, et al. 2013. The intracellular sensor NOD2 induces microRNA-29 expression in human dendritic cells to limit IL-23 release. Immunity 39:521–536.

Brest P, Lapaquette P, Souidi M, Lebrigand K, Cesaro A, Vouret-Craviari V, Mari B, Barbry P, Mosnier J-F, Hébuterne X, et al. 2011. A synonymous variant in IRGM alters a binding site for miR-196 and causes deregulation of IRGM-dependent xenophagy in Crohn's disease. Nat. Genet. 43:242–245.

Briske-Anderson MJ, Finley JW, Newman SM. 1997. The influence of culture time and passage number on the morphological and physiological development of Caco-2 cells. Proceedings of the Society for Experimental Biology and Medicine 214:248–257.

Bulik-Sullivan B, Selitsky S, Sethupathy P. 2013. Prioritization of genetic variants in the microRNA regulome as functional candidates in genome-wide association studies. Hum Mutat 34:1049–1056.

Carrer M, Liu N, Grueter CE, Williams AH, Frisard MI, Hulver MW, Bassel-Duby R, Olson EN. 2012. Control of mitochondrial metabolism and systemic energy homeostasis by microRNAs 378 and 378*. PNAS 109:15330–15335.

Carvalho BM, Guadagnini D, Tsukumo DML, Schenka AA, Latuf-Filho P, Vassallo J, Dias JC, Kubota LT, Carvalheira JBC, Saad MJA. 2012. Modulation of gut microbiota by antibiotics improves insulin signalling in high-fat fed mice. Diabetologia 55:2823–2834.

Chang T, Xie J, Li H, Li D, Liu P, Hu Y. 2016. MicroRNA-30a promotes extracellular matrix degradation in articular cartilage via downregulation of Sox9. Cell Prolif. 49:207–218.

Chen EY, Tan CM, Kou Y, Duan Q, Wang Z, Meirelles GV, Clark NR, Ma'ayan A. 2013. Enrichr: interactive and collaborative HTML5 gene list enrichment analysis tool. BMC Bioinformatics 14:128.

Chen Y, Wang C, Liu Y, Tang L, Zheng M, Xu C, Song J, Meng X. 2013. miR-122 targets NOD2 to decrease intestinal epithelial cell injury in Crohn's disease. Biochem. Biophys. Res. Commun. 438:133–139.

Chimerel C, Emery E, Summers DK, Keyser U, Gribble FM, Reimann F. 2014. Bacterial metabolite indole modulates incretin secretion from intestinal enteroendocrine L cells. Cell Rep 9:1202–1208.

Chivukula RR, Shi G, Acharya A, Mills EW, Zeitels LR, Anandam JL, Abdelnaby AA, Balch GC, Mansour JC, Yopp AC, et al. 2014. An essential mesenchymal function for miR-143/145 in intestinal epithelial regeneration. Cell 157:1104–1116.

Cho S, Wu C-J, Yasuda T, Cruz LO, Khan AA, Lin L-L, Nguyen DT, Miller M, Lee H-M, Kuo M-L, et al. 2016. miR-23~27~24 clusters control effector T cell differentiation and function. Journal of Experimental Medicine 213:235–249.

Chuang AY, Chuang JC, Zhai Z, Wu F, Kwon JH. 2014. NOD2 expression is regulated by microRNAs in colonic epithelial HCT116 cells. Inflammatory Bowel Diseases 20:126–135.

Chung ACK, Huang XR, Meng X, Lan HY. 2010. miR-192 mediates TGF-beta/Smad3-driven renal fibrosis. J. Am. Soc. Nephrol. 21:1317–1325.

Cirera-Salinas D, Pauta M, Allen RM, Salerno AG, Ramírez CM, Chamorro-Jorganes A, Wanschel AC, Lasunción MA, Morales-Ruiz M, Suárez Y, et al. 2012. miR-33 regulates cell proliferation and cell cycle progression. Cell Cycle 11:922–933.

Clarke RM. 1975. Diet, mucosal architecture and epithelial cell production in the small intestine of specified-pathogen-free and conventional rats. Lab. Anim. 9:201–209.

Cloonan N, Wani S, Xu Q, Gu J, Lea K, Heater S, Barbacioru C, Steptoe AL, Martin HC, Nourbakhsh E, et al. 2011. MicroRNAs and their isomiRs function cooperatively to target common biological pathways. Genome Biol. 12:R126.

Codocedo JF, Ríos JA, Godoy JA, Inestrosa NC. 2016. Are microRNAs the molecular link between metabolic syndrome and Alzheimer's disease? Mol. Neurobiol. 53:2320–2338.

Couzin J. 2008 Mar 28. MicroRNAs make big impression in disease after disease. Science 319:1782–1784.

Creamer B, Shorter RG, Bamforth J. 1961. The turnover and shedding of epithelial cells. Gut 2:110–116.

Creemers EE, Tijsen AJ, Pinto YM. 2012. Circulating microRNAs: novel biomarkers and extracellular communicators in cardiovascular disease? Circ. Res. 110:483–495.

Dalal SR, Kwon JH. 2010. The role of microRNA in inflammatory bowel disease. Gastroenterol Hepatol (N Y) 6:714–722.

Dalmasso G, Nguyen HTT, Yan Y, Laroui H, Charania MA, Ayyadurai S, Sitaraman SV, Merlin D. 2011. Microbiota modulate host gene expression via microRNAs. PLoS ONE 6:e19293.

David LA, Maurice CF, Carmody RN, Gootenberg DB, Button JE, Wolfe BE, Ling AV, Devlin AS, Varma Y, Fischbach MA, et al. 2014. Diet rapidly and reproducibly alters the human gut microbiome. Nature 505:559–563.

Dávalos A, Goedeke L, Smibert P, Ramírez CM, Warrier NP, Andreo U, Cirera-Salinas D, Rayner K, Suresh U, Pastor-Pareja JC, et al. 2011. miR-33a/b contribute to the regulation of fatty acid metabolism and insulin signaling. PNAS 108:9232–9237.

Delay C, Grenier-Boley B, Amouyel P, Dumont J, Lambert J-C. 2016. miRNA-dependent target regulation: functional characterization of single-nucleotide polymorphisms identified in genome-wide association studies of Alzheimer's disease. Alzheimers Res Ther 8:20.

Devaraj S, Hemarajata P, Versalovic J. 2013. The human gut microbiome and body metabolism: implications for obesity and diabetes. Clin. Chem. 59:617–628.

Dregan A, Charlton J, Chowienczyk P, Gulliford MC. 2014. Chronic inflammatory disorders and risk of type 2 diabetes mellitus, coronary heart disease, and stroke: a population-based cohort study. Circulation 130:837–844.

Duan J, Chung H, Troy E, Kasper DL. 2010. Microbial colonization drives expansion of IL-1 receptor 1-expressing and IL-17-producing gamma/delta T cells. Cell Host & Microbe 7:140–150.

Dumortier O, Hinault C, Van Obberghen E. 2013. MicroRNAs and metabolism crosstalk in energy homeostasis. Cell Metabolism 18:312–324.

Dynoodt P, Speeckaert R, De Wever O, Chevolet I, Brochez L, Lambert J, Van Gele M. 2013. miR-145 overexpression suppresses the migration and invasion of metastatic melanoma cells. Int. J. Oncol. 42:1443–1451.

Everard A, Belzer C, Geurts L, Ouwerkerk JP, Druart C, Bindels LB, Guiot Y, Derrien M, Muccioli GG, Delzenne NM, et al. 2013. Cross-talk between Akkermansia muciniphila and intestinal epithelium controls diet-induced obesity. PNAS 110:9066–9071.

Everard A, Cani PD. 2014. Gut microbiota and GLP-1. Rev Endocr Metab Disord 15:189–196.

Fasseu M, Tréton X, Guichard C, Pedruzzi E. 2010. Identification of restricted subsets of mature microRNA abnormally expressed in inactive colonic mucosa of patients with inflammatory bowel disease. PLoS ONE 5:e13160.

Feng X, Wang H, Ye S, Guan J, Tan W, Cheng S, Wei G, Wu W, Wu F, Zhou Y. 2012. Up-regulation of microRNA-126 may contribute to pathogenesis of ulcerative colitis via regulating

NF-kappaB inhibitor IκBα. PLoS ONE 7:e52782.

Fernandez-Valverde SL, Taft RJ, Mattick JS. 2011. MicroRNAs in β-cell biology, insulin resistance, diabetes and its complications. Diabetes 60:1825–1831.

Formeister EJ, Sionas AL, Lorance DK, Barkley CL, Lee GH, Magness ST. 2009. Distinct SOX9 levels differentially mark stem/progenitor populations and enteroendocrine cells of the small intestine epithelium. Am. J. Physiol. Gastrointest. Liver Physiol. 296:G1108–G1118.

Forslund K, Hildebrand F, Nielsen T, Falony G, Le Chatelier E, Sunagawa S, Prifti E, Vieira-Silva S, Gudmundsdottir V, Krogh Pedersen H, et al. 2015. Disentangling type 2 diabetes and metformin treatment signatures in the human gut microbiota. Nature 528:262–266.

Friedman RC, Farh KK-H, Burge CB, Bartel DP. 2009. Most mammalian mRNAs are conserved targets of microRNAs. Genome Research 19:92–105.

Fuller MK, Faulk DM, Sundaram N, Shroyer NF, Henning SJ, Helmrath MA. 2012. Intestinal crypts reproducibly expand in culture. Journal of Surgical Research 178:48–54.

Furet J-P, Kong L-C, Tap J, Poitou C, Basdevant A, Bouillot J-L, Mariat D, Corthier G, Doré J, Henegar C, et al. 2010. Differential adaptation of human gut microbiota to bariatric surgery-induced weight loss: links with metabolic and low-grade inflammation markers. Diabetes 59:3049–3057.

Garcia DM, Baek D, Shin C, Bell GW, Grimson A, Bartel DP. 2011. Weak seed-pairing stability and high target-site abundance decrease the proficiency of lsy-6 and other microRNAs. Nat Struct Mol Biol 18:1139–1146.

García-Segura L, Pérez-Andrade M, Miranda-Ríos J. 2013. The emerging role of microRNAs in the regulation of gene expression by nutrients. J Nutrigenet Nutrigenomics 6:16–31.

Gene Ontology Consortium. 2015. Gene Ontology Consortium: going forward. Nucleic Acids Research 43:D1049–56.

Geremia A, Biancheri P, Allan P, Corazza GR, Di Sabatino A. 2014. Innate and adaptive immunity in inflammatory bowel disease. Autoimmun Rev 13:3–10.

Ghorpade DS, Sinha AY, Holla S, Singh V, Balaji KN. 2013. NOD2-nitric oxide-responsive microRNA-146a activates Sonic hedgehog signaling to orchestrate inflammatory responses in murine model of inflammatory bowel disease. J Biol Chem 288:33037–33048.

Gil-Zamorano J, Martin R, Daimiel L, Richardson K, Giordano E, Nicod N, García-Carrasco B, Soares SMA, Iglesias-Gutiérrez E, Lasunción MA, et al. 2014. Docosahexaenoic acid modulates the enterocyte Caco-2 cell expression of microRNAs involved in lipid metabolism. J. Nutr. 144:575–585.

Gordon HA, Pesti L. 1971. The gnotobiotic animal as a tool in the study of host microbial relationships. Bacteriological reviews 25:390–429.

Gracz AD, Ramalingam S, Magness ST. 2010. Sox9 expression marks a subset of CD24-expressing small intestine epithelial stem cells that form organoids in vitro. Am. J. Physiol. Gastrointest. Liver Physiol. 298:G590–G600.

Grimson A, Farh KK-H, Johnston WK, Garrett-Engele P, Lim LP, Bartel DP. 2007. MicroRNA targeting specificity in mammals: determinants beyond seed pairing. Molecular Cell 27:91–105.

Grundy SM. 2015. Adipose tissue and metabolic syndrome: too much, too little or neither. Eur. J. Clin. Invest. 45:1209–1217.

Grün D, Lyubimova A, Kester L, Wiebrands K, Basak O, Sasaki N, Clevers H, van Oudenaarden A. 2015. Single-cell messenger RNA-sequencing reveals rare intestinal cell types. Nature 525:251–255.

Guess MG, Barthel KKB, Harrison BC, Leinwand LA. 2015. miR-30 family microRNAs regulate myogenic differentiation and provide negative feedback on the microRNA pathway. Gaetano C, editor. PLoS ONE 10:e0118229.

Guo H, Ingolia NT, Weissman JS, Bartel DP. 2010. Mammalian microRNAs predominantly act to decrease target mRNA levels. Nature 466:835–840.

Guo Z, Wu R, Gong J, Zhu W, Li Y, Wang Z, Li N, Li J. 2015. Altered microRNA expression in inflamed and non-inflamed terminal ileal mucosa of adult patients with active Crohn's disease. J. Gastroenterol. Hepatol. 30:109–116.

Han Y-C, Park CY, Bhagat G, Zhang J, Wang Y, Fan J-B, Liu M, Zou Y, Weissman IL, Gu H. 2010. microRNA-29a induces aberrant self-renewal capacity in hematopoietic progenitors, biased myeloid development, and acute myeloid leukemia. Journal of Experimental Medicine 207:475–489.

Hattori T, Kishino T, Stephen S, Eberspaecher H, Maki S, Takigawa M, de Crombrugghe B, Yasuda H. 2013. E6-AP/UBE3A protein acts as a ubiquitin ligase toward SOX9 protein. J Biol Chem 288:35138–35148.

He P, Liang J, Shao T, Guo Y, Hou Y, Li Y. 2015. HDAC5 promotes colorectal cancer cell proliferation by up-regulating DLL4 expression. Int J Clin Exp Med 8:6510–6516.

Hernández-Chirlaque C, Aranda CJ, Ocón B, Capitán-Cañadas F, Ortega-González M, Carrero JJ, Suárez MD, Zarzuelo A, Sánchez de Medina F, Martínez-Augustin O. 2016 Apr 26. GF and antibiotic-treated mice are highly susceptible to epithelial injury in DSS colitis. Journal of Crohn's and Colitis:jjw096.

Herranz H, Cohen SM. 2010. MicroRNAs and gene regulatory networks: managing the impact of noise in biological systems. Genes & Development 24:1339–1344.

Hino K, Tsuchiya K, Fukao T, Kiga K, Okamoto R, Kanai T, Watanabe M. 2008. Inducible expression of microRNA-194 is regulated by HNF-1 during intestinal epithelial cell differentiation. RNA 14:1433–1442.

Hoffman BG, Robertson G, Zavaglia B, Beach M, Cullum R, Lee S, Soukhatcheva G, Li L, Wederell ED, Thiessen N, et al. 2010. Locus co-occupancy, nucleosome positioning, and H3K4me1 regulate the functionality of FOXA2-, HNF4A-, and PDX1-bound loci in islets and liver. Genome Research 20:1037–1051.

Horie T, Ono K, Horiguchi M, Nishi H, Nakamura T, Nagao K, Kinoshita M, Kuwabara Y, Marusawa H, Iwanaga Y, et al. 2010. MicroRNA-33 encoded by an intron of sterol regulatory element-binding protein 2 (Srebp2) regulates HDL in vivo. PNAS 107:17321–17326.

Hu S, Dong TS, Dalal SR, Wu F, Bissonnette M, Kwon JH, Chang EB. 2011. The microbe-derived short chain fatty acid butyrate targets miRNA-dependent p21 gene expression in human colon cancer. PLoS ONE 6:e16221.

Huang T-C, Sahasrabuddhe NA, Kim M-S, Getnet D, Yang Y, Peterson JM, Ghosh B, Chaerkady R, Leach SD, Marchionni L, et al. 2012. Regulation of lipid metabolism by Dicer revealed through SILAC mice. J. Proteome Res. 11:2193–2205.

Huang Z, Shi T, Zhou Q, Shi S, Zhao R, Shi H, Dong L, Zhang C, Zeng K, Chen J, et al. 2014. miR-141 Regulates colonic leukocytic trafficking by targeting CXCL12β during murine colitis and human Crohn's disease. Gut 63:1247–1257.

Inukai S, Slack FJ. 2012. miR-33 connects cholesterol to the cell cycle. Cell Cycle 11:1060–1061.

Irani S, Pan X, Peck BCE, Iqbal J, Sethupathy P, Hussain MM. 2016 Jun 30. MicroRNA-30c Mimic Mitigates Hypercholesterolemia and Atherosclerosis in Mice. J Biol Chem:jbc.M116.728451.

Jackson AL, Levin AA. 2012. Developing microRNA therapeutics: approaching the unique complexities. Nucleic Acid Ther 22:213–225.

Jaladanki RN, Wang JY. 2011. Regulation of gastrointestinal mucosal growth. Colloquium Series on Integrated ….

Jayaprakash AD, Jabado O, Brown BD, Sachidanandam R. 2011. Identification and remediation of biases in the activity of RNA ligases in small-RNA deep sequencing. Nucleic Acids Research 39:e141.

Jin M, Wu Y, Wang J, Chen J, Huang Y, Rao J, Feng C. 2016. MicroRNA-24 promotes 3T3-L1 adipocyte differentiation by directly targeting the MAPK7 signaling. Biochem. Biophys. Res. Commun. 474:76–82.

Kadowaki T. 2000. Insights into insulin resistance and type 2 diabetes from knockout mouse models. J. Clin. Invest. 106:459–465.

Kamachi Y, Kondoh H. 2013. Sox proteins: regulators of cell fate specification and differentiation. Development 140:4129–4144.

Kanai Y, Hiramatsu R, Matoba S, Kidokoro T. 2005. From SRY to SOX9: mammalian testis differentiation. J. Biochem. 138:13–19.

Kang M, Yan LM, Li YM, Zhang WY, Wang H, Tang AZ, Ou HS. 2013. Inhibitory effect of microRNA-24 on fatty acid-binding protein expression on 3T3-L1 adipocyte differentiation. Genet. Mol. Res. 12:5267–5277.

Karlsson FH, Tremaroli V, Nookaew I, Bergström G, Behre CJ, Fagerberg B, Nielsen J, Bäckhed F. 2013. Gut metagenome in European women with normal, impaired and diabetic glucose control. Nature 498:99–103.

Karolina DS, Tavintharan S, Armugam A, Sepramaniam S, Pek SLT, Wong MTK, Lim SC, Sum CF, Jeyaseelan K. 2012. Circulating miRNA profiles in patients with metabolic syndrome. J. Clin. Endocrinol. Metab. 97:E2271–6.

Kashiyama K, Mitsutake N, Matsuse M, Ogi T, Saenko VA, Ujifuku K, Utani A, Hirano A, Yamashita S. 2012. miR-196a downregulation increases the expression of type I and III collagens in keloid fibroblasts. J. Invest. Dermatol. 132:1597–1604.

Khoury KA, Floch MH, Hersh T. 1969. Small intestinal mucosal cell proliferation and bacterial flora in the conventionalization of the germfree mouse. J. Exp. Med. 130:659–670.

Kim D, Kim Y-G, Seo S-U, Kim D-J, Kamada N, Prescott D, Philpott DJ, Rosenstiel P, Inohara N, Núñez G. 2016. Nod2-mediated recognition of the microbiota is critical for mucosal adjuvant activity of cholera toxin. Nat Med 22:524–530.

Kim W, Kyung Lee E. 2012. Post-transcriptional regulation in metabolic diseases. RNA Biol 9:772–780.

Knudsen LA, Petersen N, Schwartz TW, Egerod KL. 2015. The MicroRNA Repertoire in Enteroendocrine Cells: Identification of miR-375 as a Potential Regulator of the Enteroendocrine Lineage. Endocrinology 156:3971–3983.

Kole AJ, Swahari V, Hammond SM, Deshmukh M. 2011. miR-29b is activated during neuronal maturation and targets BH3-only genes to restrict apoptosis. Genes & Development 25:125–130.

Kong L, Zhu J, Han W, Jiang X, Xu M, Zhao Y, Dong Q, Pang Z, Guan Q, Gao L, et al. 2011. Significance of serum microRNAs in pre-diabetes and newly diagnosed type 2 diabetes: a clinical study. Acta Diabetol 48:61–69.

Kornfeld J-W, Baitzel C, Könner AC, Nicholls HT, Vogt MC, Herrmanns K, Scheja L, Haumaitre C, Wolf AM, Knippschild U, et al. 2013. Obesity-induced overexpression of miR-802 impairsglucose metabolism through silencing of Hnf1b. Nature 494:111–115.

Krist B, Florczyk U, Pietraszek-Gremplewicz K, Józkowicz A, Dulak J. 2015. The role of miR-378a in metabolism, angiogenesis, and muscle biology. Int J Endocrinol 2015:281756.

Kurtz CL, Fannin EE, Toth CL, Pearson DS, Vickers KC, Sethupathy P. 2015. Inhibition of

miR-29 has a significant lipid-lowering benefit through suppression of lipogenic programs in liver. Sci Rep 5:12911.

Kurtz CL, Peck BCE, Fannin EE, Beysen C, Miao J, Landstreet SR, Ding S, Turaga V, Lund PK, Turner S, et al. 2014. MicroRNA-29 fine-tunes the expression of key FOXA2-activated lipid metabolism genes and is dysregulated in animal models of insulin resistance and diabetes. Diabetes 63:3141–3148.

Larsen N, Vogensen FK, van den Berg FWJ, Nielsen DS, Andreasen AS, Pedersen BK, Al-Soud WA, Sørensen SJ, Hansen LH, Jakobsen M. 2010. Gut microbiota in human adults with type 2 diabetes differs from non-diabetic adults. PLoS ONE 5:e9085.

Larsson E, Tremaroli V, Lee YS, Koren O, Nookaew I, Fricker A, Nielsen J, Ley RE, Bäckhed F. 2012. Analysis of gut microbial regulation of host gene expression along the length of the gut and regulation of gut microbial ecology through MyD88. Gut 61:1124–1131.

le Roux CW, Welbourn R, Werling M, Osborne A, Kokkinos A, Laurenius A, Lönroth H, Fändriks L, Ghatei MA, Bloom SR, et al. 2007. Gut hormones as mediators of appetite and weight loss after Roux-en-Y gastric bypass. Ann. Surg. 246:780–785.

Lee H, Ko G. 2014. Effect of metformin on metabolic improvement and gut microbiota. Appl. Environ. Microbiol. 80:5935–5943.

Lee S, Yoon DS, Paik S, Lee K-M, Jang Y, Lee JW. 2014. microRNA-495 inhibits chondrogenic differentiation in human mesenchymal stem cells by targeting Sox9. Stem Cells and Development 23:1798–1808.

Lees CW, Barrett JC, Parkes M, Satsangi J. 2011. New IBD genetics: common pathways with other diseases. Gut 60:1739–1753.

Lewis BP, Burge CB, Bartel DP. 2005. Conserved seed pairing, often flanked by adenosines, indicates that thousands of human genes are microRNA targets. Cell 120:15–20.

Li B, Dewey CN. 2011. RSEM: accurate transcript quantification from RNA-Seq data with or without a reference genome. BMC Bioinformatics 12:323.

Li C, Kuemmerle JF. 2014. Mechanisms that mediate the development of fibrosis in patients with Crohn's disease. Inflammatory Bowel Diseases 20:1250–1258.

Li JV, Ashrafian H, Bueter M, Kinross J, Sands C, le Roux CW, Bloom SR, Darzi A, Athanasiou T, Marchesi JR, et al. 2011. Metabolic surgery profoundly influences gut microbial-host metabolic cross-talk. Gut 60:1214–1223.

Lifshitz F, Wapnir RA, Wehman HJ, Diaz-bensussen S, Pergolizzi R. 1978. The effects of small intestinal colonization by fecal and colonic bacteria on intestinal function in rats. J. Nutr. 108:1913–1923.

Lin J, Cao Q, Zhang J, Li Y, Shen B, Zhao Z, Chinnaiyan AM, Bronner MP. 2013. MicroRNA

expression patterns in indeterminate inflammatory bowel disease. Modern Pathology 26:148–154.

Lin J, Welker NC, Zhao Z, Li Y, Zhang J, Reuss SA, Zhang X, Lee H, Liu Y, Bronner MP. 2013. Novel specific microRNA biomarkers inidiopathic inflammatory bowel diseaseunrelated to disease activity. Modern Pathology 27:602–608.

Lindow M, Kauppinen S. 2012. Discovering the first microRNA-targeted drug. The Journal of Cell Biology 199:407–412.

Liu EY, Li M, Wang W, Li Y. 2013. MaCH-admix: genotype imputation for admixed populations. Genet. Epidemiol. 37:25–37.

Liu S, da Cunha AP, Rezende RM, Cialic R, Wei Z, Bry L, Comstock LE, Gandhi R, Weiner HL. 2016. The host shapes the gut microbiota via fecal microRNA. Cell Host & Microbe 19:32–43.

Liu X, Fortin K, Mourelatos Z. 2008. MicroRNAs: Biogenesis and Molecular Functions. Brain Pathology 18:113–121.

Lord CC, Betters JL, Ivanova PT, Milne SB, Myers DS, Madenspacher J, Thomas G, Chung S, Liu M, Davis MA, et al. 2012. CGI-58/ABHD5-derived signaling lipids regulate systemic inflammation and insulin action. Diabetes 61:355–363.

Loscalzo J. 2013. Gut microbiota, the genome, and diet in atherogenesis. N Engl J Med 368:1647–1649.

Ludwig K, Fassan M, Mescoli C, Pizzi M, Balistreri M, Albertoni L, Pucciarelli S, Scarpa M, Sturniolo GC, Angriman I, et al. 2013. PDCD4/miR-21 dysregulation in inflammatory bowel disease-associated carcinogenesis. Virchows Arch. 462:57–63.

Ma F, Xu S, Liu X, Zhang Q, Xu X, Liu M, Hua M, Li N, Yao H, Cao X. 2011. The microRNA miR-29 controls innate and adaptive immune responses to intracellular bacterial infection by targeting interferon-γ. Nat Immunol 12:861–869.

Mah AT, Van Landeghem L, Gavin HE, Magness ST, Lund PK. 2014. Impact of diet-induced obesity on intestinal stem cells: hyperproliferation but impaired intrinsic function that requires insulin/IGF1. Endocrinology 155:3302–3314.

Maharshak N, Shenhar-Tsarfaty S, Aroyo N, Orpaz N, Guberman I, Canaani J, Halpern Z, Dotan I, Berliner S, Soreq H. 2013. MicroRNA-132 modulates cholinergic signaling and inflammation in human inflammatory bowel disease. Inflammatory Bowel Diseases 19:1346–1353.

Marette A, Liu Y, Sweeney G. 2014. Skeletal muscle glucose metabolism and inflammation in the development of the metabolic syndrome. Rev Endocr Metab Disord 15:299–305.

Marquart TJ, Allen RM, Ory DS, Baldán A. 2010. miR-33 links SREBP-2 induction to repression of sterol transporters. PNAS 107:12228–12232.

Martinez I, Cazalla D, Almstead LL, Steitz JA, DiMaio D. 2011. miR-29 and miR-30 regulate B-Myb expression during cellular senescence. PNAS 108:522–527.

Martinez-Sanchez A, Dudek KA, Murphy CL. 2012. Regulation of human chondrocyte function through direct inhibition of cartilage master regulator SOX9 by microRNA-145 (miRNA-145). J Biol Chem 287:916–924.

Martínez-Borra J, López-Larrea C, González S, Fuentes D, Dieguez A, Deschamps EM, Pérez-Pariente JM, López-Vázquez A, de Francisco R, Rodrigo L. 2002. High serum tumor necrosis factor-alpha levels are associated with lack of response to infliximab in fistulizing Crohn's disease. Am. J. Gastroenterol. 97:2350–2356.

McKenna LB, Schug J, Vourekas A, McKenna JB, Bramswig NC, Friedman JR, Kaestner KH. 2010. MicroRNAs control intestinal epithelial differentiation, architecture, and barrier function. Gastroenterology 139:1654–64– 1664.e1.

Melkman-Zehavi T, Oren R, Kredo-Russo S, Shapira T, Mandelbaum AD, Rivkin N, Nir T, Lennox KA, Behlke MA, Dor Y, et al. 2011. miRNAs control insulin content in pancreatic β-cells via downregulation of transcriptional repressors. EMBO J. 30:835–845.

Mikkelsen KH, Frost M, Bahl MI, Licht TR, Jensen US, Rosenberg J, Pedersen O, Hansen T, Rehfeld JF, Holst JJ, et al. 2015. Effect of antibiotics on gut microbiota, gut hormones and glucose metabolism. Buchowski M, editor. PLoS ONE 10:e0142352.

Mitchell PS, Parkin RK, Kroh EM, Fritz BR, Wyman SK, Pogosova-Agadjanyan EL, Peterson A, Noteboom J, O'Briant KC, Allen A, et al. 2008. Circulating microRNAs as stable blood-based markers for cancer detection. PNAS 105:10513–10518.

Mithieux G, Andreelli F, Magnan C. 2009. Intestinal gluconeogenesis: key signal of central control of energy and glucose homeostasis. Current Opinion in Clinical Nutrition and Metabolic Care 12:419–423.

Mithieux G, Gautier-Stein A. 2014. Intestinal glucose metabolism revisited. Diabetes Res. Clin. Pract. 105:295–301.

Mittelbrunn M, Gutiérrez-Vázquez C, Villarroya-Beltri C, González S, Sánchez-Cabo F, González MÁ, Bernad A, Sánchez-Madrid F. 2011. Unidirectional transfer of microRNA-loaded exosomes from T cells to antigen-presenting cells. Nat Commun 2:282.

Mologni L, Dekhil H, Ceccon M, Purgante S, Lan C, Cleris L, Magistroni V, Formelli F, Gambacorti-Passerini CB. 2010. Colorectal Tumors Are Effectively Eradicated by Combined Inhibition of -Catenin, KRAS, and the Oncogenic Transcription Factor ITF2. Cancer Res. 70:7253–7263.

Montecalvo A, Larregina AT, Shufesky WJ, Stolz DB, Sullivan MLG, Karlsson JM, Baty CJ, Gibson GA, Erdos G, Wang Z, et al. 2012. Mechanism of transfer of functional microRNAs between mouse dendritic cells via exosomes. Blood 119:756–766.

Moossavi S, Zhang H, Sun J, Rezaei N. 2013. Host-microbiota interaction and intestinal stem cells in chronic inflammation and colorectal cancer. Expert Rev Clin Immunol 9:409–422.

Mori Akiyama Y, Akiyama H, Rowitch DH, de Crombrugghe B. 2003. Sox9 is required for determination of the chondrogenic cell lineage in the cranial neural crest. PNAS 100:9360–9365.

Mukherji S, Ebert MS, Zheng GXY, Tsang JS, Sharp PA, van Oudenaarden A. 2011. MicroRNAs can generate thresholds in target gene expression. Nat. Genet. 43:854–859.

Mullany LE, Herrick JS, Wolff RK, Buas MF, Slattery ML. 2016. Impact of polymorphisms in microRNA biogenesis genes on colon cancer risk and microRNA expression levels: a population-based, case-control study. BMC Med Genomics 9:21.

Mustata RC, Van Loy T, Lefort A, Libert F, Strollo S, Vassart G, Garcia M-I. 2011. Lgr4 is required for Paneth cell differentiation and maintenance of intestinal stem cells ex vivo. EMBO reports 12:558–564.

Najafi-Shoushtari SH, Kristo F, Li Y, Shioda T, Cohen DE, Gerszten RE, Naar AM. 2010. microRNA-33 and the SREBP host genes cooperate to control cholesterol homeostasis. Science 328:1566.

Nakato G, Hase K, Sato T, Kimura S, Sakakibara S, Sugiyama M, Obata Y, Hanazato M, Iwanaga T, Ohno H. 2016. Epithelium-intrinsic microRNAs contribute to mucosal immune homeostasis by promoting M-cell maturation. PLoS ONE 11:e0150379.

Nathan G, Kredo-Russo S, Geiger T, Lenz A, Kaspi H, Hornstein E, Efrat S. 2015. miR-375 promotes redifferentiation of adult human β cells expanded in vitro. Camussi G, editor. PLoS ONE 10:e0122108.

Nezami BG, Mwangi SM, Lee JE, Jeppsson S, Anitha M, Yarandi SS, Farris AB, Srinivasan S. 2014. MicroRNA 375 mediates palmitate-induced enteric neuronal damage and high-fat diet-induced delayed intestinal transit in mice. Gastroenterology 146:473–83.e3.

Ng R, Wu H, Xiao H, Chen X, Willenbring H, Steer CJ, Song G. 2014. Inhibition of microRNA-24 expression in liver prevents hepatic lipid accumulation and hyperlipidemia. Hepatology 60:554–564.

Nguyen HTT, Dalmasso G, Müller S, Carrière J, Seibold F, Darfeuille-Michaud A. 2014. Crohn's disease-associated adherent invasive Escherichia coli modulate levels of microRNAs in intestinal epithelial cells to reduce autophagy. Gastroenterology 146:508–519.

Noah TK, Donahue B, Shroyer NF. 2011. Intestinal development and differentiation. Exp. Cell Res. 317:2702–2710.

Nunn AC. 2012. The role of SOX9 in neural progenitor identity. Lovell-Badge R; Briscoe J, editors. [Mill Hill, London NW7 1AA]: UCL (University College London).

O'Shea EF, Cotter PD, Stanton C, Ross RP, Hill C. 2012. Production of bioactive substances by

intestinal bacteria as a basis for explaining probiotic mechanisms: bacteriocins and conjugated linoleic acid. Int. J. Food Microbiol. 152:189–205.

Odamaki T, Kato K, Sugahara H, Hashikura N, Takahashi S, Xiao J-Z, Abe F, Osawa R. 2016. Age-related changes in gut microbiota composition from newborn to centenarian: a cross-sectional study. BMC Microbiology 16:90.

Oglesby IK, Chotirmall SH, McElvaney NG, Greene CM. 2013. Regulation of cystic fibrosis transmembrane conductance regulator by microRNA-145, -223, and -494 is altered in ΔF508 cystic fibrosis airway epithelium. J. Immunol. 190:3354–3362.

Olaru AV, Selaru FM, Mori Y, Vazquez C, David S, Paun B, Cheng Y, Jin Z, Yang J, Agarwal R, et al. 2011. Dynamic changes in the expression of MicroRNA-31 during inflammatory bowel disease-associated neoplastic transformation. Inflammatory Bowel Diseases 17:221–231.

Olaru AV, Yamanaka S, Vazquez C, Mori Y, Cheng Y, Abraham JM, Bayless TM, Harpaz N, Selaru FM, Meltzer SJ. 2013. MicroRNA-224 negatively regulates p21 expression during late neoplastic progression in inflammatory bowel disease. Inflammatory Bowel Diseases 19:471–480.

Osella M, Bosia C, Corà D, Caselle M. 2011. The role of incoherent microRNA-mediated feedforward loops in noise buffering. PLoS Comput. Biol. 7:e1001101.

Ott CE, Grünhagen J, Jäger M, Horbelt D, Schwill S. 2011. MicroRNAs differentially expressed in postnatal aortic development downregulate elastin via 3′ UTR and coding-sequence binding sites. Zhou Z, editor. PLoS ONE 6:e16250.

Pandey AK, Verma G, Vig S, Srivastava S, Srivastava AK, Datta M. 2011. miR-29a levels are elevated in the db/db mice liver and its overexpression leads to attenuation of insulin action on PEPCK gene expression in HepG2 cells. Molecular and Cellular Endocrinology 332:125–133.

Patro R, Duggal G, Kingsford C. 2015. Salmon: Accurate, Versatile and Ultrafast Quantification from RNA-seq Data using Lightweight-Alignment. bioRxiv.

Peck BCE, Weiser M, Lee SE, Gipson GR, Iyer VB, Sartor RB, Herfarth HH, Long MD, Hansen JJ, Isaacs KL, et al. 2015. MicroRNAs Classify Different Disease Behavior Phenotypes of Crohn's Disease and May Have Prognostic Utility. Inflammatory Bowel Diseases 21:2178–2187.

Pekow JR, Dougherty U, Mustafi R, Zhu H, Kocherginsky M, Rubin DT, Hanauer SB, Hart J, Chang EB, Fichera A, et al. 2012. miR-143 and miR-145 are downregulated in ulcerative colitis: Putative regulators of inflammation and protooncogenes. Inflammatory Bowel Diseases 18:94–100.

Penhoat A, Fayard L, Stefanutti A, Mithieux G, Rajas F. 2014. Intestinal gluconeogenesis is crucial to maintain a physiological fasting glycemia in the absence of hepatic glucose production in mice. Metabolism 63:104–111.

Perreault N, Beaulieu JF. 1996. Use of the dissociating enzyme thermolysin to generate viable

human normal intestinal epithelial cell cultures. Exp. Cell Res. 224:354–364.

Pédron T, Mulet C, Dauga C, Frangeul L, Chervaux C, Grompone G, Sansonetti PJ. 2012. A crypt-specific core microbiota resides in the mouse colon. mBio 3:e00116–12–e00116–12.

Poy MN, Eliasson L, Krützfeldt J, Kuwajima S, Ma X, Macdonald PE, Pfeffer S, Tuschl T, Rajewsky N, Rorsman P, et al. 2004. A pancreatic islet-specific microRNA regulates insulin secretion. Nature 432:226–230.

Poy MN, Hausser J, Trajkovski M, Braun M, Collins S, Rorsman P, Zavolan M, Stoffel M. 2009. miR-375 maintains normal pancreatic alpha- and beta-cell mass. PNAS 106:5813–5818.

Prideaux L, Kang S, Wagner J, Buckley M, Mahar JE, De Cruz P, Wen Z, Chen L, Xia B, van Langenberg DR, et al. 2013. Impact of ethnicity, geography, and disease on the microbiota in health and inflammatory bowel disease. Inflammatory Bowel Diseases 19:2906–2918.

Primo MN, Bak RO, Schibler B, Mikkelsen JG. 2012. Regulation of pro-inflammatory cytokines TNFα and IL24 by microRNA-203 in primary keratinocytes. Cytokine 60:741–748.

Puigserver P, Rodgers JT. 2006. Foxa2, a novel transcriptional regulator of insulin sensitivity. Nat Med 12:38–39.

Pullen TJ, da Silva Xavier G, Kelsey G, Rutter GA. 2011. miR-29a and miR-29b contribute to pancreatic beta-cell-specific silencing of monocarboxylate transporter 1 (Mct1). Mol Cell Biol 31:3182–3194.

Qin J, Li Y, Cai Z, Li S, Zhu J, Zhang F, Liang S, Zhang W, Guan Y, Shen D, et al. 2012. A metagenome-wide association study of gut microbiota in type 2 diabetes. Nature 490:55–60.

Quiat D, Olson EN. 2013. MicroRNAs in cardiovascular disease: from pathogenesis to prevention and treatment. J. Clin. Invest. 123:11–18.

Rabot S, Membrez M, Bruneau A, Gérard P, Harach T, Moser M, Raymond F, Mansourian R, Chou CJ. 2010. GF C57BL/6J mice are resistant to high-fat-diet-induced insulin resistance and have altered cholesterol metabolism. The FASEB Journal 24:4948–4959.

Ramírez CM, Goedeke L, Rotllan N, Yoon J-H, Cirera-Salinas D, Mattison JA, Suárez Y, de Cabo R, Gorospe M, Fernández-Hernando C. 2013. MicroRNA 33 regulates glucose metabolism. Mol Cell Biol 33:2891–2902.

Rasband WS. 2008. ImageJ. http://rsbweb. nih. gov/ij/.

Rasmussen BA, Breen DM, Duca FA, Côté CD, Zadeh-Tahmasebi M, Filippi BM, Lam TKT. 2014. Jejunal leptin-PI3K signaling lowers glucose production. Cell Metabolism 19:155–161.

Rayner KJ, Esau CC, Hussain FN, McDaniel AL, Marshall SM, van Gils JM, Ray TD, Sheedy FJ, Goedeke L, Liu X, et al. 2011. Inhibition of miR-33a/b in non-human primates raises plasma HDL and lowers VLDL triglycerides. Nature 478:404–407.

Rayner KJ, Sheedy FJ, Esau CC, Hussain FN, Temel RE, Parathath S, van Gils JM, Rayner AJ, Chang AN, Suárez Y, et al. 2011. Antagonism of miR-33 in mice promotes reverse cholesterol transport and regression of atherosclerosis. J. Clin. Invest. 121:2921–2931.

Rayner KJ, Suárez Y, Dávalos A, Parathath S, Fitzgerald ML, Tamehiro N, Fisher EA, Moore KJ, Fernández-Hernando C. 2010. miR-33 contributes to the regulation of cholesterol homeostasis. Science 328:1570–1573.

Reddy BS. 1972. Studies on the mechanism of calcium and magnesium absorption in germfree rats. Archives of Biochemistry and Biophysics 149:15–21.

Reinehr T, Roth CL, Schernthaner G-H, Kopp H-P, Kriwanek S, Schernthaner G. 2007. Peptide YY and glucagon-like peptide-1 in morbidly obese patients before and after surgically induced weight loss. OBES SURG 17:1571–1577.

Reusch J, Stewart MW, Perkins CM, Cirkel DT, Ye J, Perry CR, Reinhardt RR, Bode BW. 2014. Efficacy and safety of once-weekly glucagon-like peptide 1 receptor agonist albiglutide (HARMONY 1 trial): 52-week primary endpoint results from a randomized, double-blind, placebo-controlled trial in patients with type 2 diabetes mellitus not controlled on pioglitazone, with or without metformin. Diabetes Obes Metab 16:1257–1264.

Richards P, Pais R, Habib AM, Brighton CA, Yeo GSH, Reimann F, Gribble FM. 2016. High-fat diet impairs the function of glucagon-like peptide-1 producing L-cells. Peptides 77:21–27.

Robinson MD, McCarthy DJ, Smyth GK. 2009. edgeR: a Bioconductor package for differential expression analysis of digital gene expression data. Bioinformatics 26:139–140.

Roche KC, Gracz AD, Liu XF, Newton V, Akiyama H, Magness ST. 2015. SOX9 maintains reserve stem cells and preserves radioresistance in mouse small intestine. Gastroenterology 149:1553–1563.e10.

Rockich BE, Hrycaj SM, Shih HP, Nagy MS, Ferguson MAH, Kopp JL, Sander M, Wellik DM, Spence JR. 2013. Sox9 plays multiple roles in the lung epithelium during branching morphogenesis. PNAS 110:E4456–64.

Romao JM, Jin W, Dodson MV, Hausman GJ, Moore SS, Guan LL. 2011. MicroRNA regulation in mammalian adipogenesis. Exp. Biol. Med. (Maywood) 236:997–1004.

Rotllan N, Price N, Pati P, Goedeke L, Fernández-Hernando C. 2016. microRNAs in lipoprotein metabolism and cardiometabolic disorders. Atherosclerosis 246:352–360.

Rottiers V, Naar AM. 2012. MicroRNAs in metabolism and metabolic disorders. Nat Rev Mol Cell Biol 13:239–250.

Sarkar A, Hochedlinger K. 2013. The sox family of transcription factors: versatile regulators of stem and progenitor cell fate. Cell Stem Cell 12:15–30.

Savage DC, Siegel JE, Snellen JE, Whitt DD. 1981. Transit time of epithelial cells in the small

intestines of germfree mice and ex-germfree mice associated with indigenous microorganisms. Appl. Environ. Microbiol. 42:996–1001.

Schauer PR, Bhatt DL, Kirwan JP, Wolski K, Brethauer SA, Navaneethan SD, Aminian A, Pothier CE, Kim ESH, Nissen SE, et al. 2014. Bariatric surgery versus intensive medical therapy for diabetes--3-year outcomes. N Engl J Med 370:2002–2013.

Schauer PR, Kashyap SR, Wolski K, Brethauer SA, Kirwan JP, Pothier CE, Thomas S, Abood B, Nissen SE, Bhatt DL. 2012. Bariatric surgery versus intensive medical therapy in obese patients with diabetes. N Engl J Med 366:1567–1576.

Schirbel A, Kessler S, Rieder F, West G, Rebert N, Asosingh K, McDonald C, Fiocchi C. 2013. Pro-angiogenic activity of TLRs and NLRs: a novel link between gut microbiota and intestinal angiogenesis. Gastroenterology 144:613–623.e9.

Seiler KM, Schenhals EL, Furstenberg von RJ, Allena BK, Smith BJ, Scaria D, Bresler MN, Dekaney CM, Henning SJ. 2015. Tissue underlying the intestinal epithelium elicits proliferation of intestinal stem cells following cytotoxic damage. Cell and Tissue Research 361:427–438.

Semova I, Carten JD, Stombaugh J, Mackey LC, Knight R, Farber SA, Rawls JF. 2012. Microbiota regulate intestinal absorption and metabolism of fatty acids in the zebrafish. Cell Host & Microbe 12:277–288.

Sethupathy P. 2013. Illuminating microRNA Transcription from the Epigenome. Curr. Genomics 14:68–77.

Sethupathy P. 2016. The Promise and Challenge of Therapeutic MicroRNA Silencing in Diabetes and Metabolic Diseases. Curr. Diab. Rep. 16:52.

Sharma R, Schumacher U. 1996. The diet and gut microflora influence the distribution of enteroendocrine cells in the rat intestine. Experientia 52:664–670.

She Z-Y, Yang W-X. 2015. SOX family transcription factors involved in diverse cellular events during development. Eur. J. Cell Biol. 94:547–563.

Shenoy A, Blelloch RH. 2014. Regulation of microRNA function in somatic stem cell proliferation and differentiation. Nat Rev Mol Cell Biol 15:565–576.

Shi Z, Chiang C-I, Mistretta T-A, Major A, Mori Akiyama Y. 2013. SOX9 directly regulates IGFBP-4 in the intestinal epithelium. Am. J. Physiol. Gastrointest. Liver Physiol. 305:G74–83.

Shin N-R, Lee J-C, Lee H-Y, Kim M-S, Whon TW, Lee M-S, Bae J-W. 2014. An increase in the Akkermansia spp. population induced by metformin treatment improves glucose homeostasis in diet-induced obese mice. Gut 63:727–735.

Siciliano V, Garzilli I, Fracassi C, Criscuolo S, Ventre S, di Bernardo D. 2013. miRNAs confer phenotypic robustness to gene networks by suppressing biological noise. Nat Commun 4:2364.

Soh J, Iqbal J, Queiroz J, Fernández-Hernando C, Hussain MM. 2013. MicroRNA-30c reduces hyperlipidemia and atherosclerosis in mice by decreasing lipid synthesis and lipoprotein secretion. Nat Med 19:892–900.

Sommer F, Bäckhed F. 2013. The gut microbiota--masters of host development and physiology. Nat Rev Micro 11:227–238.

Song C-Q, Zhang J-H, Shi J-C, Cao X-Q, Song C-H, Hassan A, Wang P, Dai L-P, Zhang J-Y, Wang K-J. 2014. Bioinformatic prediction of SNPs within miRNA binding sites of inflammatory genes associated with gastric cancer. Asian Pacific Journal of Cancer Prevention 15:937–943.

Sorefan K, Pais H, Hall AE, Kozomara A, Griffiths-Jones S, Moulton V, Dalmay T. 2012. Reducing ligation bias of small RNAs in libraries for next generation sequencing. Silence 3:4.

Squadrito ML, Baer C, Burdet F, Maderna C, Gilfillan GD, Lyle R, Ibberson M, De Palma M. 2014. Endogenous RNAs modulate microRNA sorting to exosomes and transfer to acceptor cells. Cell Rep 8:1432–1446.

Stein CA, Hansen JB, Lai J, Wu S, Voskresenskiy A, Hog A, Worm J, Hedtjarn M, Souleimanian N, Miller P, et al. 2009. Efficient gene silencing by delivery of locked nucleic acid antisense oligonucleotides, unassisted by transfection reagents. Nucleic Acids Research 38:e3–e3.

Su W-L, Kleinhanz RR, Schadt EE. 2011. Characterizing the role of miRNAs within gene regulatory networks using integrative genomics techniques. Molecular Systems Biology 7:490–490.

Takagi T, Naito Y, Mizushima K, Hirata I, Yagi N, Tomatsuri N, Ando T, Oyamada Y, Isozaki Y, Hongo H, et al. 2010. Increased expression of microRNA in the inflamed colonic mucosa of patients with active ulcerative colitis. J. Gastroenterol. Hepatol. 25 Suppl 1:S129–33.

Tan GC, Chan E, Molnar A, Sarkar R, Alexieva D, Isa IM, Robinson S, Zhang S, Ellis P, Langford CF, et al. 2014. 5' isomiR variation is of functional and evolutionary importance. Nucleic Acids Research 42:9424–9435.

Tattikota SG, Rathjen T, Hausser J, Khedkar A, Kabra UD, Pandey V, Sury M, Wessels H-H, Mollet IG, Eliasson L, et al. 2015. miR-184 regulates pancreatic β-cell function according to glucose metabolism. J Biol Chem 290:20284–20294.

Tlaskalová-Hogenová H, Štěpánková R, Kozáková H, Hudcovic T, Vannucci L, Tučková L, Rossmann P, Hrnčíř T, Kverka M, Zákostelská Z, et al. 2011. The role of gut microbiota (commensal bacteria) and the mucosal barrier in the pathogenesis of inflammatory and autoimmune diseases and cancer: contribution of GF and gnotobiotic animal models of human diseases. Cell. Mol. Immunol. 8:110–120.

Tolhurst G, Heffron H, Lam YS, Parker HE, Habib AM, Diakogiannaki E, Cameron J, Grosse J, Reimann F, Gribble FM. 2012. Short-chain fatty acids stimulate glucagon-like peptide-1 secretion via the G-protein-coupled receptor FFAR2. Diabetes 61:364–371.

Trajkovski M, Hausser J, Soutschek J, Bhat B, Akin A, Zavolan M, Heim MH, Stoffel M. 2011. MicroRNAs 103 and 107 regulate insulin sensitivity. Nature 474:649–653.

Tremaroli V, Bäckhed F. 2012. Functional interactions between the gut microbiota and host metabolism. Nature 489:242–249.

Troy S, Soty M, Ribeiro L, Laval L, Migrenne S, Fioramonti X, Pillot B, Fauveau V, Aubert R, Viollet B, et al. 2008. Intestinal gluconeogenesis is a key factor for early metabolic changes after gastric bypass but not after gastric lap-band in mice. Cell Metabolism 8:201–211.

Tsang J, Zhu J, van Oudenaarden A. 2007. MicroRNA-mediated feedback and feedforward loops are recurrent network motifs in mammals. Molecular Cell 26:753–767.

Tserel L, Runnel T, Kisand K, Pihlap M, Bakhoff L, Kolde R, Peterson H, Vilo J, Peterson P, Rebane A. 2011. MicroRNA expression profiles of human blood monocyte-derived dendritic cells and macrophages reveal miR-511 as putative positive regulator of Toll-like receptor 4. J Biol Chem 286:26487–26495.

Turchinovich A, Samatov TR, Tonevitsky AG, Burwinkel B. 2013. Circulating miRNAs: cell-cell communication function? Front Genet 4:119.

Turnbaugh PJ, Bäckhed F, Fulton L, Gordon JI. 2008. Diet-induced obesity is linked to marked but reversible alterations in the mouse distal gut microbiome. Cell Host & Microbe 3:213–223.

Uribe A, Alam M, Johansson O, Midtvedt T, Theodorsson E. 1994. Microflora modulates endocrine cells in the gastrointestinal mucosa of the rat. Gastroenterology 107:1259–1269.

Van Beers EH, Al RH, Rings EH, Einerhand AW, Dekker J, Büller HA. 1995. Lactase and sucrase-isomaltase gene expression during Caco-2 cell differentiation. Biochem. J. 308 (Pt 3):769–775.

van de Bunt M, Gaulton KJ, Parts L, Moran I, Johnson PR, Lindgren CM, Ferrer J, Gloyn AL, McCarthy MI. 2013. The miRNA profile of human pancreatic islets and beta-cells and relationship to type 2 diabetes pathogenesis. PLoS ONE 8:e55272.

Van Landeghem L, Santoro MA, Krebs AE, Mah AT, Dehmer JJ, Gracz AD, Scull BP, McNaughton K, Magness ST, Lund PK. 2012. Activation of two distinct Sox9-EGFP-expressing intestinal stem cell populations during crypt regeneration after irradiation. Am. J. Physiol. Gastrointest. Liver Physiol. 302:G1111–32.

van Rooij E, Purcell AL, Levin AA. 2012. Developing microRNA therapeutics. Circ. Res. 110:496–507.

van Rooij E, Sutherland LB, Thatcher JE, DiMaio JM, Naseem RH, Marshall WS, Hill JA, Olson EN. 2008. Dysregulation of microRNAs after myocardial infarction reveals a role of miR-29 in cardiac fibrosis. PNAS 105:13027–13032.

Velasquez-Manoff M. 2015. Gut microbiome: the peacekeepers. Nature 518:S3–11.

Vickers KC, Palmisano BT, Shoucri BM, shamburek RD, Remaley AT. 2011. MicroRNAs are transported in plasma and delivered to recipient cells by high-density lipoproteins. Nat. Cell Biol. 13:423–433.

Vickers KC, Remaley AT. 2012. Lipid-based carriers of microRNAs and intercellular communication. Current Opinion in Lipidology 23:91–97.

Vickers KC, Shoucri BM, Levin MG, Wu H, Pearson DS, Osei-Hwedieh D, Collins FS, Remaley AT, Sethupathy P. 2013. MicroRNA-27b is a regulatory hub in lipid metabolism and is altered in dyslipidemia. Hepatology 57:533–542.

Vijay-Kumar M, Aitken JD, Carvalho FA, Cullender TC, Mwangi S, Srinivasan S, Sitaraman SV, Knight R, Ley RE, Gewirtz AT. 2010. Metabolic syndrome and altered gut microbiota in mice lacking Toll-like receptor 5. Science 328:228–231.

Vilà-Brau A, De Sousa-Coelho AL, Mayordomo C, Haro D, Marrero PF. 2011. Human HMGCS2 regulates mitochondrial fatty acid oxidation and FGF21 expression in HepG2 cell line. J Biol Chem 286:20423–20430.

Wang D, Xia M, Yan X, Li D, Wang L, Xu Y, Jin T, Ling W. 2012. Gut microbiota metabolism of anthocyanin promotes reverse cholesterol transport in mice via repressing miRNA-10b. Circ. Res. 111:967–981.

Wang K, Singh D, Zeng Z, Coleman SJ, Huang Y, Savich GL, He X, Mieczkowski P, Grimm SA, Perou CM, et al. 2010. MapSplice: accurate mapping of RNA-seq reads for splice junction discovery. Nucleic Acids Research 38:e178.

Wang Y, Huang C, Reddy Chintagari N, Bhaskaran M, Weng T, Guo Y, Xiao X, Liu L. 2013. miR-375 regulates rat alveolar epithelial cell trans-differentiation by inhibiting Wnt/ -catenin pathway. Nucleic Acids Research 41:3833–3844.

Wang Z, Klipfell E, Bennett BJ, Koeth R, Levison BS, DuGar B, Feldstein AE, Britt EB, Fu X, Chung Y-M, et al. 2011. Gut flora metabolism of phosphatidylcholine promotes cardiovascular disease. Nature 472:57–63.

Williams MD, Mitchell GM. 2012. MicroRNAs in insulin resistance and obesity. Exp Diabetes Res 2012:484696–8.

Wolfrum C, Asilmaz E, Luca E, Friedman JM, Stoffel M. 2004. Foxa2 regulates lipid metabolism and ketogenesis in the liver during fasting and in diabetes. Nature 432:1027–1032.

Wolfrum C, Stoffel M. 2006. Coactivation of Foxa2 through Pgc-1beta promotes liver fatty acid oxidation and triglyceride/VLDL secretion. Cell Metabolism 3:99–110.

Wostmann BS. 1973. Intestinal bile acids and cholesterol absorption in the germfree rat. J. Nutr. 103:982–990.

Wostmann BS. 1996. Germfree and Gnotobiotic Animal Models: Background and Applications.

Boca Raton, FL: Taylor \& Francis.

Wu F, Zhang S, Dassopoulos T, Harris ML, Bayless TM, Meltzer SJ, Brant SR, Kwon JH. 2010. Identification of microRNAs associated with ileal and colonic Crohn's disease. Inflammatory Bowel Diseases 16:1729–1738.

Wu F, Zikusoka M, Trindade A, Dassopoulos T, Harris ML, Bayless TM, Brant SR, Chakravarti S, Kwon JH. 2008. MicroRNAs are differentially expressed in ulcerative colitis and alter expression of macrophage inflammatory peptide-2 alpha. Gastroenterology 135:1624–1635.e24.

Wu T, Zhou H, Hong Y, Li J, Jiang X, Huang H. 2012. miR-30 family members negatively regulate osteoblast differentiation. J Biol Chem 287:7503–7511.

Wu TD, Nacu S. 2010. Fast and SNP-tolerant detection of complex variants and splicing in short reads. Bioinformatics 26:873–881.

Xiang Y, Cheng J, Wang D, Hu X, Xie Y, Stitham J, Atteya G, Du J, Tang WH, Lee SH, et al. 2015. Hyperglycemia repression of miR-24 coordinately upregulates endothelial cell expression and secretion of von Willebrand factor. Blood 125:3377–3387.

Xiao Changchun, Calado DP, Galler G, Thai T-H, Patterson HC, Wang J, Rajewsky N, Bender TP, Rajewsky K. 2007. miR-150 controls B cell differentiation by targeting the transcription factor c-Myb. Cell 131:146–159.

Xiao Changting, Dash S, Morgantini C, Adeli K, Lewis GF. 2015. Gut peptides are novel regulators of intestinal lipoprotein secretion: experimental and pharmacological manipulation of mipoprotein metabolism. Diabetes 64:2310–2318.

Xu L, Yang B-F, Ai J. 2013. MicroRNA transport: a new way in cell communication. J. Cell. Physiol. 228:1713–1719.

Xu N, Meisgen F, Butler LM, Han G, Wang X-J, Söderberg-Nauclér C, Ståhle M, Pivarcsi A, Sonkoly E. 2013. MicroRNA-31 is overexpressed in psoriasis and modulates inflammatory cytokine and chemokine production in keratinocytes via targeting serine/threonine kinase 40. J. Immunol. 190:678–688.

Yan J-W, Lin J-S, He X-X. 2013. The emerging role of miR-375 in cancer. Int. J. Cancer 135:1011–1018.

Yang B, Guo H, Zhang Y, Chen L, Ying D, Dong S. 2011. MicroRNA-145 regulates chondrogenic differentiation of mesenchymal stem cells by targeting Sox9. PLoS ONE 6:e21679.

Ye D, Guo S, Al-Sadi R, Ma TY. 2011. MicroRNA regulation of intestinal epithelial tight junction permeability. Gastroenterology 141:1323–1333.

Yokoi N, Hoshino M, Hidaka S, Yoshida E, Beppu M, Hoshikawa R, Sudo K, Kawada A, Takagi S, Seino S. 2013. A novel rat model of type 2 diabetes: The Zucker Fatty Diabetes

Mellitus ZFDM rat. J Diabetes Res 2013.

Yoon JC, Puigserver P, Chen G, Donovan J, Wu Z, Rhee J, Adelmant G, Stafford J, Kahn CR, Granner DK, et al. 2001. Control of hepatic gluconeogenesis through the transcriptional coactivator PGC-1. Nature 413:131–138.

Yoshikawa T, Otsuka M, Kishikawa T, Takata A, Ohno M, Shibata C, Kang YJ, Yoshida H, Koike K. 2013. Unique haploinsufficient role of the microRNA-processing molecule Dicer1 in a murine colitis-associated tumorigenesis model. Wang Y, editor. PLoS ONE 8:e71969.

Yu C-C, Tsai L-L, Wang M-L, Yu C-H, Lo W-L, Chang Y-C, Chiou G-Y, Chou M-Y, Chiou S-H. 2013. miR-145 targets the SOX9/ADAM17 axis to inhibit tumor-initiating cells and IL-6-mediated paracrine effects in head and neck cancer. Cancer Res. 73:3425–3440.

Yu F, Deng H, Yao H, Liu Q, Su F, Song E. 2010. miR-30 reduction maintains self-renewal and inhibits apoptosis in breast tumor-initiating cells. Oncogene 29:4194–4204.

Zaiss MM, Rapin A, Lebon L, Dubey LK, Mosconi I, Sarter K, Piersigilli A, Menin L, Walker AW, Rougemont J, et al. 2015. The intestinal microbiota contributes to the ability of helminths to modulate allergic inflammation. Immunity 43:998–1010.

Zampetaki A, Kiechl S, Drozdov I, Willeit P, Mayr U, Prokopi M, Mayr A, Weger S, Oberhollenzer F, Bonora E, et al. 2010. Plasma microRNA profiling reveals loss of endothelial miR-126 and other microRNAs in type 2 diabetes. Circ. Res. 107:810–817.

Zhang B-W, Cai H-F, Wei X-F, Sun J-J, Lan X-Y, Lei C-Z, Lin F-P, Qi X-L, Plath M, Chen H. 2016. miR-30-5p regulates muscle differentiation and alternative splicing of muscle-related genes by targeting MBNL. Int J Mol Sci 17:1–16.

Zhang C, Zhao Z, Osman H, Watson R, Nalbantoglu I, Lin J. 2014. Differential expression of miR-31 between inflammatory bowel disease and microscopic colitis. Microrna 3:155–159.

Zhang P, Huang A, Ferruzzi J, Mecham RP, Starcher BC, Tellides G, Humphrey JD, Giordano FJ, Niklason LE, Sessa WC. 2012. Inhibition of microRNA-29 enhances elastin levels in cells haploinsufficient for elastin and in bioengineered vessels--brief report. Arteriosclerosis, Thrombosis, and Vascular Biology 32:756–759.

Zhang X, Shen D, Fang Z, Jie Z, Qiu X, Zhang C, Chen Y, Ji L. 2013. Human gut microbiota changes reveal the progression of glucose intolerance. Federici M, editor. PLoS ONE 8:e71108.

Zhang Y, Guo X, Xiong L, Kong X, Xu Y, Liu C, Zou L, Li Z, Zhao J, Lin N. 2012. MicroRNA-101 suppresses SOX9-dependent tumorigenicity and promotes favorable prognosis of human hepatocellular carcinoma. FEBS Letters 586:4362–4370.

Zhang Z-W, Men T, Feng R-C, Li Y-C, Zhou D, Teng C-B. 2013. miR-375 inhibits proliferation of mouse pancreatic progenitor cells by targeting YAP1. Cell. Physiol. Biochem. 32:1808–1817.

Zhong C-Y, Sun W-W, Ma Y, Zhu H, Yang P, Wei H, Zeng B-H, Zhang Q, Liu Y, Li W-X, et

al. 2015. Microbiota prevents cholesterol loss from the body by regulating host gene expression in mice. Sci Rep 5:10512.

Zhu Y, You W, Wang H, Li Y, Qiao N, Shi Y, Zhang C, Bleich D, Han X. 2013. MicroRNA-24/MODY gene regulatory pathway mediates pancreatic β-cell dysfunction. Diabetes 62:3194–3206.

Zinman B, Gerich J, Buse JB, Lewin A, Schwartz S, Raskin P, Hale PM, Zdravkovic M, Blonde L, Investigators TL-4S. 2009. Efficacy and Safety of the Human Glucagon-Like Peptide-1 Analog Liraglutide in Combination With Metformin and Thiazolidinedione in Patients With Type 2 Diabetes (LEAD-4 Met+TZD). Diabetes Care 32:1224–1230.

Zweibaum A, Triadou N, Kedinger M, Augeron C, Robine-Léon S, Pinto M, Rousset M, Haffen K. 1983. Sucrase-isomaltase: a marker of foetal and malignant epithelial cells of the human colon. Int. J. Cancer 32:407–412.